Gravitational waves from the early universe

Chiara Caprini
CERN and University of Geneva

Summary of the lecture

- GW equation of motion in FLRW and its relevant solutions
- Characterisation of a stochastic GW background from the early universe
- What is and will be known on the SGWB, with a digression on PTA measurement
- A few examples of SGWB sources with characteristic solutions

C.C. and D.G. Figueroa, “Cosmological backgrounds of GWs”, arXiv:1801.04268
M. Maggiore, “Gravitational waves”, volume 1 and 2, Oxford University Press

GW propagation equation in FLRW

From Einstein equations in FLRW universe at first order in cosmological perturbation theory

$$\ddot{h}_{ij}(\mathbf{x},t) + 3\,H\,\dot{h}_{ij}(\mathbf{x},t) - \frac{\nabla^2}{a^2}\,h_{ij}(\mathbf{x},t) = 16\pi G\,\boxed{\Pi_{ij}(\mathbf{x},t)}$$

Source: tensor anisotropic stress

Perfect fluid

$$T_{\mu\nu} = \bar{T}_{\mu\nu} + \delta T_{\mu\nu}$$

In the cosmological context: energy momentum tensor of the matter content of the universe (background + perturbations)

$$\delta T_{ij} = \bar{p}\,\delta g_{ij} + a^2[\delta p\,\delta_{ij} + (\partial_i\partial_j - \frac{1}{3}\delta_{ij}\nabla^2)\sigma + 2\partial_{(i}v_{j)}\boxed{+\,\Pi_{ij}}]$$

$$(\partial_i v_i = 0,\ \partial_i\Pi_{ij} = 0,\ \Pi_{ii} = 0)$$

NO GWs FROM THE HOMOGENEOUS MATTER COMPONENT

GW propagation equation in FLRW

From Einstein equations in FLRW universe at first order in cosmological perturbation theory

$$\ddot{h}_{ij}(\mathbf{x},t) + 3\,H\,\dot{h}_{ij}(\mathbf{x},t) - \frac{\nabla^2}{a^2}\,h_{ij}(\mathbf{x},t) = 16\pi G\,\boxed{\Pi_{ij}(\mathbf{x},t)}$$

Source: tensor anisotropic stress

One exploits the translational invariance and performs a F.T. in space

$$h_{ij}(\mathbf{x},t) = \sum_{r=+,\times} \int \frac{d^3\mathbf{k}}{(2\pi)^3}\, h_r(\mathbf{k},t)\, e^{-i\mathbf{k}\cdot\mathbf{x}}\, e^r_{ij}(\hat{\mathbf{k}})$$

$$\Pi_{ij}(\mathbf{x},t) = \sum_{r=+,\times} \int \frac{d^3\mathbf{k}}{(2\pi)^3}\, \Pi_r(\mathbf{k},t)\, e^{-i\mathbf{k}\cdot\mathbf{x}}\, e^r_{ij}(\hat{\mathbf{k}})$$

GW propagation equation in FLRW

From Einstein equations in FLRW universe at first order in cosmological perturbation theory

$$\ddot{h}_{ij}(\mathbf{x},t) + 3\,H\,\dot{h}_{ij}(\mathbf{x},t) - \frac{\nabla^2}{a^2}\,h_{ij}(\mathbf{x},t) = 16\pi G\,\boxed{\Pi_{ij}(\mathbf{x},t)}$$

Source: tensor anisotropic stress

One exploits the translational invariance and performs a F.T. in space

$$h_{ij}(\mathbf{x},t) = \sum_{r=+,\times} \int \frac{d^3\mathbf{k}}{(2\pi)^3}\, h_r(\mathbf{k},t)\, e^{-i\mathbf{k}\cdot\mathbf{x}}\, e^r_{ij}(\hat{\mathbf{k}})$$

The evolution equation decouples for each polarisation mode

$$h_r''(\mathbf{k},\eta) + 2\,\mathcal{H}\,h_r'(\mathbf{k},\eta) + k^2\,h_r(\mathbf{k},\eta) = 16\pi G\,a^2\,\Pi_r(\mathbf{k},\eta)$$

conformal time, Hubble factor and comoving wavenumber

GW propagation equation in FLRW

$$h_r''(\mathbf{k},\eta) + 2\,\mathcal{H}\,h_r'(\mathbf{k},\eta) + k^2\,h_r(\mathbf{k},\eta) = 16\pi G\,a^2\,\Pi_r(\mathbf{k},\eta)$$

Solution of the homogeneous equation

Power-law scale factor $a(\eta) = a_n \eta^n$

Covering matter (n=2) and radiation domination (n=1), and De Sitter inflation n=-1)

$$h_r(\mathbf{k},\eta) = \frac{A_r(\mathbf{k})}{a_n \eta^{n-1}}\,j_{n-1}(k\eta) + \frac{B_r(\mathbf{k})}{a_n \eta^{n-1}}\,y_{n-1}(k\eta)$$

Two notable limiting cases: sub-Hubble and super-Hubble modes

$$H_r(\mathbf{k},\eta) = a\,h_r(\mathbf{k},\eta) \qquad H_r''(\mathbf{k},\eta) + \left(k^2 - \frac{a''}{a}\right) H_r(\mathbf{k},\eta) = 0$$

$$a''/a \propto \mathcal{H}^2$$

GW propagation equation in FLRW

CASE 1: Sub-Hubble modes, relevant for **propagation after the source stops**

$$k^2 \gg \mathcal{H}^2 \qquad h_r(\mathbf{k},\eta) = \frac{A_r(\mathbf{k})}{a(\eta)}\, e^{ik\eta} + \frac{B_r(\mathbf{k})}{a(\eta)}\, e^{-ik\eta}$$

In this limit, GWs are plane waves with redshifting amplitude

What are the coefficients $A_r(\mathbf{k})$ and $B_r(\mathbf{k})$ from the initial condition?

Suppose the source operates in a time interval $\eta_{\rm fin}$ - $\eta_{\rm in}$ in the radiation dominated era

$$H_r^{\rm rad}(\mathbf{k},\eta<\eta_{\rm fin}) = \frac{16\pi G}{k}\int_{\eta_{\rm in}}^{\eta} d\tau\, a(\tau)^3\, \sin[k(\eta-\tau)]\,\Pi_r(\mathbf{k},\tau)$$

Matching at $\eta_{\rm fin}$ with the homogeneous solution to find the GW signal today

$$H_r^{\rm rad}(\mathbf{k},\eta>\eta_{\rm fin}) = A_r^{\rm rad}(\mathbf{k})\cos(k\eta) + B_r^{\rm rad}(\mathbf{k})\sin(k\eta)$$

$$A_r^{\rm rad}(\mathbf{k}) = \frac{16\pi G}{k}\int_{\eta_{\rm in}}^{\eta_{\rm fin}} d\tau\, a(\tau)^3\, \sin(-k\tau)\,\Pi_r(\mathbf{k},\tau)$$

$$B_r^{\rm rad}(\mathbf{k}) = \frac{16\pi G}{k}\int_{\eta_{\rm in}}^{\eta_{\rm fin}} d\tau\, a(\tau)^3\, \cos(k\tau)\,\Pi_r(\mathbf{k},\tau)$$

GW propagation equation in FLRW

CASE 2: Super-Hubble modes, relevant for **inflationary tensor perturbations**

$$k^2 \ll \mathcal{H}^2 \qquad h_r(\mathbf{k},\eta) = A_r(\mathbf{k}) + B_r(\mathbf{k}) \int^{\eta} \frac{d\eta'}{a^2(\eta')}$$

Decaying mode, negligible

Full solution with inflationary initial conditions
Hubble re-entry at the radiation-matter transition

Initial condition from inflation, $A_r(\mathbf{k})$ constant

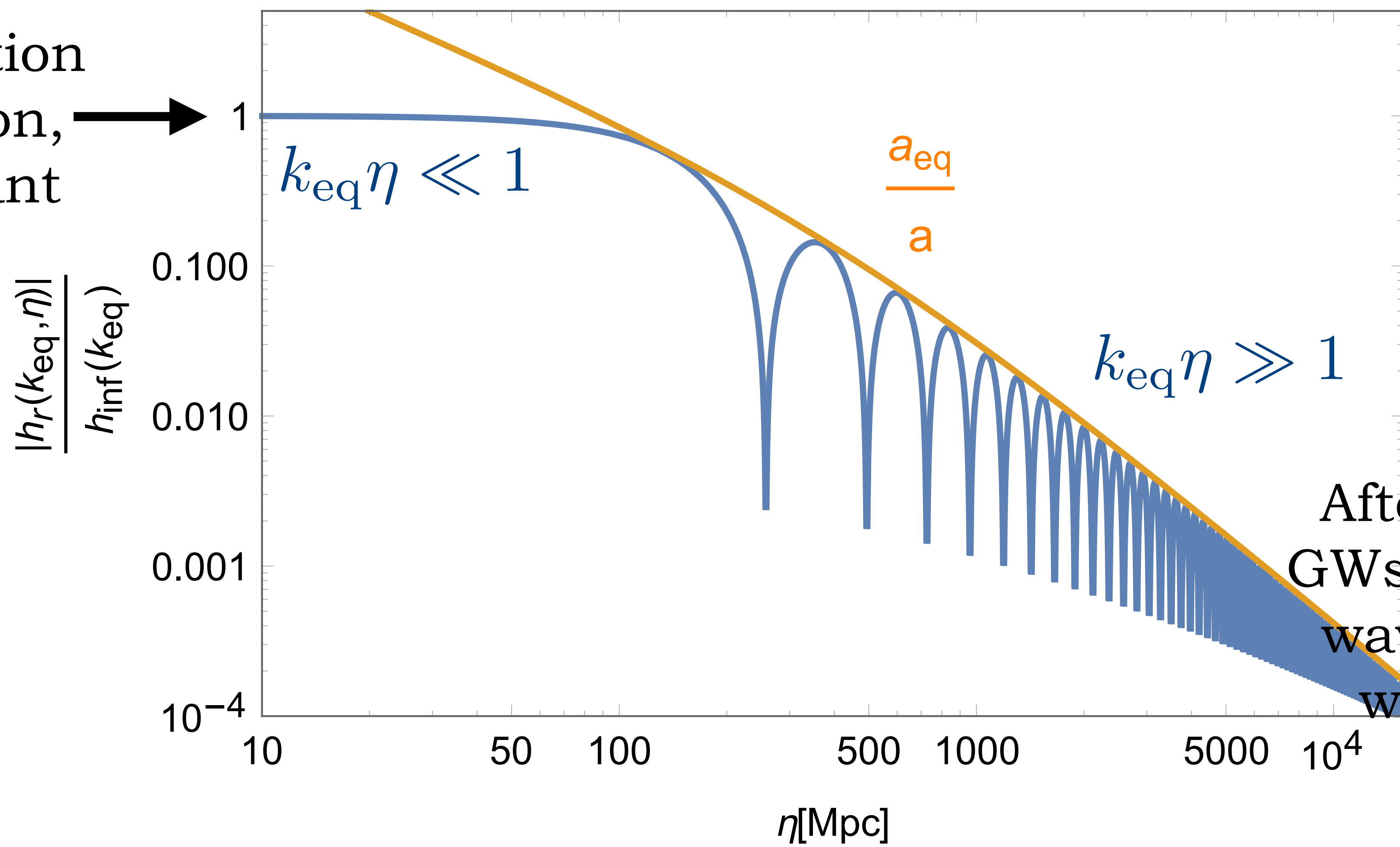

After Hubble re-entry, GWs oscillating as plane waves and redshifting with the expansion

Why sources in the early universe produce SGWBs?

A stochastic GW background is a signal for which *only the statistical properties can be accessed* because it is given by the incoherent superposition of sources that cannot be individually resolved

LIGO website

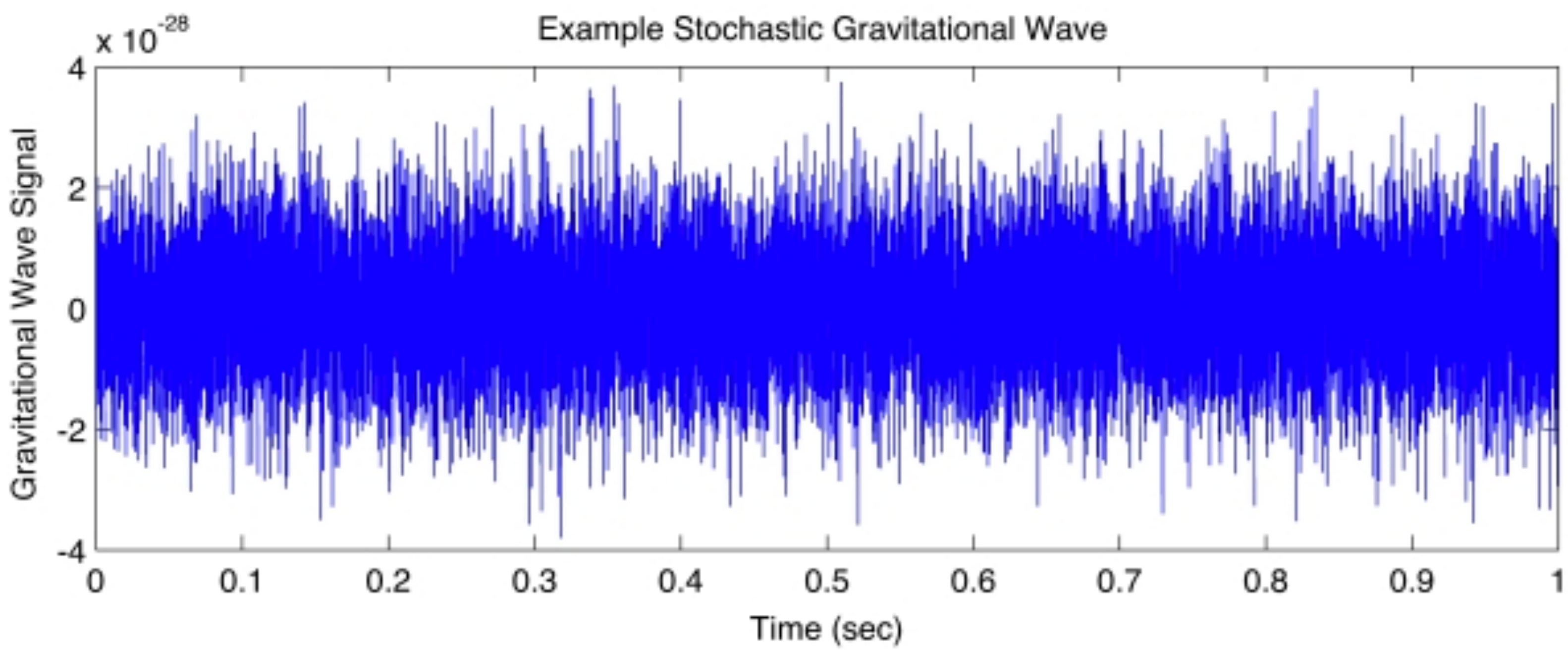

- For example, the superposition of deterministic GW signals from astrophysical binary sources with too low signal-to-noise ratio, or too much overlap in time and frequency -> confusion noise (Examples: LVK, LISA, PTAs…)

- Early universe GW sources produce SGWBs because they are homogeneously and isotropically distributed over the entire universe, and correlated on scales much smaller than the detector resolution

Why sources in the early universe produce SGWBs?

A GW source acting at time t_* in the early universe cannot produce a signal correlated on length/time scales larger than the causal horizon at that time

$$\boxed{\ell_* \leq H_*^{-1}}$$

ℓ_* characteristic length-scale of the source
(typical size of variation of the tensor anisotropic stresses)

Why sources in the early universe produce SGWBs?

A GW source acting at time t_* in the early universe cannot produce a signal correlated on length/time scales larger than the causal horizon at that time

$$\boxed{\ell_* \leq H_*^{-1}}$$

Angular size on the sky today of a region in which the SGWB signal is correlated

$$\Theta_* = \frac{\ell_*}{d_A(z_*)}$$

Angular diameter distance

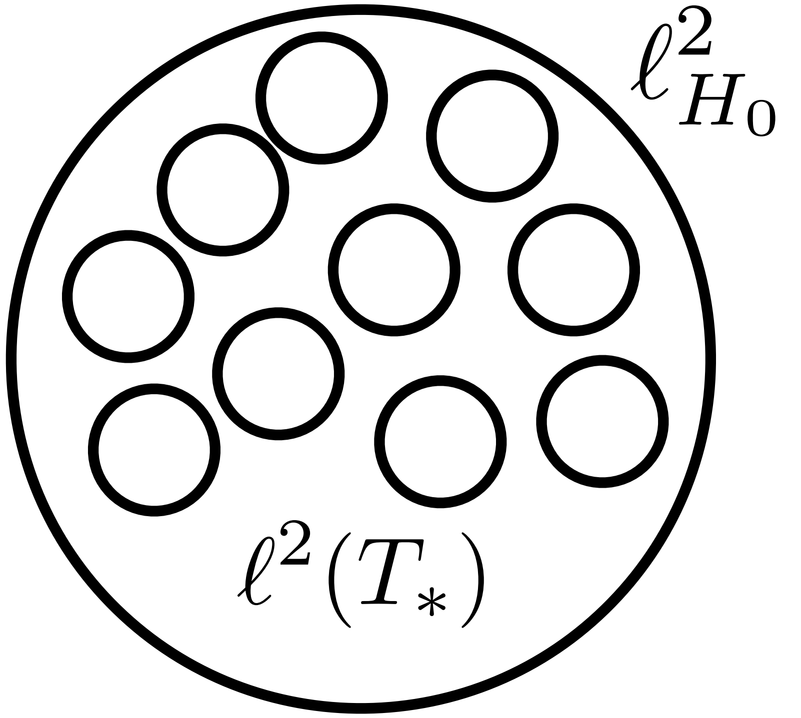

Number of uncorrelated regions accessible today $\sim \Theta_*^{-2}$

Suppose a GW detector angular resolution of 10 deg $\longrightarrow$ $z_* \lesssim 17$

$$\Theta(z_* = 1090) \simeq 0.9\,\mathrm{deg} \qquad\qquad \Theta(T_* = 100\,\mathrm{GeV}) \simeq 10^{-12}\mathrm{deg}$$

Only the statistical properties of the signal can be accessed

Why sources in the early universe produce SGWBs?

- We access today the GW signal from many independent horizon volumes: $h_{ij}(\mathbf{x},t)$ must be treated as a random variable, only its statistical properties can be accessed, e.g. its correlator $\langle h_r(\mathbf{x},\eta_1)\, h_s(\mathbf{y},\eta_2)\rangle$

  where <…> is an ensemble average

- The universe is homogeneous and isotropic, so the GW source is operating everywhere at the same time with the same average properties ("a-causal" initial conditions from Inflation)

- Under the ergodic hypothesis, the ensemble average can be substituted with volume / time averages: we identify this average with the volume / time one necessary to define the GW energy momentum tensor

- Notable exception: *SGWB from Inflation* (intrinsic quantum fluctuations that become classical (stochastic) outside the horizon)

Characterisation of a primordial SGWB

The SGWB is in general homogenous and isotropic, unpolarised and Gaussian

As the FLRW space-time

$$\langle h_{ij}(\mathbf{x},\eta_1)\,h_{lm}(\mathbf{y},\eta_2)\rangle = F_{ijlm}(|\mathbf{x}-\mathbf{y}|,\eta_1,\eta_2)$$

Certainly some *induced anisotropy*, e.g. the dipole with respect to the cosmological frame

More challenging to detect than the “monopole”

If the sourcing process preserves parity

$$\langle h_{+2}(\mathbf{k},\eta)h_{+2}(\mathbf{k},\eta) - h_{-2}(\mathbf{k},\eta)h_{-2}(\mathbf{k},\eta)\rangle = \langle h_{+}(\mathbf{k},\eta)h_{\times}(\mathbf{k},\eta)\rangle = 0$$

Helicity basis $e_{ij}^{\pm 2} = \dfrac{e_{ij}^{+} \pm i\, e_{ij}^{\times}}{2}$

There are exceptions!

Central limit theorem: the signal comes from the superposition of many independent regions

Characterisation of a primordial SGWB

Power spectrum of the GW amplitude $h_c(k,t)$

$$\langle h_r(\mathbf{k},\eta)\, h_p^*(\mathbf{q},\eta)\rangle = \frac{8\pi^5}{k^3}\,\underbrace{\delta^{(3)}(\mathbf{k}-\mathbf{q})}_{\text{Statistical homogeneity and isotropy}}\,\delta_{rp}\, h_c^2(k,\eta)$$

Unpolarised

Gaussianity: the two-point correlation function is enough to fully describe the SGWB

$$\langle h_{ij}(\mathbf{x},\eta)\, h_{ij}(\mathbf{x},\eta)\rangle = 2\int_0^{+\infty}\frac{dk}{k}\, h_c^2(k,\eta)$$

Related to the variance of the GW amplitude in real space

For *freely propagating sub-Hubble modes*, and taking the time-average:

$$h_r(\mathbf{k},\eta) = \frac{A_r(\mathbf{k})}{a(\eta)}\, e^{ik\eta} + \frac{B_r(\mathbf{k})}{a(\eta)}\, e^{-ik\eta}$$

$$\langle h_r(\mathbf{k},\eta)\, h_p^*(\mathbf{q},\eta)\rangle = \frac{1}{a^2(\eta)}\left[\langle A_r(\mathbf{k})\, A_p^*(\mathbf{q})\rangle + \langle B_r(\mathbf{k})\, B_p^*(\mathbf{q})\rangle\right] \qquad h_c(k,\eta) \propto \frac{1}{a^2(\eta)}$$

Characterisation of a primordial SGWB

Power spectrum of the GW energy density $\dfrac{d\rho_{\rm GW}}{d\log k}$

$$\rho_{\rm GW} = \frac{\langle \dot h_{ij}(\mathbf{x},t)\, \dot h_{ij}(\mathbf{x},t)\rangle}{32\pi G} = \frac{\langle h'_{ij}(\mathbf{x},\eta)\, h'_{ij}(\mathbf{x},\eta)\rangle}{32\pi G\, a^2(\eta)} = \int_0^{+\infty} \frac{dk}{k}\, \frac{d\rho_{\rm GW}}{d\log k}$$

$$\langle h'_r(\mathbf{k},\eta)\, {h'_p}^*(\mathbf{q},\eta)\rangle = \frac{8\pi^5}{k^3}\, \delta^{(3)}(\mathbf{k}-\mathbf{q})\, \delta_{rp}\, {h'_c}^2(k,\eta)$$

For *freely propagating sub-Hubble modes*, and taking the time-average:

$${h'_c}^2(k,\eta) \simeq k^2\, h_c^2(k,\eta) \qquad\qquad \frac{d\rho_{\rm GW}}{d\log k} = \frac{k^2\, h_c^2(k,\eta)}{16\pi G\, a^2(\eta)}$$

$$\rho_{\rm GW} \propto \frac{1}{a(\eta)^4}$$

GW energy density scales like radiation for freely propagating sub-Hubble modes (free massless particles)

Characterisation of a primordial SGWB

GW energy density parameter

Evaluated today, for a source that operated at time η_*

$$h^2\,\Omega_{\rm GW}(k,\eta_0) = \frac{h^2\rho_*}{\rho_c}\left(\frac{a_*}{a_0}\right)^4\left(\frac{1}{\rho_*}\frac{d\rho_{\rm GW}}{d{\rm log}k}(k,\eta_*)\right)$$

To make connection with the <u>detection process</u> one assumes that

- The source has stopped operating so the waves are freely propagating
- The expansion of the universe is negligible over the time of the measurement so that the SGWB appears stationary
- One can F.T. in time as well $\quad f = \dfrac{1}{2\pi}\dfrac{k}{a_0}$

Power spectral density

$$\langle \bar{h}_r(f,\hat{\mathbf{k}})\bar{h}^*_p(g,\hat{\mathbf{q}})\rangle = a_0^4\, f^2\, g^2 \langle A_r(\mathbf{k})\, A^*_p(\mathbf{q})\rangle =$$
$$= \frac{1}{8\pi}\,\delta(f-g)\,\delta^{(2)}(\hat{\mathbf{k}}-\hat{\mathbf{q}})\,\delta_{rp}\,S_h(f)$$

$$\Omega_{\rm GW}(f) = \frac{4\pi^2}{3H_0^2}\,f^3\,S_h(f)$$

What is/will be known about the SGWB

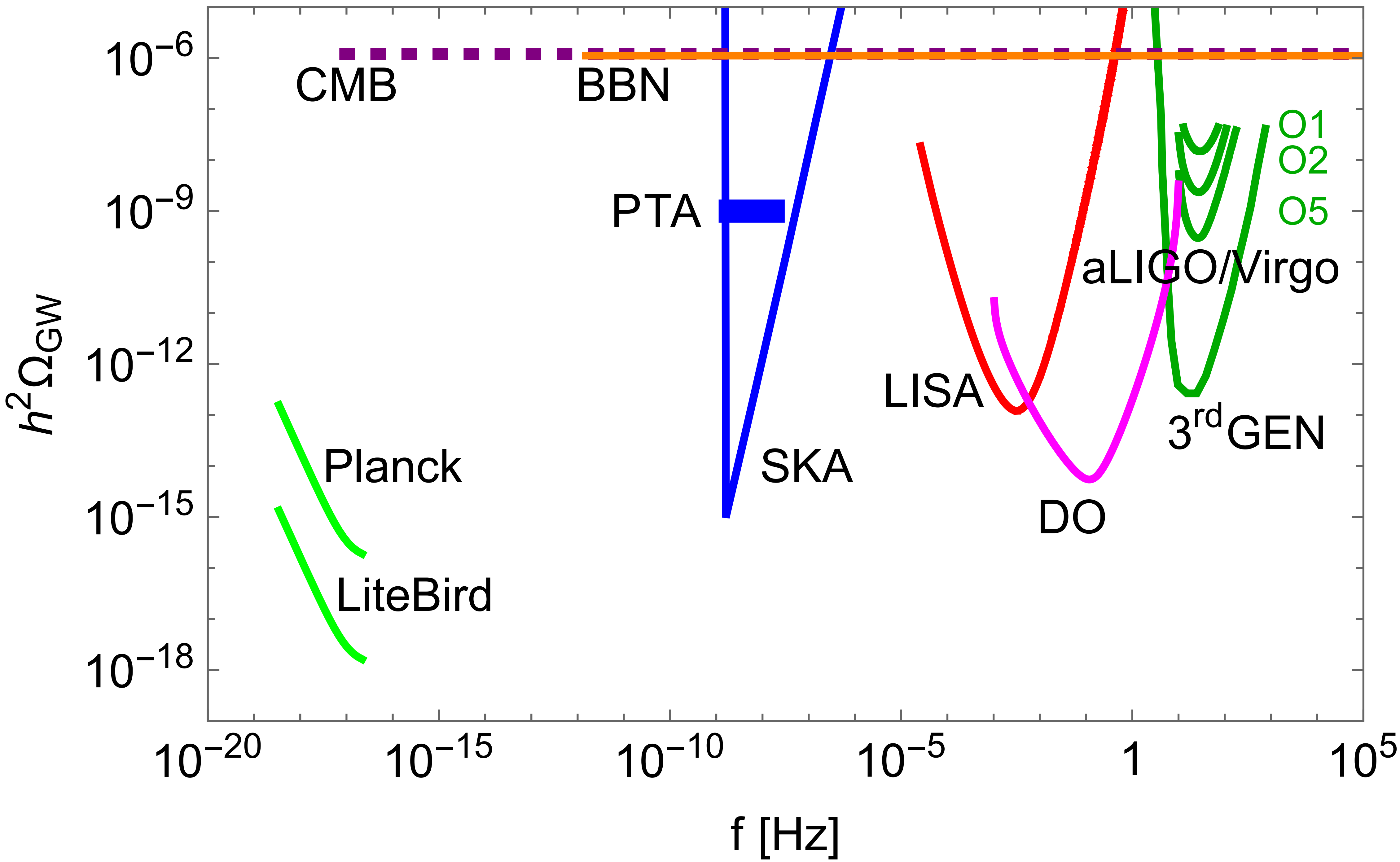

What is/will be known about the SGWB

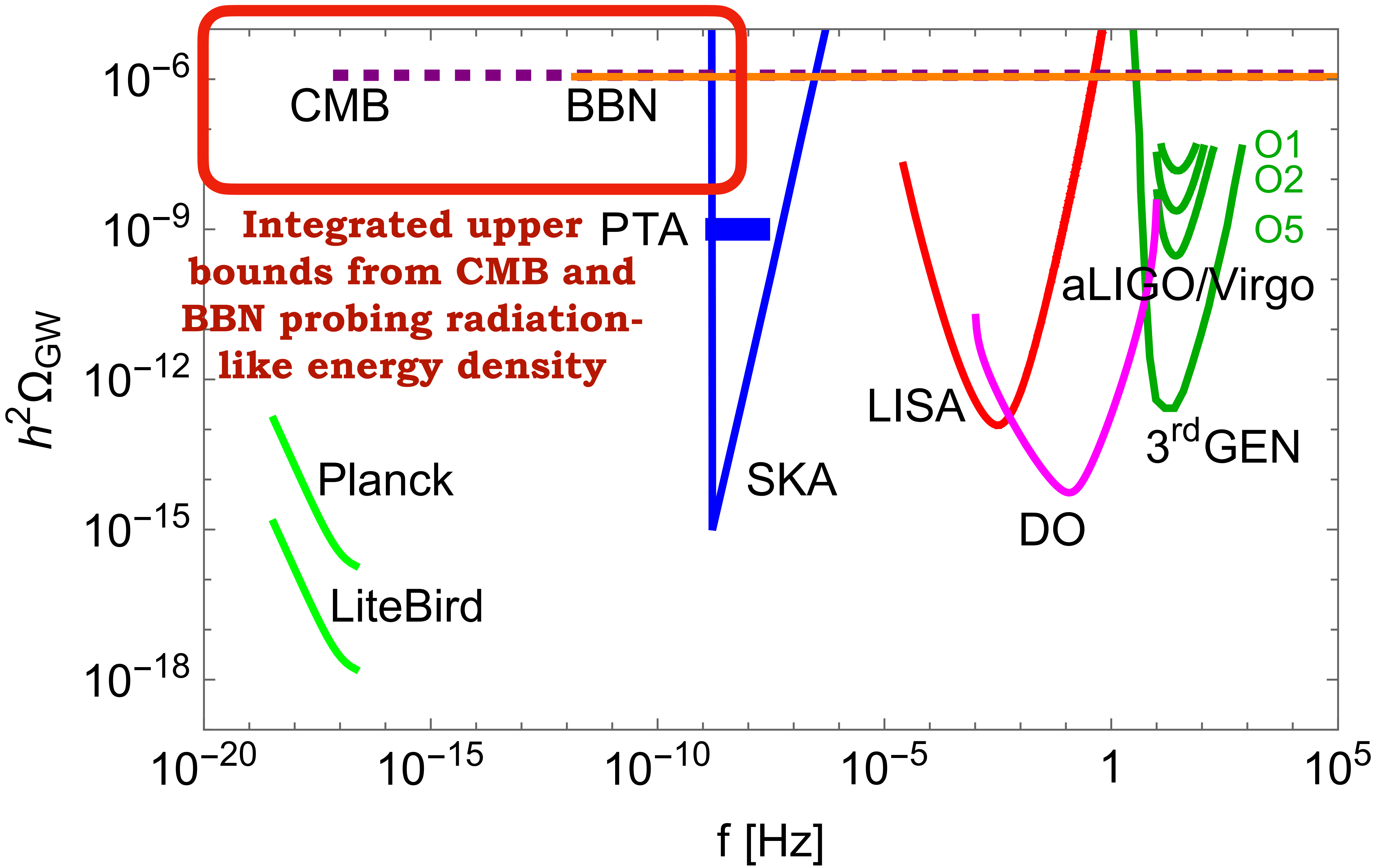

What is/will be known about the SGWB

- GW contribute to the energy density in the universe and change its background evolution

$$H^2(T) = \frac{8\pi G}{3} \Sigma_i \rho_i(T)$$

- The abundances of elements produced at Big Bang Nucleosynthesis (BBN) depend on the relative abundance of neutrons and protons, which depends on the Hubble scale at T ~ MeV

- The Cosmic Microwave Background (CMB) monopole and anisotropy spectrum depend on the Hubble scale at decoupling T ~ 0.3 eV, on the matter-radiation equality…

- Bounds on the *integrated GW energy density* at/previous to the BBN and CMB epochs

$$\left(\frac{\rho_{\rm GW}}{\rho_c}\right)_0 = \int \frac{df}{f}\,\Omega_{\rm GW}(f) = \Omega_\gamma^0 \left(\frac{g_S(T_0)}{g_S(T)}\right)^{4/3} \boxed{\left(\frac{\rho_{\rm GW}}{\rho_\gamma}\right)_T}$$

CAREFUL! Plot "wrong"…

What is/will be known about the SGWB

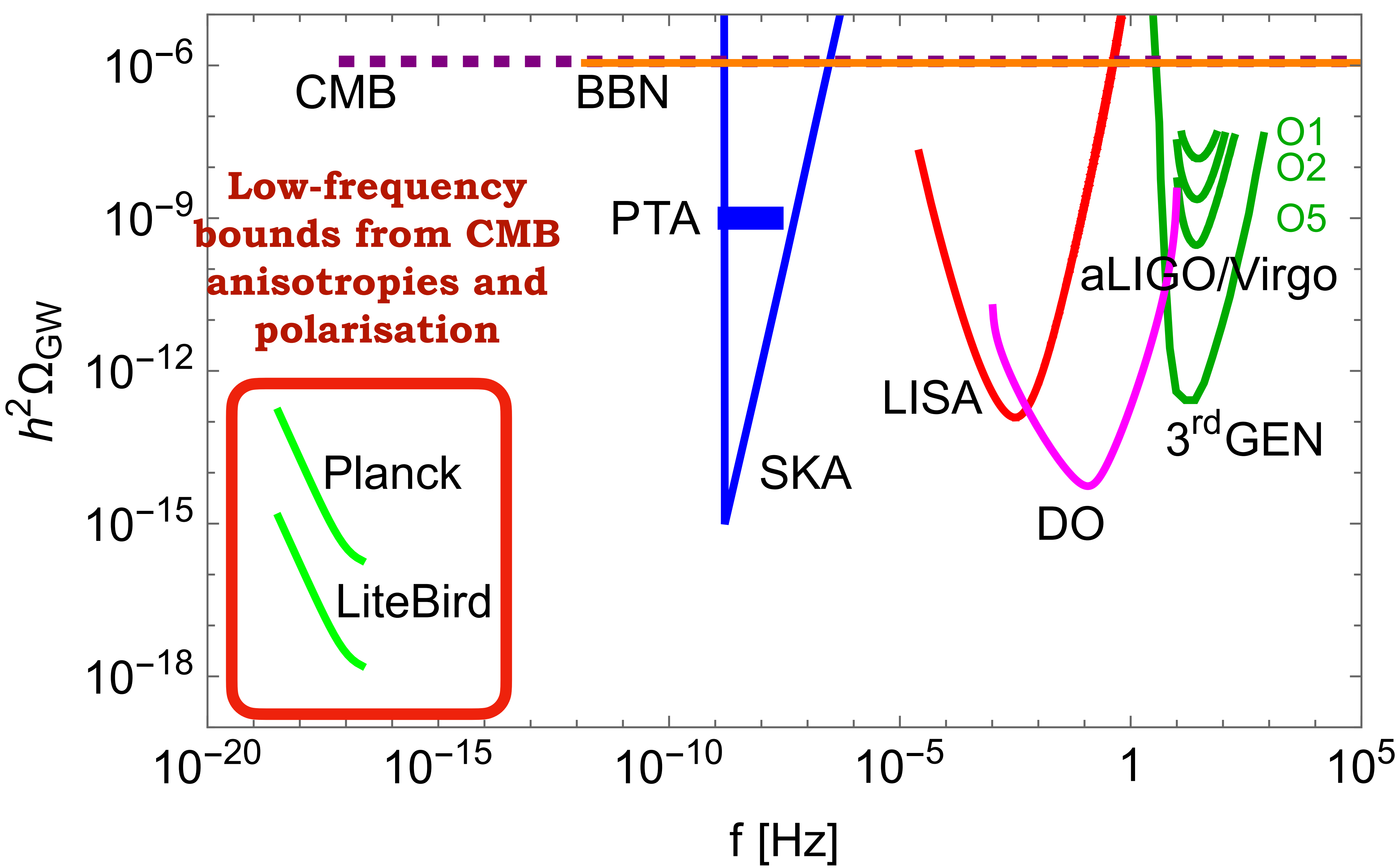

Cosmic microwave background

frequency range of detection: 10^{-18} Hz < f < 10^{-16} HZ

- temperature anisotropy: limit by Planck

$$\frac{\delta T}{T} = -\int_{t_{\rm dec}}^{t_0} \dot{h}_{ij}\, n^i n^j\, dt$$

$$P_h(k) = A_t(k_0)\,(k\,\eta_0)^{n_t} \qquad C_{\ell,T}^{\Theta\Theta} \simeq \frac{\sqrt{\pi}}{3} A_t(k_0)\,\frac{\ell(\ell+2)!}{(\ell-2)!}\,\frac{\Gamma\left[\frac{7-n_t}{2}\right]\Gamma\left[\ell+\frac{n_t}{2}\right]}{\Gamma\left[4-\frac{n_t}{2}\right]\Gamma\left[\ell+7-\frac{n_t}{2}\right]}$$

$$\propto \ \ell^{n_t-2} \qquad \text{for} \quad 1 \ll \ell \lesssim 60$$

- polarisation: BB spectrum measured by BICEP and Planck generated at photon decoupling time, from Thomson scattering of electrons by a quadrupole temperature anisotropy in the photons

polarisation patterns

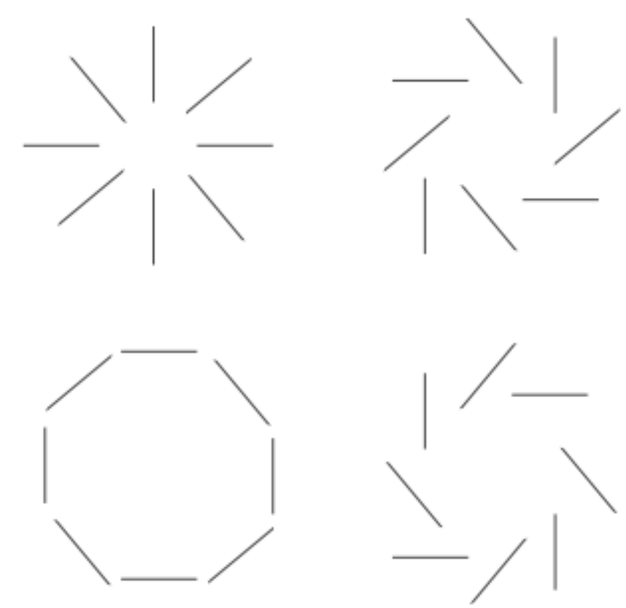

E mode B mode

generated by primordial scalar and tensor perturbations

generated only by primordial tensor perturbations or by foregrounds

Cosmic microwave background

Galloni et al: arXiv:2208.00188

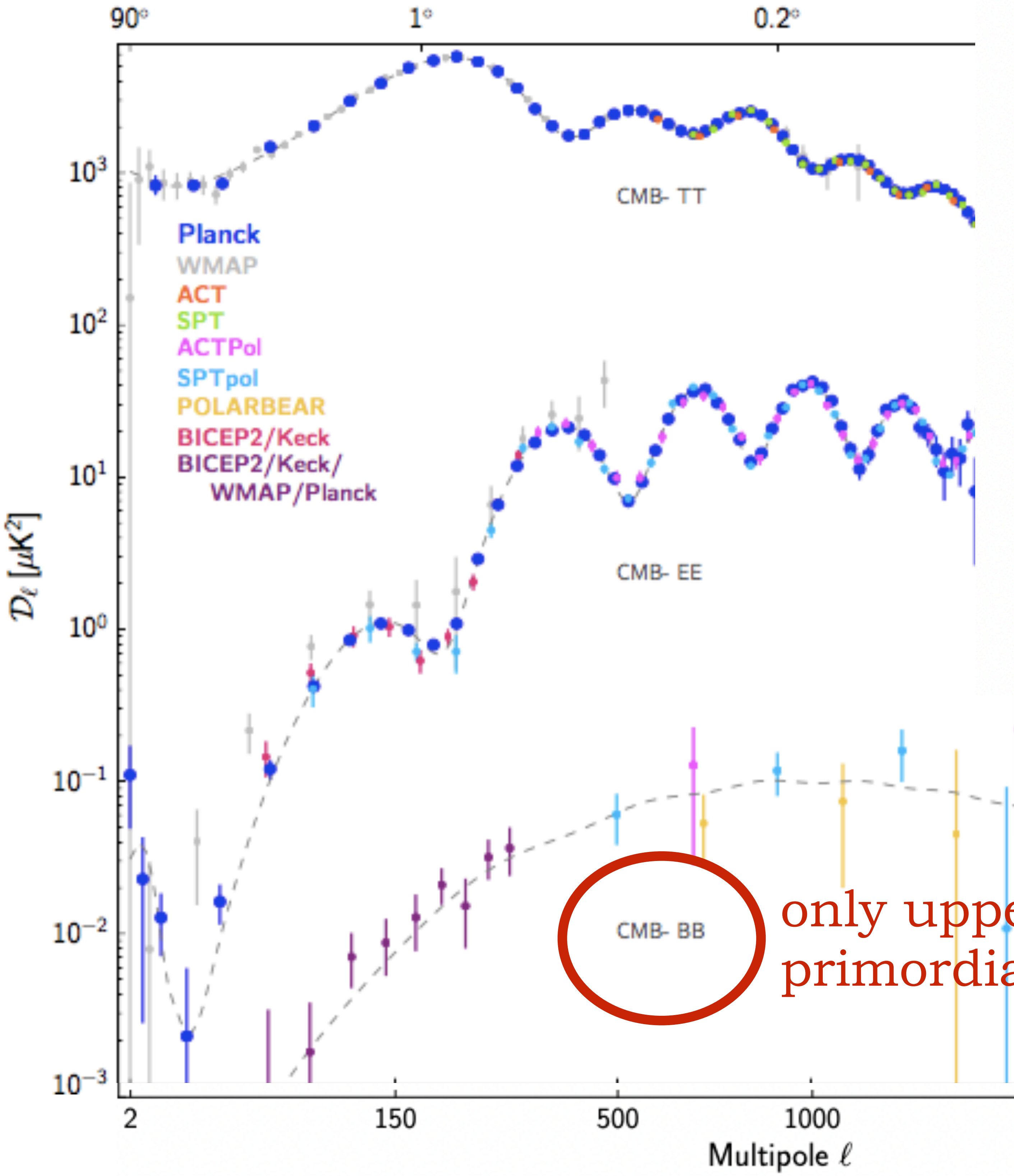

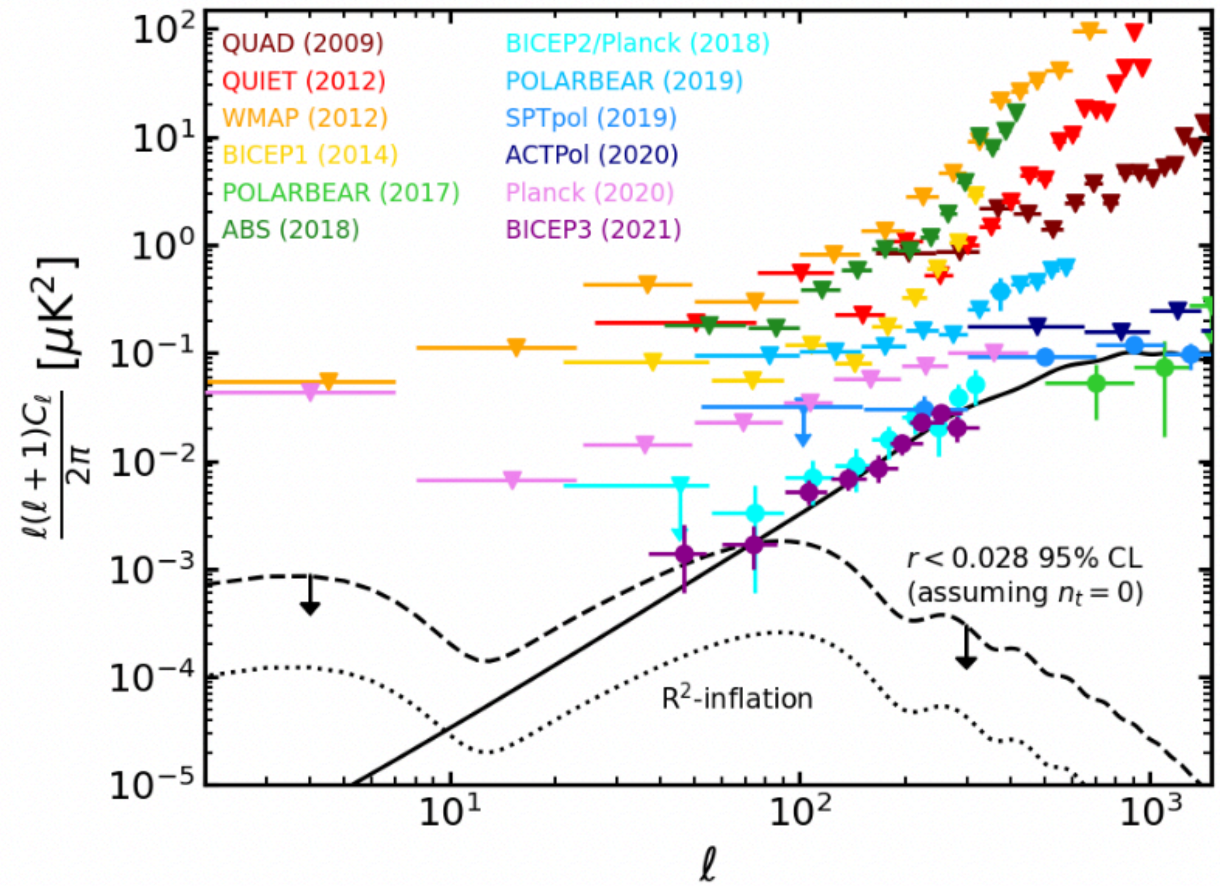

only upper bounds on the primordial component for now

Planck collaboration: arXiv:1807.06205

Cosmic microwave background

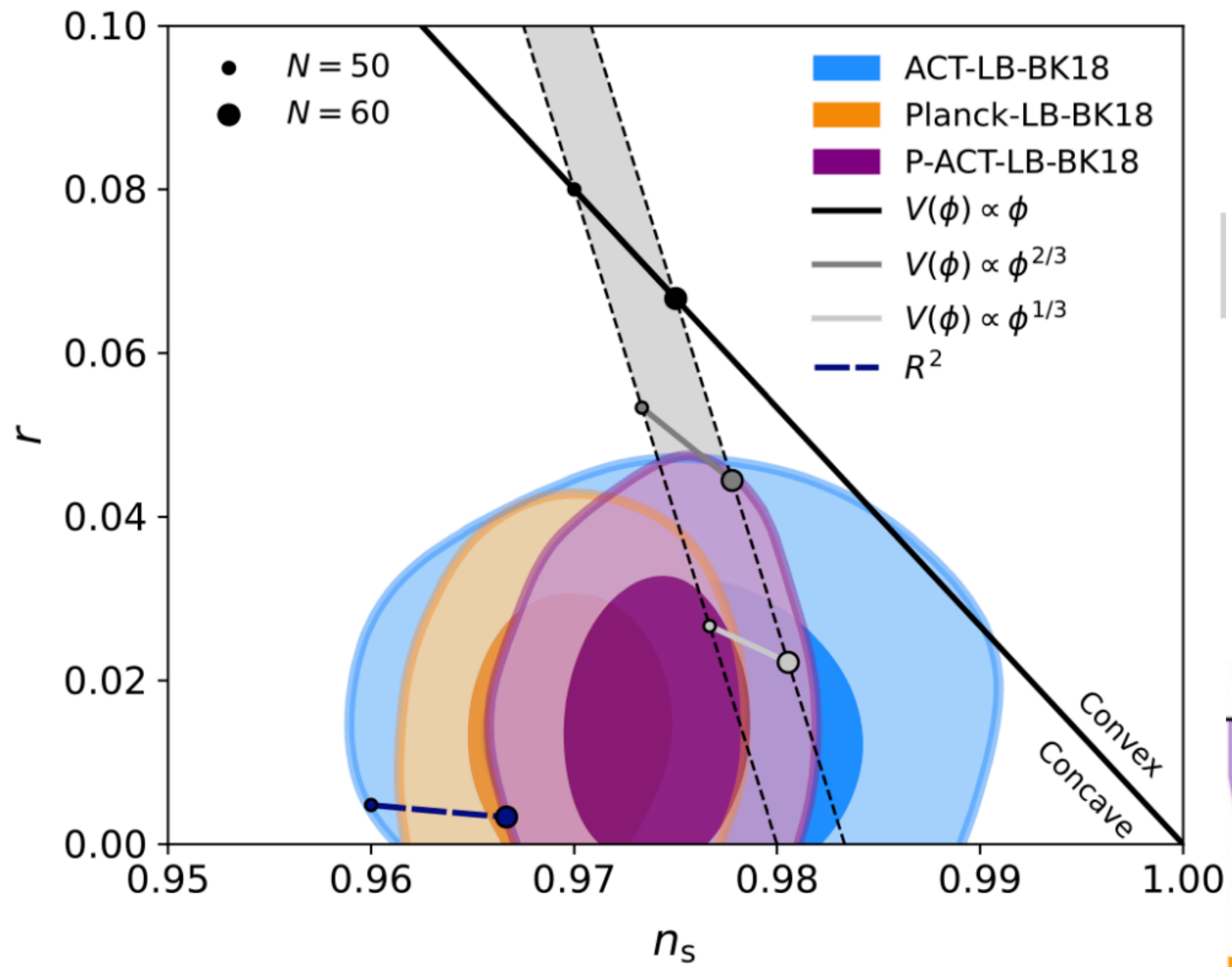

Calabrese et al, arXiv:2503.14454

This constraint is usually represented in the context of Inflation as a bound on the tensor-to-scalar ratio

A. Challinor, https://indico-dpt.unige.ch/event/1/contributions/31/attachments/16/19/Challinor_Geneva2025.pdf

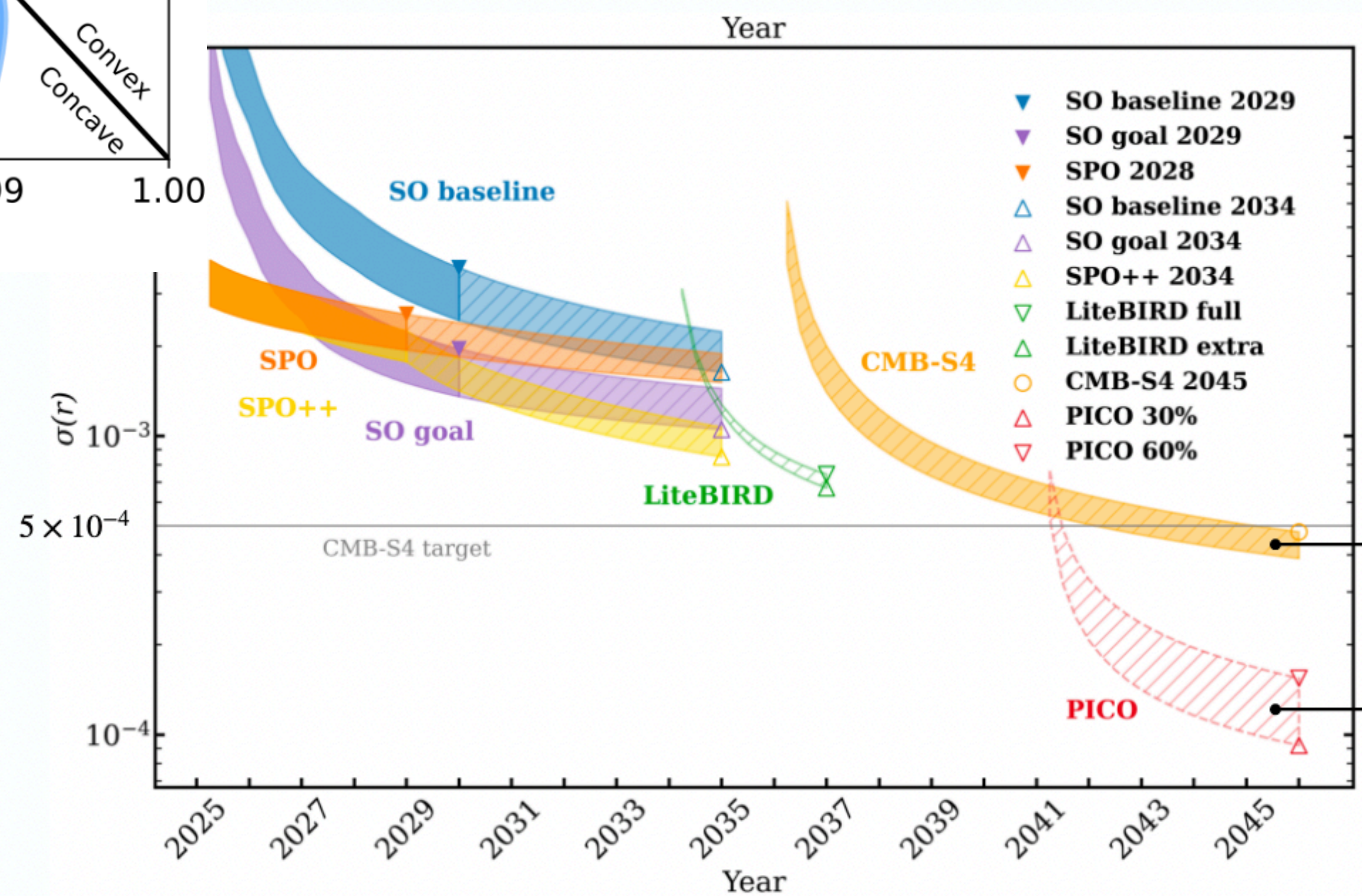

Projected sensitivity on the tensor-to-scalar ratio

What is/will be known about the SGWB

Present and future GW obsevatories:
LIGO VIRGO KAGRA

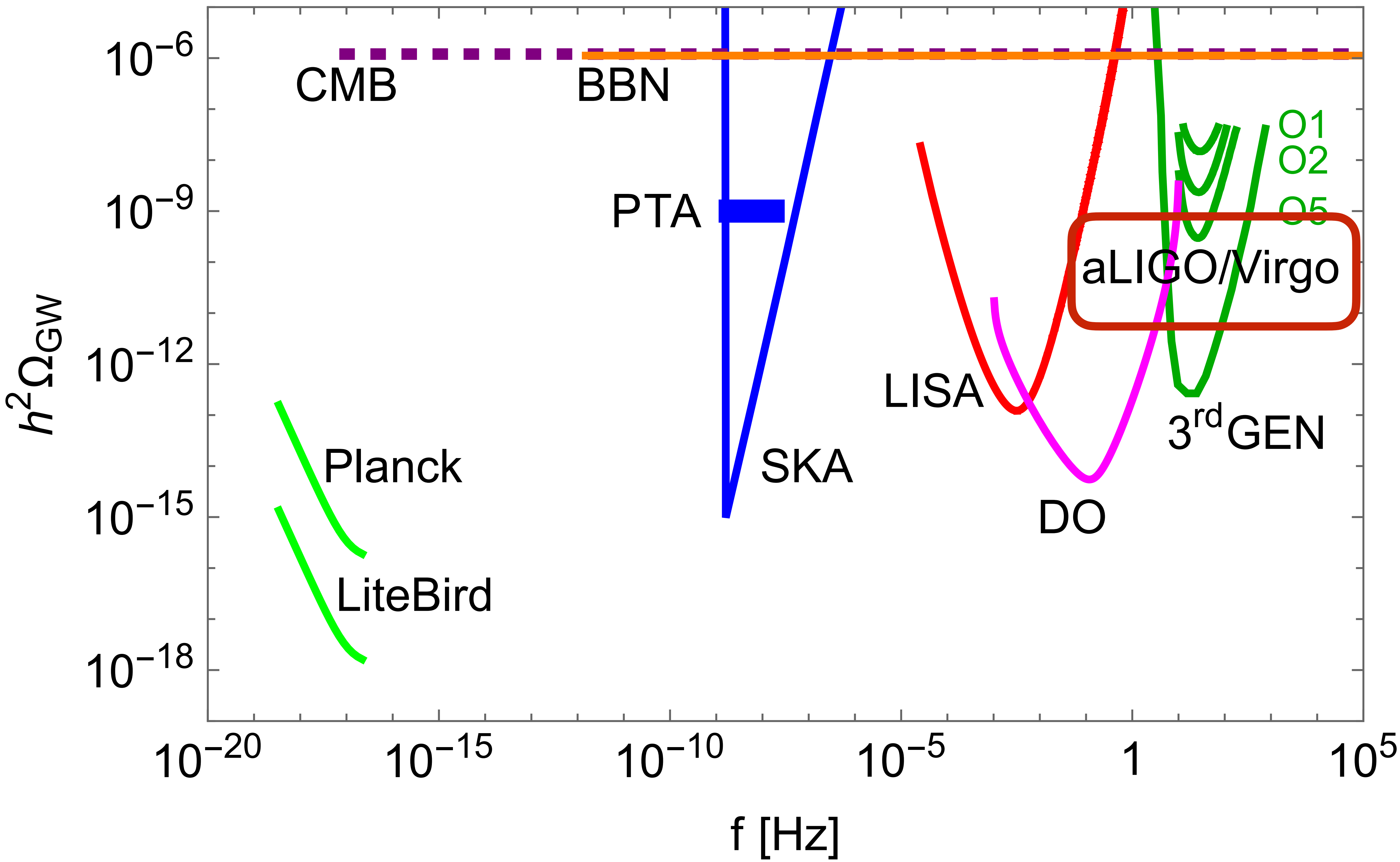

Earth-based interferometers

LIGO/Virgo (operating)

arm length L = 4 km

frequency range of detection:
10 Hz < f < 5kHZ

3rd generation ET, CE (future)

arm length L ~15-20 km

frequency range of detection:
1 Hz < f < 10^4 HZ

factor 20 improvement in sensitivity

DETECTION TARGETS:

- Black hole coalescing binaries of masses few to hundred solar masses (BHBs)
- Neutron Star and NS-BH binaries / SN explosions
- Stochastic GW background

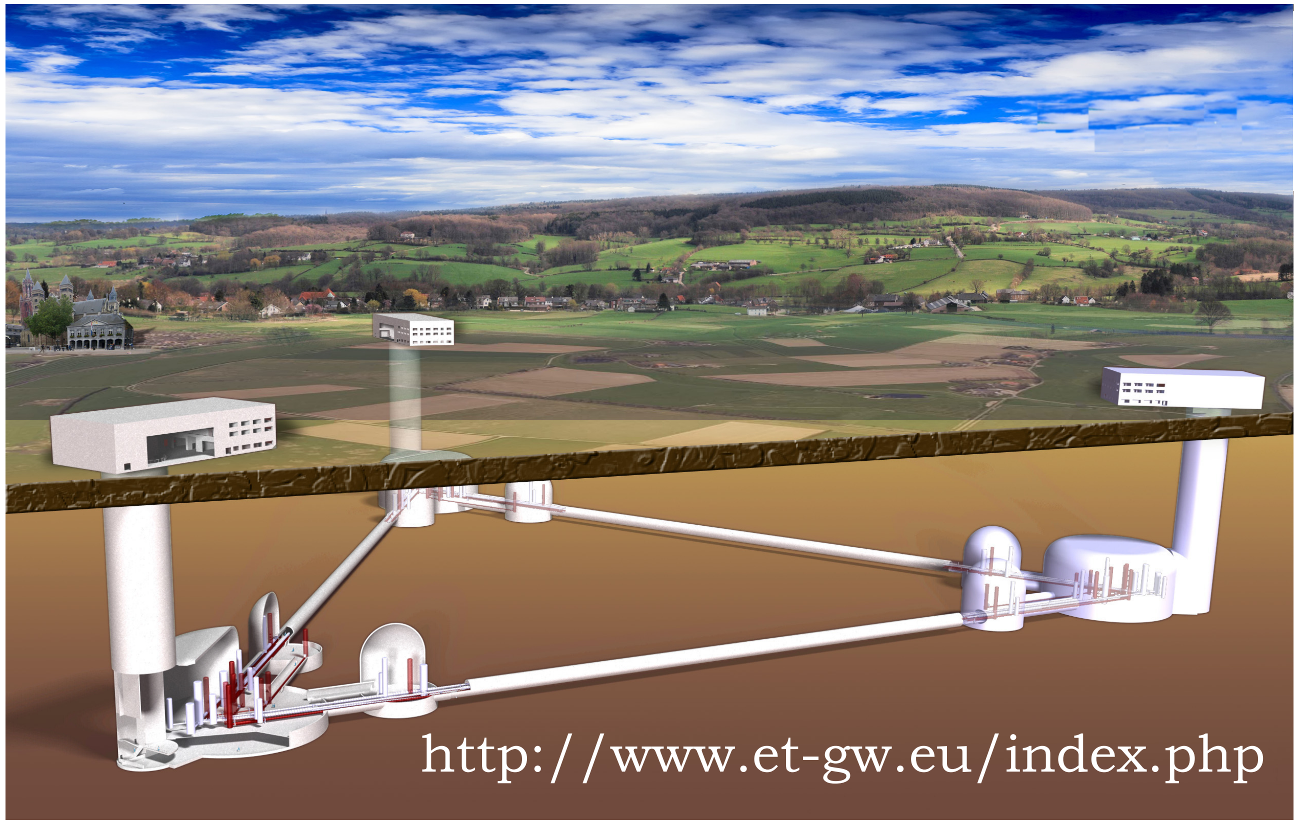

Earth-based interferometers

Candidate	$M(M_\odot)$	$\mathcal{M}(M_\odot)$	$m_1(M_\odot)$	$m_2(M_\odot)$	$\chi_{\rm eff}$	D_L(Gpc)	z	$M_f(M_\odot)$	χ_f	$\Delta\Omega(\deg^2)$	SNR
GW191103_012549	$20.0^{+3.7}_{-1.8}$	$8.34^{+0.66}_{-0.57}$	$11.8^{+6.2}_{-2.2}$	$7.9^{+1.7}_{-2.4}$	$0.21^{+0.16}_{-0.10}$	$0.99^{+0.50}_{-0.47}$	$0.20^{+0.09}_{-0.09}$	$19.0^{+3.8}_{-1.7}$	$0.75^{+0.06}_{-0.05}$	2500	$8.9^{+0.3}_{-0.5}$
GW191105_143521	$18.5^{+2.1}_{-1.3}$	$7.82^{+0.61}_{-0.45}$	$10.7^{+3.7}_{-1.6}$	$7.7^{+1.4}_{-1.9}$	$-0.02^{+0.13}_{-0.09}$	$1.15^{+0.43}_{-0.48}$	$0.23^{+0.07}_{-0.09}$	$17.6^{+2.1}_{-1.2}$	$0.67^{+0.04}_{-0.05}$	640	$9.7^{+0.3}_{-0.5}$
GW191109_010717	112^{+20}_{-16}	$47.5^{+9.6}_{-7.5}$	65^{+11}_{-11}	47^{+15}_{-13}	$-0.29^{+0.42}_{-0.31}$	$1.29^{+1.13}_{-0.65}$	$0.25^{+0.18}_{-0.12}$	107^{+18}_{-15}	$0.61^{+0.18}_{-0.19}$	1600	$17.3^{+0.5}_{-0.5}$
GW191113_071753	$34.5^{+10.5}_{-9.8}$	$10.7^{+1.1}_{-1.0}$	29^{+12}_{-14}	$5.9^{+4.4}_{-1.3}$	$0.00^{+0.37}_{-0.29}$	$1.37^{+1.15}_{-0.62}$	$0.26^{+0.18}_{-0.11}$	34^{+11}_{-10}	$0.45^{+0.33}_{-0.11}$	3600	$7.9^{+0.5}_{-1.1}$
GW191126_115259	$20.7^{+3.4}_{-2.0}$	$8.65^{+0.95}_{-0.71}$	$12.1^{+5.5}_{-2.2}$	$8.3^{+1.9}_{-2.4}$	$0.21^{+0.15}_{-0.11}$	$1.62^{+0.74}_{-0.74}$	$0.30^{+0.12}_{-0.13}$	$19.6^{+3.5}_{-2.0}$	$0.75^{+0.06}_{-0.05}$	1400	$8.3^{+0.2}_{-0.5}$
GW191127_050227	80^{+39}_{-22}	$29.9^{+11.7}_{-9.1}$	53^{+47}_{-20}	24^{+17}_{-14}	$0.18^{+0.34}_{-0.36}$	$3.4^{+3.1}_{-1.9}$	$0.57^{+0.40}_{-0.29}$	76^{+39}_{-21}	$0.75^{+0.13}_{-0.29}$	980	$9.2^{+0.7}_{-0.6}$
GW191129_134029	$17.5^{+2.4}_{-1.2}$	$7.31^{+0.43}_{-0.28}$	$10.7^{+4.1}_{-2.1}$	$6.7^{+1.5}_{-1.7}$	$0.06^{+0.16}_{-0.08}$	$0.79^{+0.26}_{-0.33}$	$0.16^{+0.05}_{-0.06}$	$16.8^{+2.5}_{-1.2}$	$0.69^{+0.03}_{-0.05}$	850	$13.1^{+0.2}_{-0.3}$
GW191204_110529	$47.1^{+9.1}_{-7.8}$	$19.8^{+3.6}_{-3.2}$	$27.3^{+10.8}_{-5.9}$	$19.2^{+5.5}_{-6.0}$	$0.05^{+0.25}_{-0.26}$	$1.9^{+1.7}_{-1.1}$	$0.34^{+0.25}_{-0.18}$	$45.0^{+8.7}_{-7.5}$	$0.71^{+0.11}_{-0.11}$	3400	$8.9^{+0.4}_{-0.6}$
GW191204_171526	$20.19^{+1.64}_{-0.95}$	$8.56^{+0.41}_{-0.28}$	$11.7^{+3.3}_{-1.7}$	$8.4^{+1.3}_{-1.7}$	$0.16^{+0.08}_{-0.05}$	$0.64^{+0.20}_{-0.26}$	$0.13^{+0.04}_{-0.05}$	$19.18^{+1.71}_{-0.93}$	$0.73^{+0.04}_{-0.03}$	310	$17.4^{+0.2}_{-0.3}$
GW191215_223052	$43.3^{+5.3}_{-4.3}$	$18.4^{+2.2}_{-1.7}$	$24.9^{+7.1}_{-4.1}$	$18.1^{+3.8}_{-4.1}$	$-0.04^{+0.17}_{-0.21}$	$1.93^{+0.89}_{-0.86}$	$0.35^{+0.13}_{-0.14}$	$41.4^{+5.1}_{-4.1}$	$0.68^{+0.07}_{-0.07}$	530	$11.2^{+0.3}_{-0.4}$
GW191216_213338	$19.80^{+2.70}_{-0.93}$	$8.33^{+0.22}_{-0.19}$	$12.1^{+4.6}_{-2.2}$	$7.7^{+1.6}_{-1.9}$	$0.11^{+0.13}_{-0.06}$	$0.34^{+0.12}_{-0.13}$	$0.07^{+0.02}_{-0.03}$	$18.87^{+2.81}_{-0.93}$	$0.70^{+0.03}_{-0.04}$	910	$18.6^{+0.2}_{-0.2}$
GW191219_163120	$32.3^{+2.2}_{-2.7}$	$4.31^{+0.12}_{-0.17}$	$31.1^{+2.2}_{-2.8}$	$1.17^{+0.07}_{-0.06}$	$0.00^{+0.07}_{-0.09}$	$0.55^{+0.24}_{-0.16}$	$0.11^{+0.05}_{-0.03}$	$32.2^{+2.2}_{-2.7}$	$0.14^{+0.06}_{-0.06}$	1500	$9.1^{+0.5}_{-0.8}$
GW191222_033537	79^{+16}_{-11}	$33.8^{+7.1}_{-5.0}$	$45.1^{+10.9}_{-8.0}$	$34.7^{+9.3}_{-10.5}$	$-0.04^{+0.20}_{-0.25}$	$3.0^{+1.7}_{-1.7}$	$0.51^{+0.23}_{-0.26}$	$75.5^{+15.3}_{-9.9}$	$0.67^{+0.08}_{-0.11}$	2000	$12.5^{+0.2}_{-0.3}$
GW191230_180458	86^{+19}_{-12}	$36.5^{+8.2}_{-5.6}$	$49.4^{+14.0}_{-9.6}$	37^{+11}_{-12}	$-0.05^{+0.26}_{-0.31}$	$4.3^{+2.1}_{-1.9}$	$0.69^{+0.26}_{-0.27}$	82^{+17}_{-11}	$0.68^{+0.11}_{-0.13}$	1100	$10.4^{+0.3}_{-0.4}$
GW200105_162426	$11.0^{+1.5}_{-1.4}$	$3.42^{+0.08}_{-0.08}$	$9.1^{+1.7}_{-1.7}$	$1.91^{+0.33}_{-0.24}$							
GW200112_155838	$63.9^{+5.7}_{-4.6}$	$27.4^{+2.6}_{-2.1}$	$35.6^{+6.7}_{-4.5}$	$28.3^{+4.4}_{-5.9}$							
GW200115_042309	$7.4^{+1.7}_{-1.7}$	$2.43^{+0.05}_{-0.07}$	$5.9^{+2.0}_{-2.5}$	$1.44^{+0.85}_{-0.28}$							
GW200128_022011	75^{+17}_{-12}	$32.0^{+7.5}_{-5.5}$	$42.2^{+11.6}_{-8.1}$	$32.6^{+9.5}_{-9.2}$							
GW200129_065458	$63.3^{+4.5}_{-3.4}$	$27.2^{+2.1}_{-2.3}$	$34.5^{+9.9}_{-3.1}$	$29.0^{+3.3}_{-9.3}$							
GW200202_154313	$17.58^{+1.78}_{-0.67}$	$7.49^{+0.24}_{-0.20}$	$10.1^{+3.5}_{-1.4}$	$7.3^{+1.1}_{-1.7}$							
GW200208_130117	$65.3^{+8.1}_{-6.8}$	$27.7^{+3.7}_{-3.1}$	$37.7^{+9.3}_{-6.2}$	$27.4^{+6.3}_{-7.3}$							
GW200208_222617	63^{+100}_{-26}	$19.8^{+10.5}_{-5.2}$	51^{+103}_{-30}	$12.3^{+9.2}_{-5.5}$							
GW200209_085452	$62.6^{+13.9}_{-9.4}$	$26.7^{+6.0}_{-4.2}$	$35.6^{+10.5}_{-6.8}$	$27.1^{+7.8}_{-7.8}$							
GW200210_092254	$27.0^{+7.1}_{-4.3}$	$6.56^{+0.38}_{-0.40}$	$24.1^{+7.5}_{-4.6}$	$2.83^{+0.47}_{-0.42}$							
GW200216_220804	81^{+20}_{-14}	$32.9^{+9.3}_{-8.5}$	51^{+22}_{-13}	30^{+14}_{-16}							
GW200219_094415	$65.0^{+12.6}_{-8.2}$	$27.6^{+5.6}_{-3.8}$	$37.5^{+10.1}_{-6.9}$	$27.9^{+7.4}_{-8.4}$							
GW200220_061928	148^{+55}_{-33}	62^{+23}_{-15}	87^{+40}_{-23}	61^{+26}_{-25}							
GW200220_124850	67^{+17}_{-12}	$28.2^{+7.3}_{-5.1}$	$38.9^{+14.1}_{-8.6}$	$27.9^{+9.2}_{-9.0}$							
GW200224_222234	$72.3^{+7.2}_{-5.3}$	$31.1^{+3.3}_{-2.7}$	$40.0^{+6.7}_{-4.5}$	$32.7^{+4.8}_{-7.2}$							
GW200225_060421	$33.5^{+3.6}_{-3.0}$	$14.2^{+1.5}_{-1.4}$	$19.3^{+5.0}_{-3.0}$	$14.0^{+2.8}_{-3.5}$							
GW200302_015811	$57.8^{+9.6}_{-6.9}$	$23.4^{+4.7}_{-3.0}$	$37.8^{+8.7}_{-8.5}$	$20.0^{+8.1}_{-5.7}$							
GW200306_093714	$43.9^{+11.8}_{-7.5}$	$17.5^{+3.5}_{-3.0}$	$28.3^{+17.1}_{-7.7}$	$14.8^{+6.5}_{-6.4}$							
GW200308_173609*	92^{+169}_{-48}	34^{+44}_{-18}	60^{+166}_{-29}	24^{+36}_{-13}							
GW200311_115853	$61.9^{+5.3}_{-4.2}$	$26.6^{+2.4}_{-2.0}$	$34.2^{+6.4}_{-3.8}$	$27.7^{+4.1}_{-5.9}$							
GW200316_215756	$21.2^{+7.2}_{-2.0}$	$8.75^{+0.62}_{-0.55}$	$13.1^{+10.2}_{-2.9}$	$7.8^{+2.0}_{-2.9}$							
GW200322_091133*	50^{+132}_{-22}	$15.0^{+29.5}_{-4.0}$	38^{+130}_{-22}	$11.3^{+24.3}_{-6.0}$							

Individually resolved BHBs, NSBs, NS-BH

Last catalogue GWTC-3:

90 binary mergers detected, including NS-BH and NS-NS mergers

LVK Collaboration: arXiv:2111.03606

Earth-based interferometers

Stochastic GW background: for now, only upper bounds

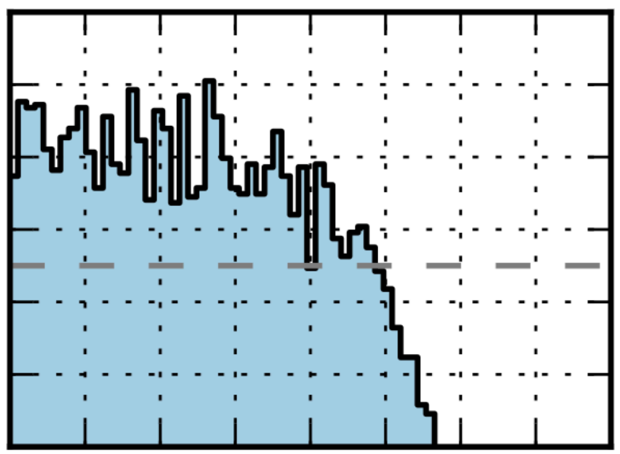

Upper bound on generic

$$\Omega_{\mathrm{GW}}(f) = \Omega_{\mathrm{ref}} \left(\frac{f}{25\,\mathrm{Hz}} \right)^{\alpha}$$

Most probably no cosmological SGWB detection by LVK, masked by astrophysical foreground detection expected for ~2030

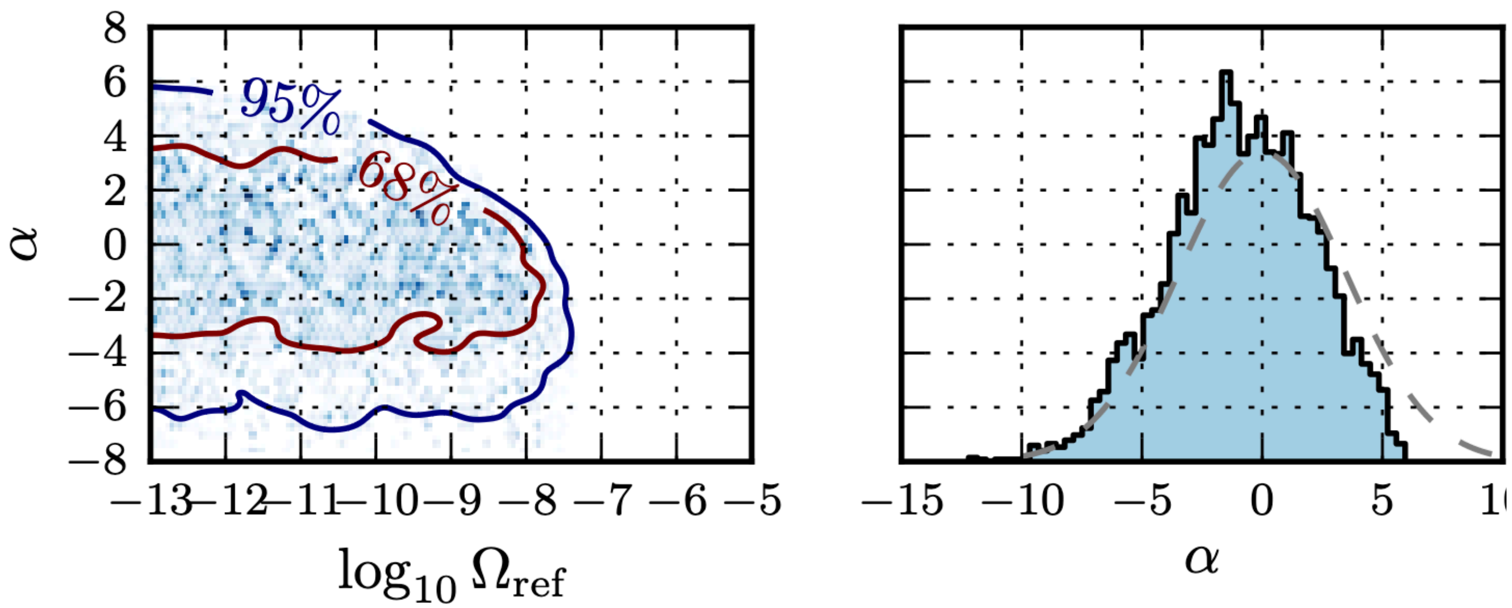

SGWB from BHBs and NSBs

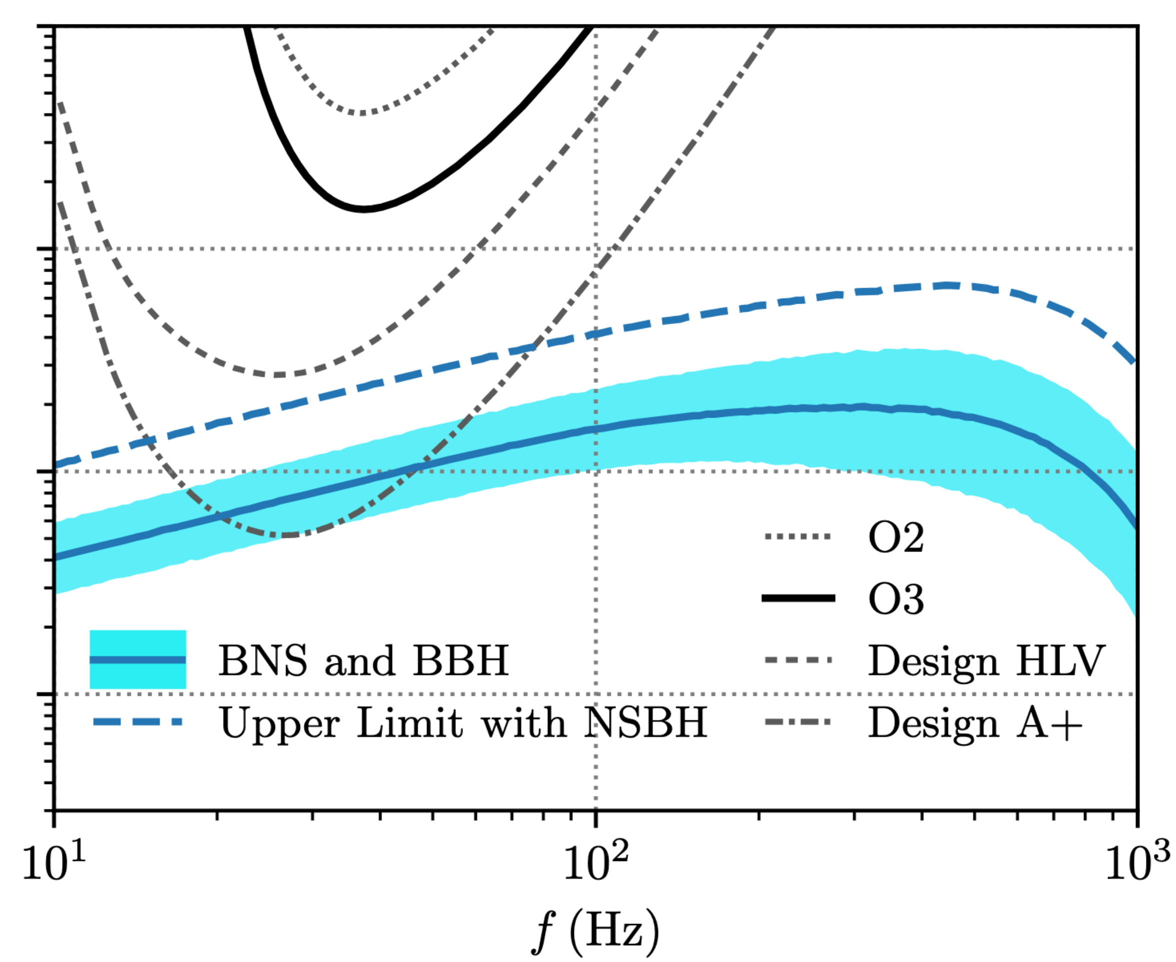

Detection via cross-correlation of signals from different detectors

LVK Collaborations, arXiv:2101.12130

What is/will be known about the SGWB

Present and future GW observatories: LISA

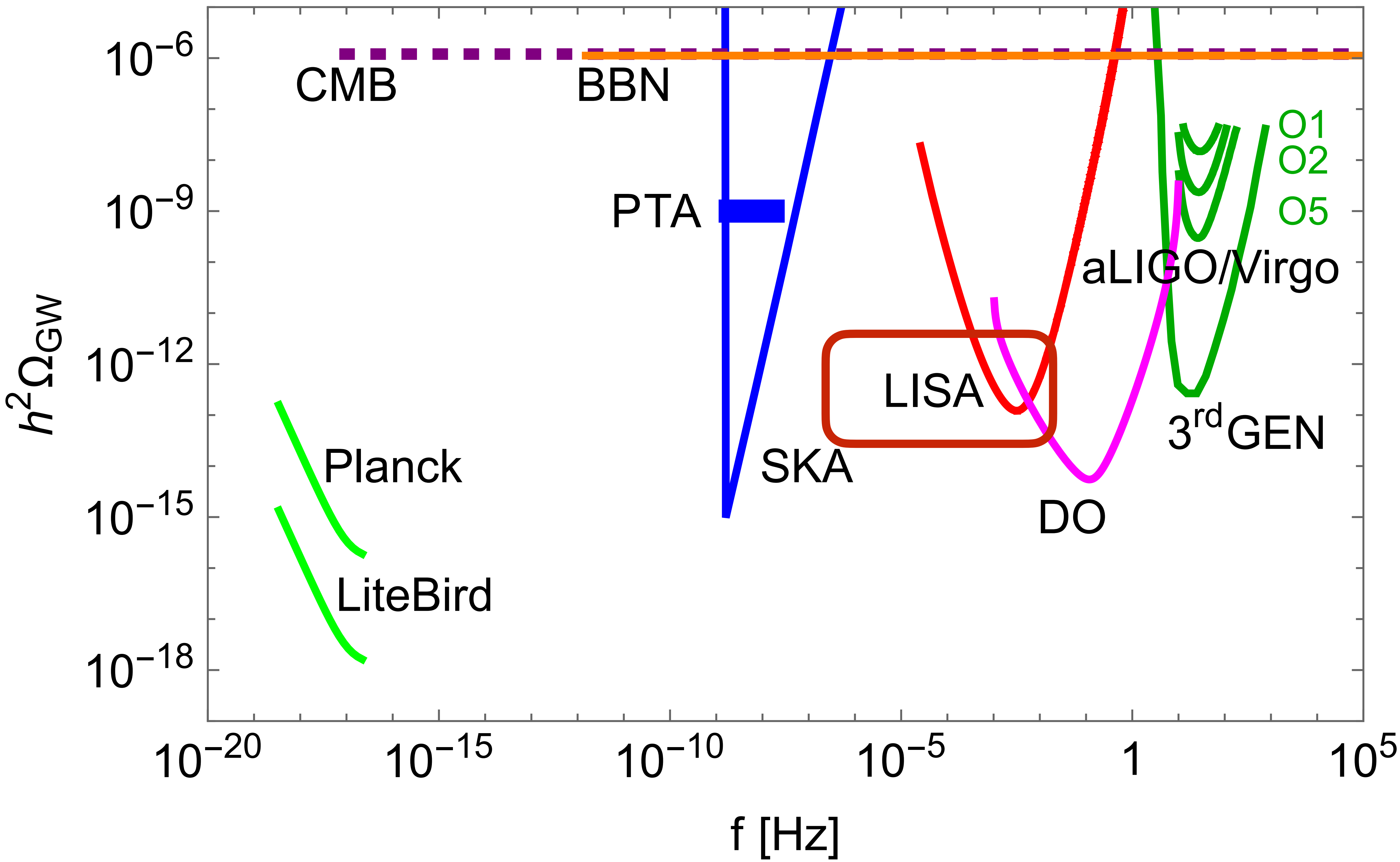

Space-based interferometers: LISA

LISA: Laser Interferometer Space Antenna

- no seismic noise
- much longer arms than on Earth

frequency range of detection:

$$10^{-4}\,\mathrm{Hz} < f < 1\,\mathrm{Hz}$$

- Launch in ~2035
- two masses in free fall per spacecraft
- 2.5 million km arms
- picometer displacement of masses

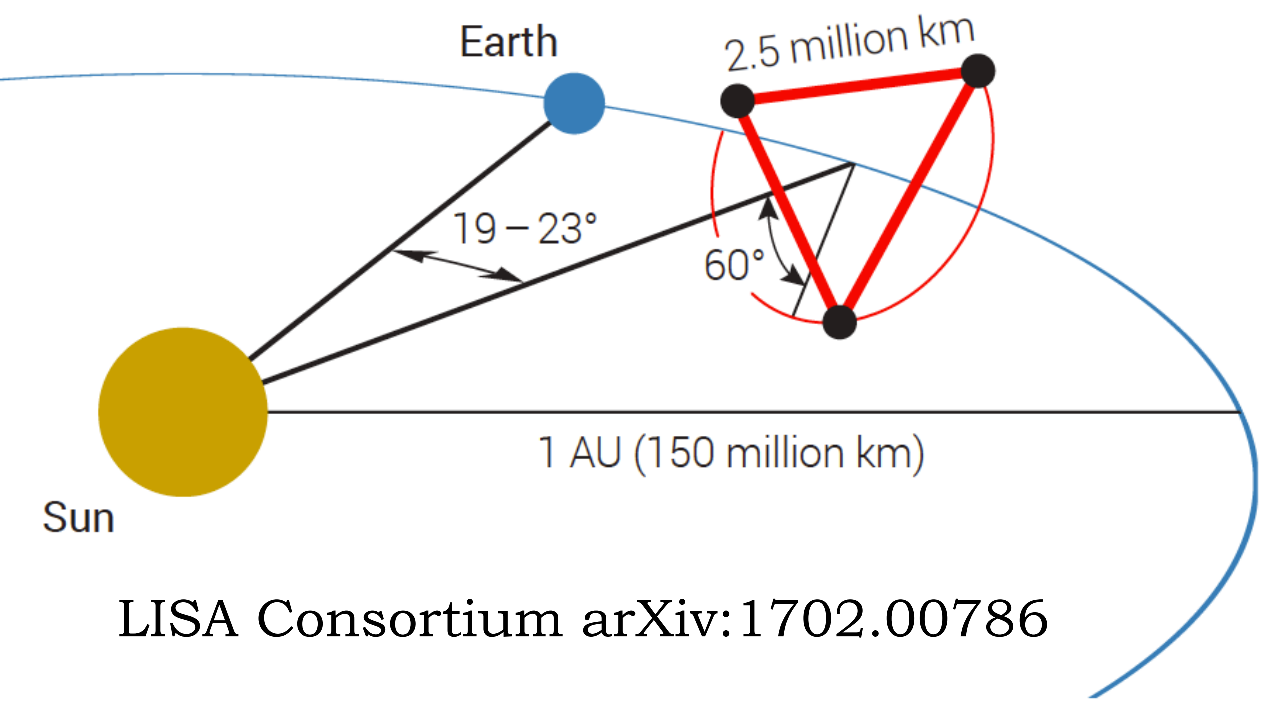

LISA Consortium arXiv:1702.00786

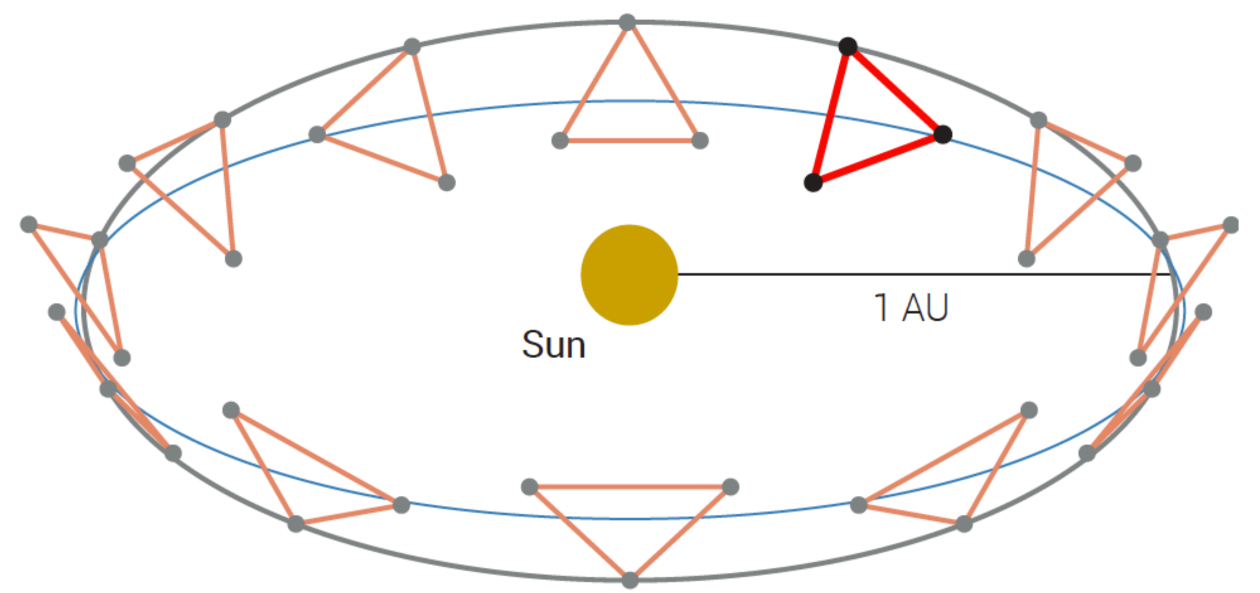

Space-based interferometers: LISA

DETECTION TARGETS:

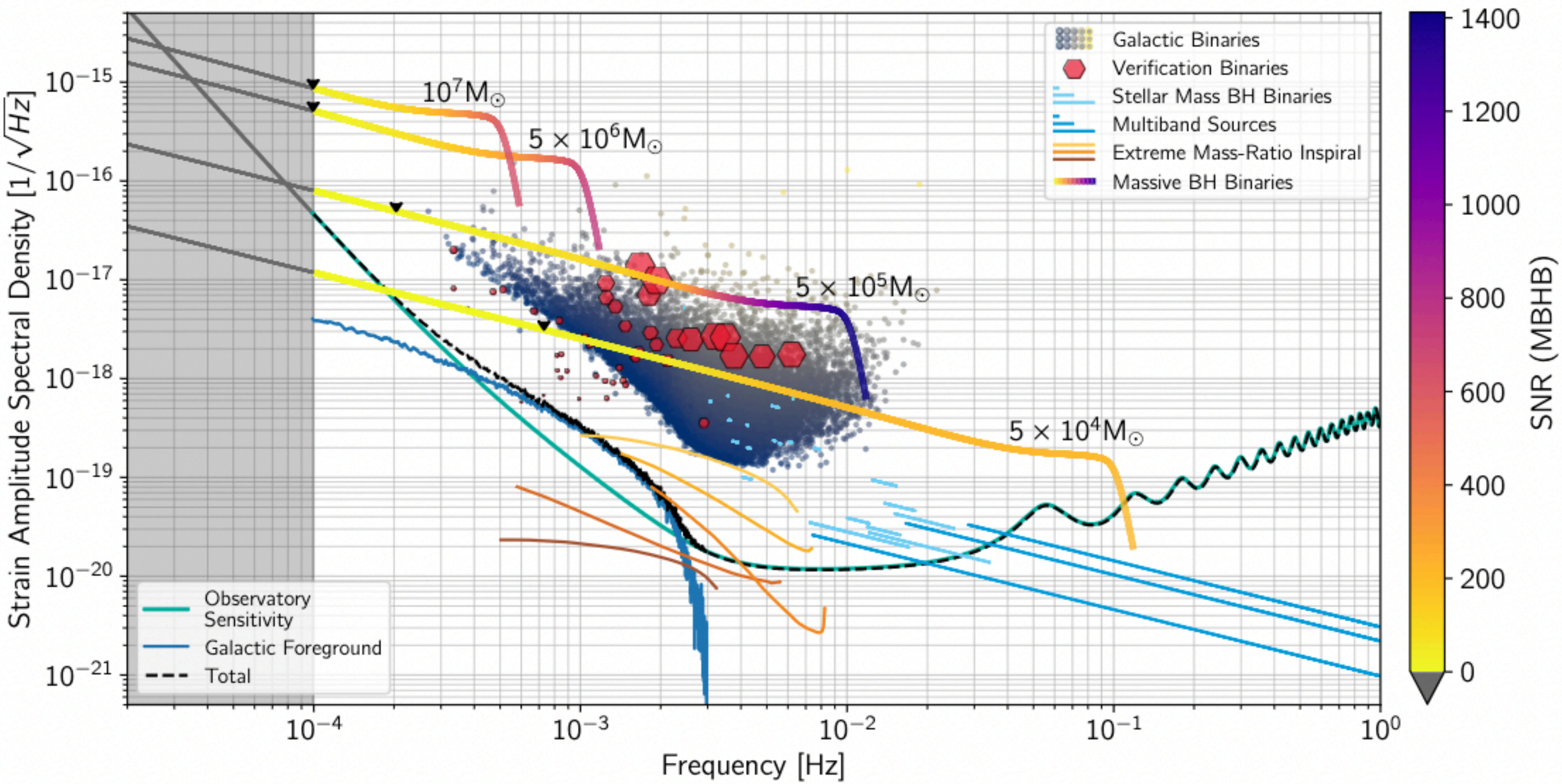

M. Colpi et al, arXiv:2402.07571 - LISA Red Book

Space-based interferometers: LISA

Stochastic GW background

- Confusion noise from the binaries in the Galaxy (mainly WD binaries)
- Confusion noise from extra-galactic binaries (WD binaries and BHBs)
- Candidates from the early universe, in particular at the EW scale

Detecting a SGWB with LISA is challenging: no cross-correlation, need to assume knowledge of the noise (possibility of null channels)

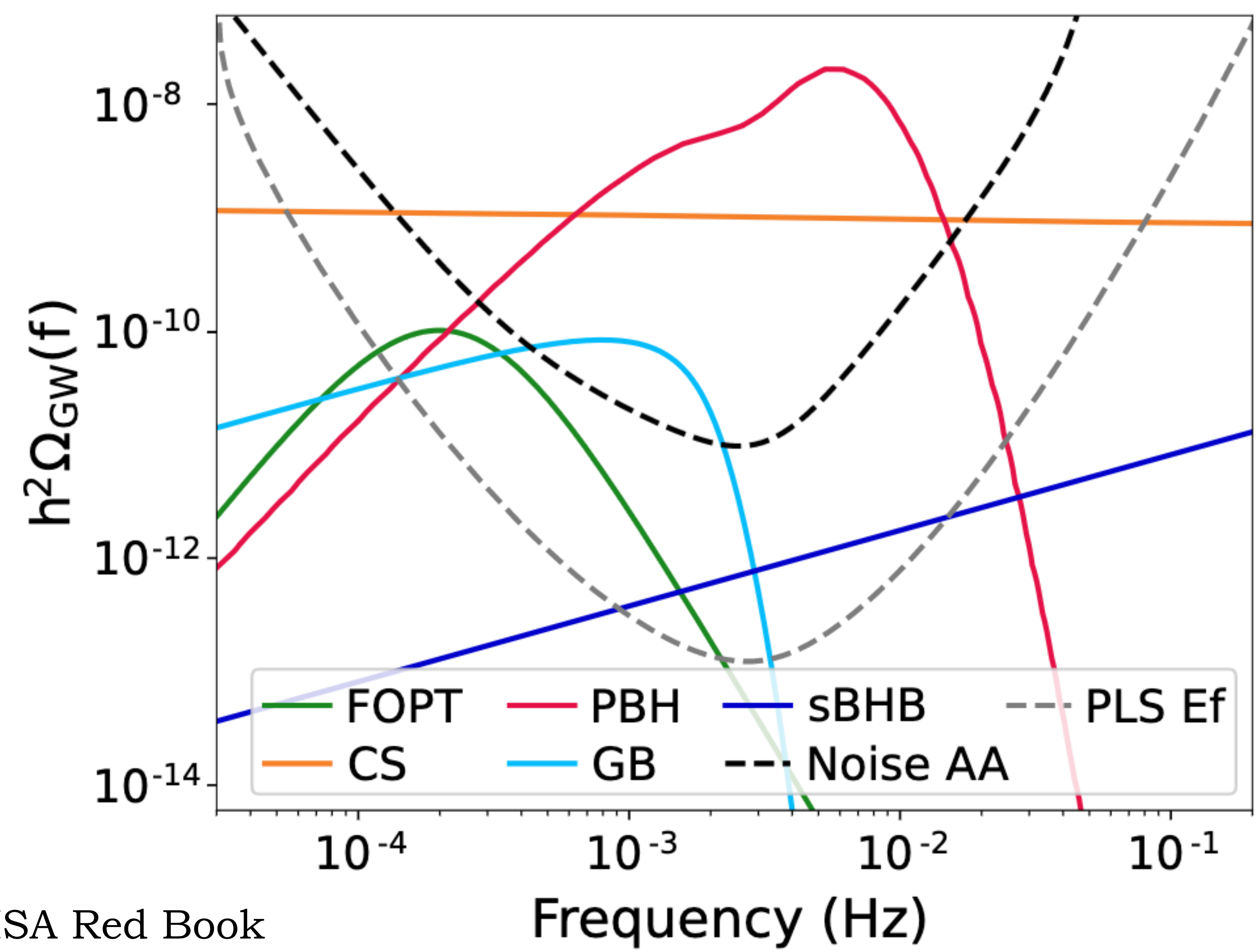

M. Colpi et al, arXiv:2402.07571 - LISA Red Book

What is/will be known about the SGWB

Present and future GW observatories:
Pulsar Timing Arrays

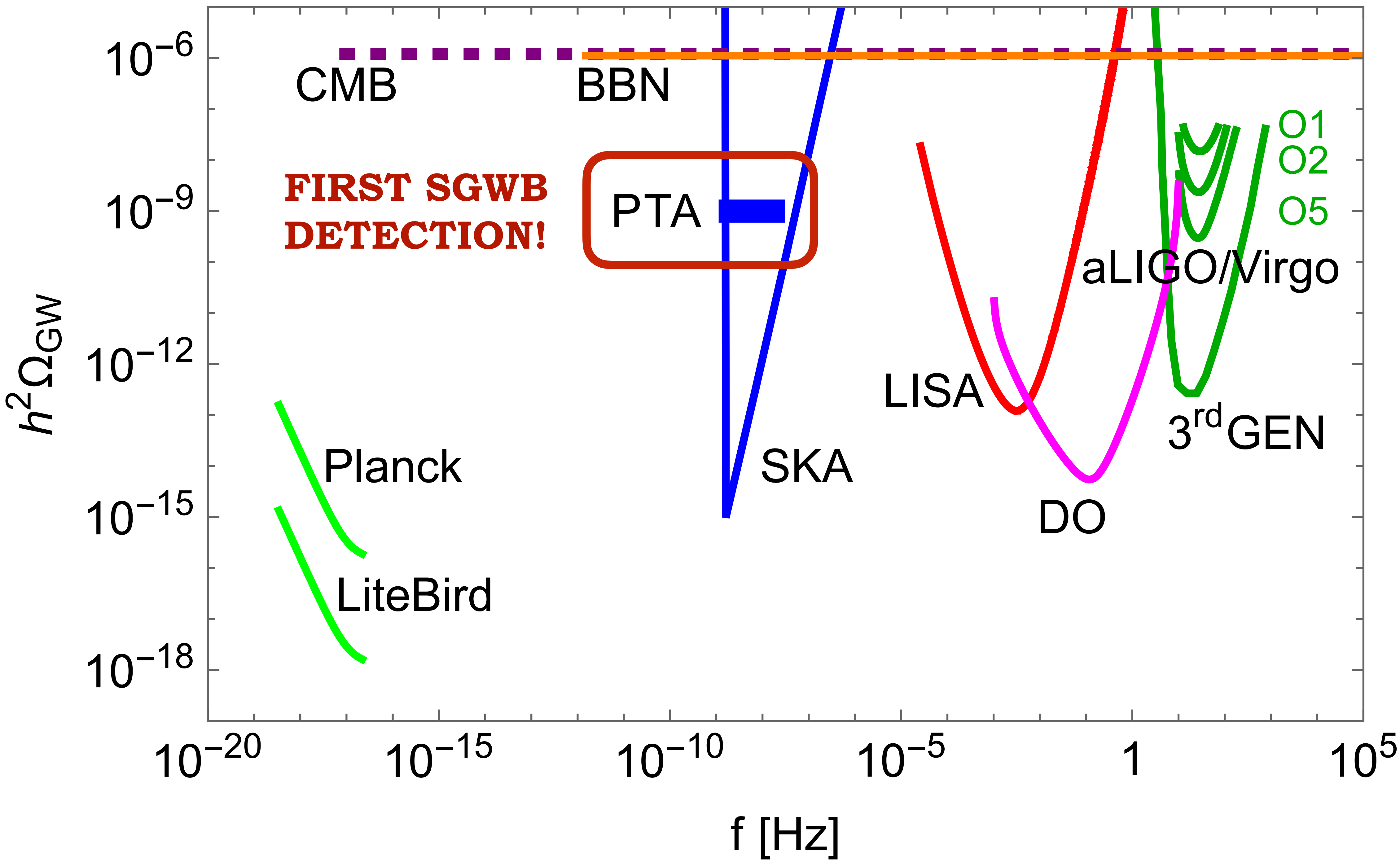

Pulsar timing arrays

CPTA, EPTA, NANOGrav, PPTA -> IPTA

frequency range of detection: 10^{-9} Hz < f < 10^{-7} HZ

- rotating, magnetised neutron stars emitting periodic radio-frequency EM pulses -> can be used as clocks in the sky
- the radio pulses are emitted at very regular time intervals, but their arrival times can be altered by a GW passing between the pulsar and the Earth
- First a timing model of the pulsar is constructed, which is then compared to observations to infer the *timing residuals* where the GW effect is looked for

DETECTION TARGETS:

Individual emission and stochastic background from inspiralling Super Massive Black Hole Binaries (SMBHBs) with masses ~10^9 $M_\odot$ at the centre of galaxies

Pulsar timing arrays

Principle of the measurement: gravitational redshift caused by gravitational waves emitted by far-away sources and travelling through spacetime between the pulsars and the Earth

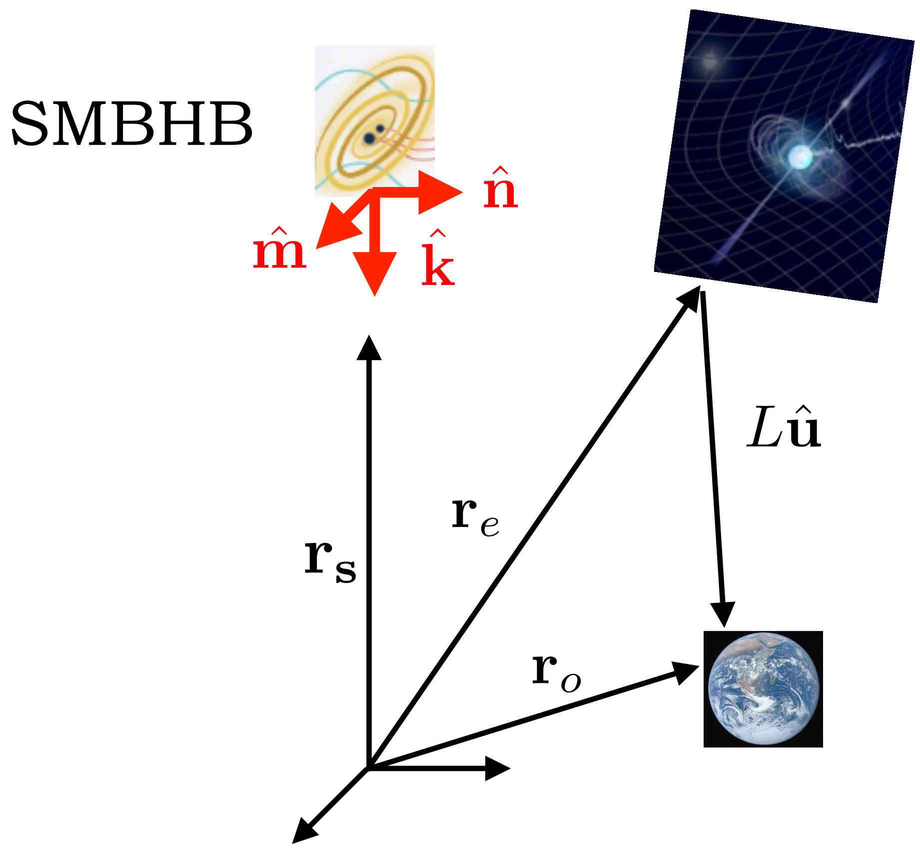

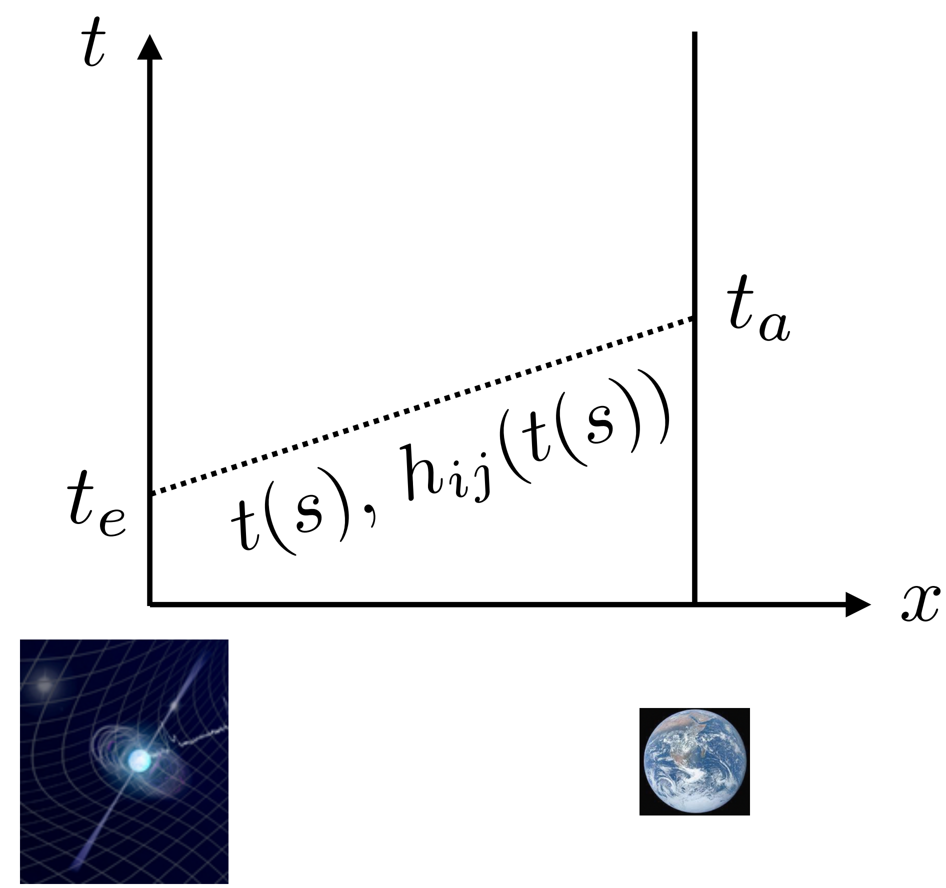

Photon from pulsar:

$$dt = \pm\sqrt{(\delta_{ij} + h_{ij})\mathrm{d}x^i\mathrm{d}x^j} \qquad t_a - t_e = L + \frac{1}{2}\hat{u}^i\hat{u}^j\int_0^L \mathrm{d}s\, h_{ij}(t_e + s, \mathbf{r_e} + s\hat{\mathbf{u}})$$

Effect of the metric perturbation on a single beam:
not measurable unless one knows the reference quantities

Pulsar timing arrays

Principle of the measurement: compare with the next pulse

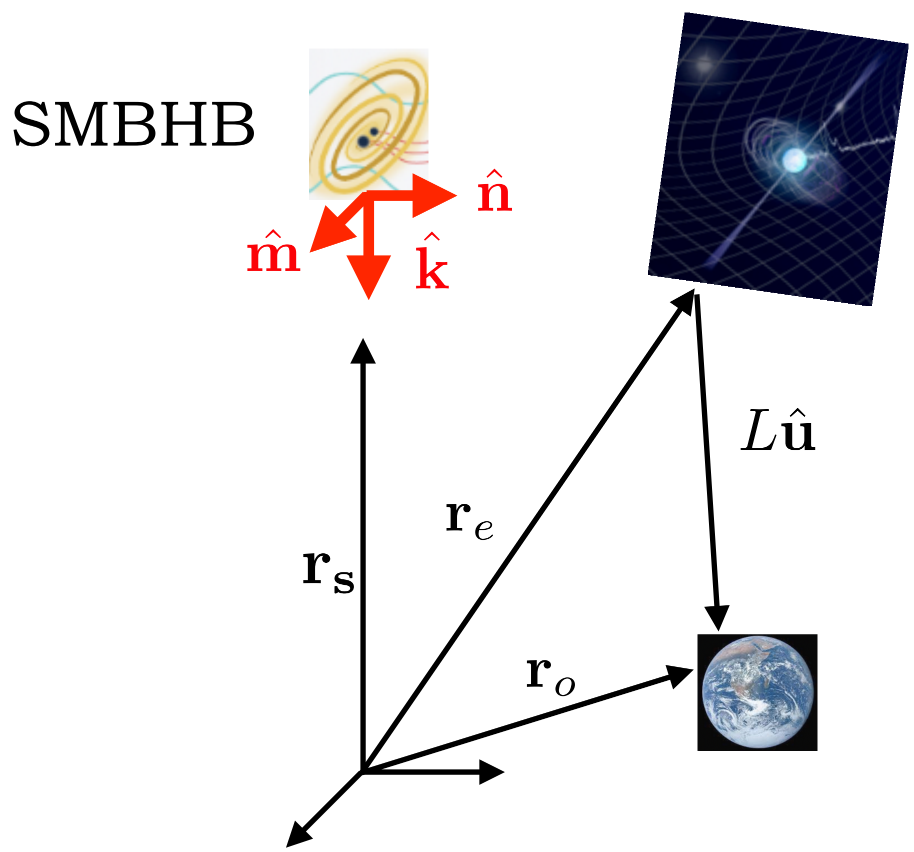

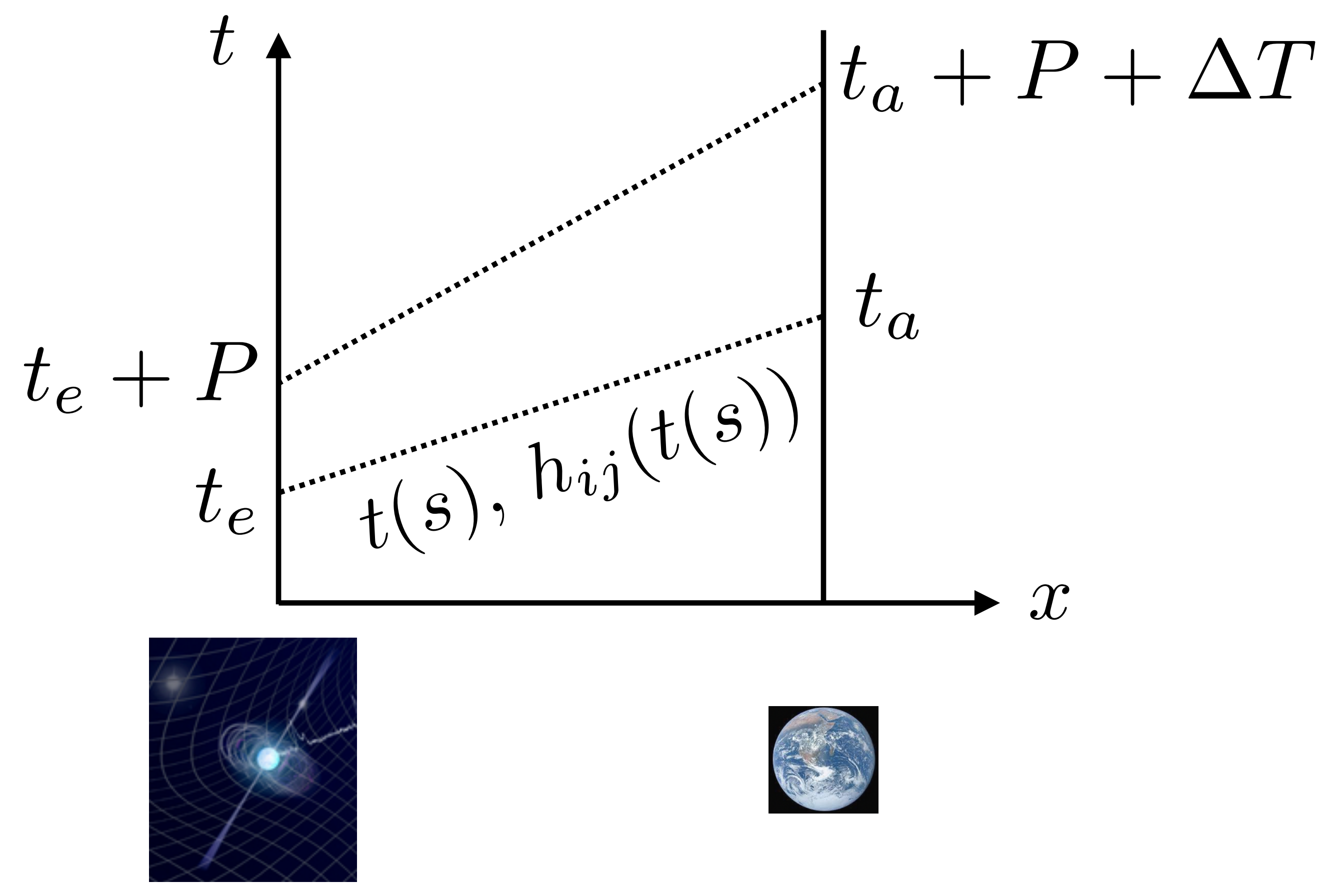

$$\Delta T = \frac{1}{2}\hat{u}^i\hat{u}^j \int_0^L \mathrm{d}s\, [h_{ij}(t_e + P + s, \mathbf{r_e} + s\hat{\mathbf{u}}) - h_{ij}(t_e + s, \mathbf{r_e} + s\hat{\mathbf{u}})]$$

This effect is present only because the gravitational wave is time-dependent

"Gravitational Waves Vol 2",
M. Maggiore, Oxford University Press 2018

S. Taylor, arXiv:2105.13270

Pulsar timing arrays

Principle of the measurement: compare with the next pulse

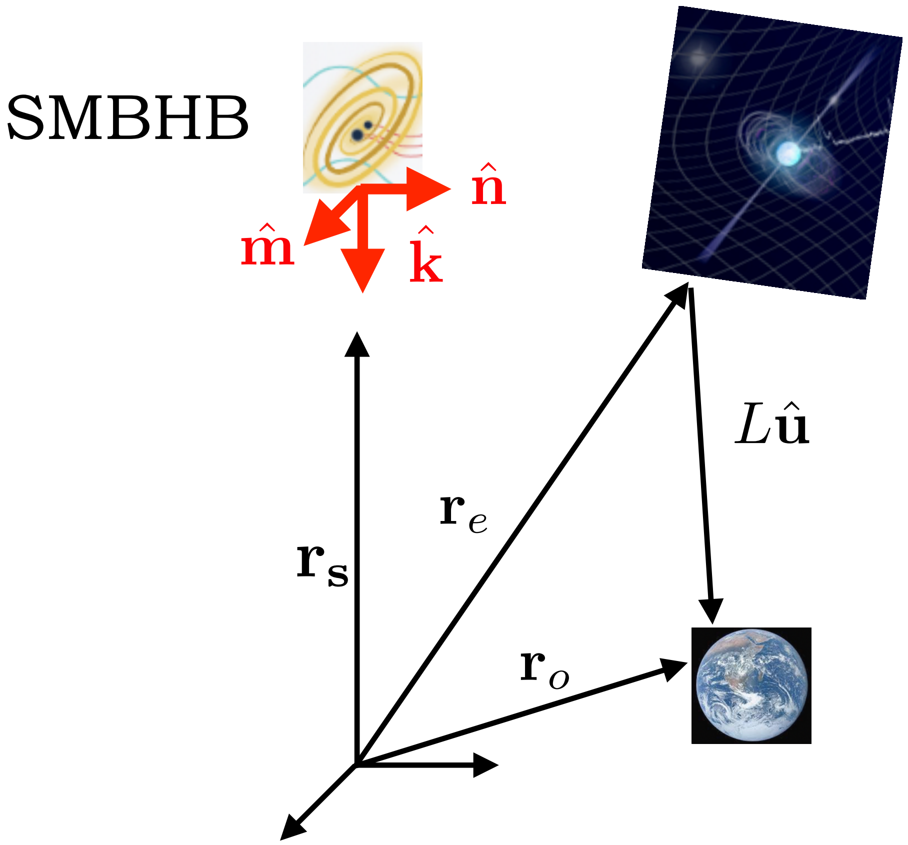

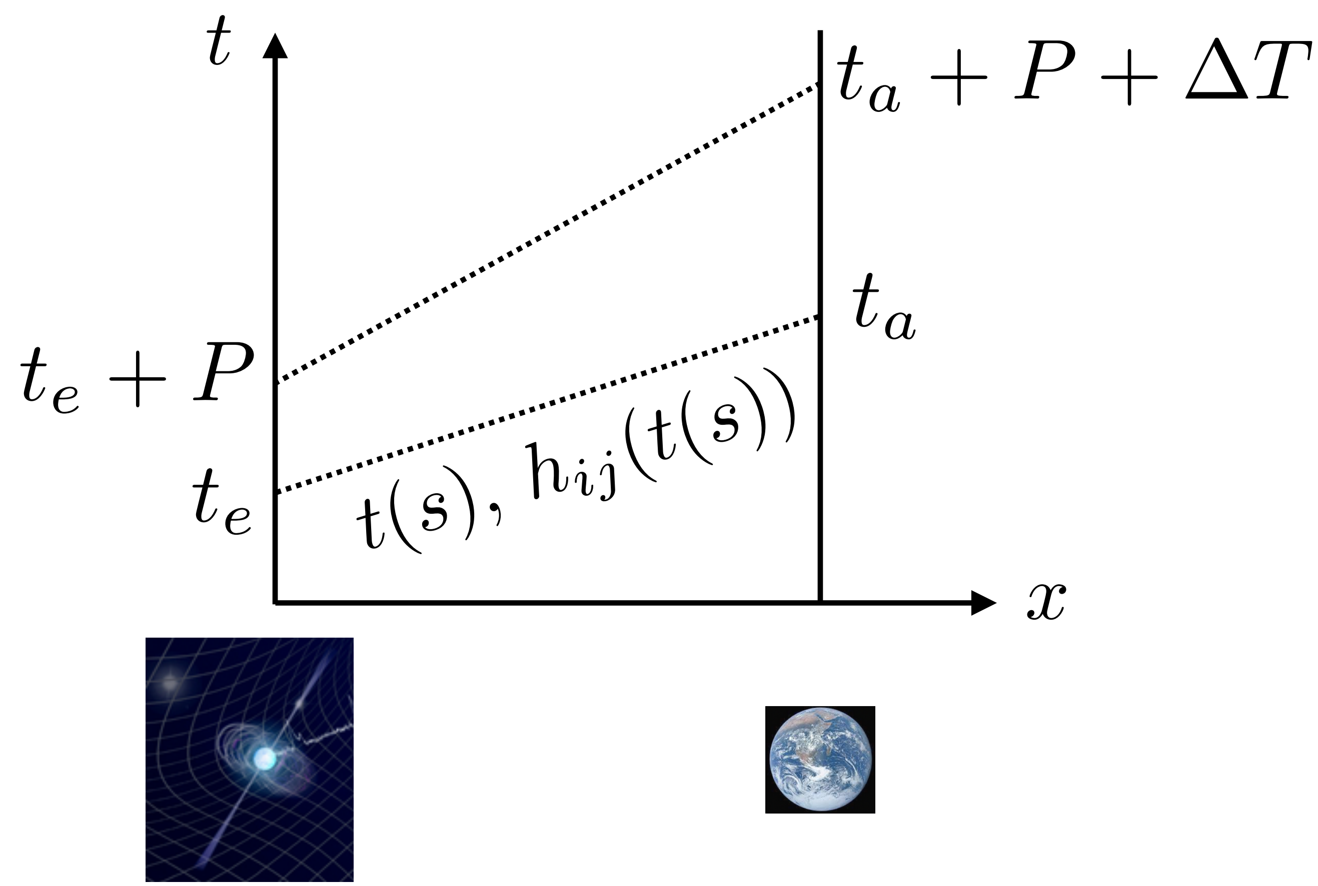

$$\Delta T = \frac{1}{2}\frac{\hat{u}^i\hat{u}^j}{1-\hat{\mathbf{k}}\cdot\hat{\mathbf{u}}}\int_{t_e-\hat{\mathbf{k}}\cdot\mathbf{r_e}}^{t_e+L-\hat{\mathbf{k}}\cdot\mathbf{r_e}-L\hat{\mathbf{k}}\cdot\mathbf{u}} \mathrm{d}X\,[h_{ij}(X+P)-h_{ij}(X)]$$

Wave propagating in k direction: $h_{ij}(X)$ with $X = t_e + s - \hat{\mathbf{k}}\cdot\mathbf{r_e} - s\,\hat{\mathbf{k}}\cdot\hat{\mathbf{u}}$

Pulsar timing arrays

Supposing the source is the inspiral of a super massive black hole binary: what is the typical scale of the time variation of the metric perturbation?

$$f(\tau) = \frac{1}{\pi}\left(\frac{5}{256}\right)^{3/8} \frac{1}{(G\,M_c)^{5/8}\,\tau^{3/8}} \simeq 10^{-8}\,\mathrm{Hz}$$

for $M_c \simeq 10^9\,M_\odot$, $\tau = 4\times 10^4\,\mathrm{yrs}$

Time to coalescence

Chirp mass
$$M_c = \frac{(m_1\,m_2)^{3/5}}{(m_1+m_2)^{1/5}}$$

GW varies on a scale of about 3 years

Period of the pulsar: millisecond

$$f_{\rm GW} P \ll 1$$

$$\Delta T = \frac{1}{2}\frac{\hat{u}^i\hat{u}^j}{1-\hat{\mathbf{k}}\cdot\hat{\mathbf{u}}}\int_{t_e-\hat{\mathbf{k}}\cdot\mathbf{r_e}}^{t_e+L-\hat{\mathbf{k}}\cdot\mathbf{r_e}-L\hat{\mathbf{k}}\cdot\mathbf{u}} \mathrm{d}X\,[h_{ij}(X+P)-h_{ij}(X)]$$

Taylor expand

Relative change in the rate of the pulses measured on Earth because of the GW passing by:

$$\frac{\Delta T}{P} \simeq \frac{1}{2}\frac{\hat{u}^i\hat{u}^j}{1-\hat{\mathbf{k}}\cdot\hat{\mathbf{u}}}\,[h_{ij}(t_e+L,\mathbf{r_o}) - h_{ij}(t_e,\mathbf{r_e})]$$

Earth term Pulsar term

Pulsar timing arrays

Supposing the source is the inspiral of a super massive black hole binary: what is the typical scale of the time variation of the metric perturbation?

$$f(\tau) = \frac{1}{\pi}\left(\frac{5}{256}\right)^{3/8} \frac{1}{(G\,M_c)^{5/8}\,\tau^{3/8}} \simeq 10^{-8}\,\mathrm{Hz}$$

for $M_c \simeq 10^9\,M_\odot$, $\tau = 4 \times 10^4\,\mathrm{yrs}$

Time to coalescence

Chirp mass

$$M_c = \frac{(m_1\,m_2)^{3/5}}{(m_1 + m_2)^{1/5}}$$

GW varies on a scale of about 3 years

Period of the pulsar: millisecond

$$f_{\mathrm{GW}}\,P \ll 1$$

$$\Delta T = \frac{1}{2}\frac{\hat{u}^i\hat{u}^j}{1 - \hat{\mathbf{k}}\cdot\hat{\mathbf{u}}}\int_{t_e - \hat{\mathbf{k}}\cdot\mathbf{r_e}}^{t_e + L - \hat{\mathbf{k}}\cdot\mathbf{r_e} - L\hat{\mathbf{k}}\cdot\mathbf{u}} \mathrm{d}X\,[h_{ij}(X+P) - h_{ij}(X)]$$

Taylor expand

NB: this is the change in the frequency of the pulses due to the GWs, calculated between two successive geodesics, and NOT the redshift experienced by a photon on the same geodesic (usual gravitational redshift, depending on $\dot{h}_{ij}$)

However, the two expressions become the same in the limit of infinitesimal P

Pulsar timing arrays

Relative change in the rate of the pulses measured on Earth because of the GW passing by:

$$\frac{\Delta T}{P} \simeq \frac{1}{2}\frac{\hat{u}^i\hat{u}^j}{1-\hat{\mathbf{k}}\cdot\hat{\mathbf{u}}}\left[h_{ij}(t_e+L,\mathbf{r_o}) - h_{ij}(t_e,\mathbf{r_e})\right]$$

$$\sim 7\cdot 10^{-23}\,\frac{\mathrm{pc}}{d_L}\left(\frac{M_c}{M_\odot}\right)^{5/3}\left(\frac{f_{\rm GW}}{10^{-8}\,\mathrm{Hz}}\right)^{2/3} \simeq 7\cdot 10^{-16}$$

$M_c \simeq 10^9\,M_\odot$
$d_L = 100\,\mathrm{Mpc}$

Timing residuals: $R(T) = \int_{t_{\rm ref}}^{t_{\rm ref}+T} \mathrm{d}t\,\frac{\Delta T}{P}$

$$R(T_{\rm GW} = 3\,\mathrm{yrs}) \simeq 60\,\mathrm{nsec}$$

A GW with period of a few years induces a timing residual of order 100 nsec, the precision of pulsar monitoring!

This renders the measurement possible, provided one has at least a few years of data

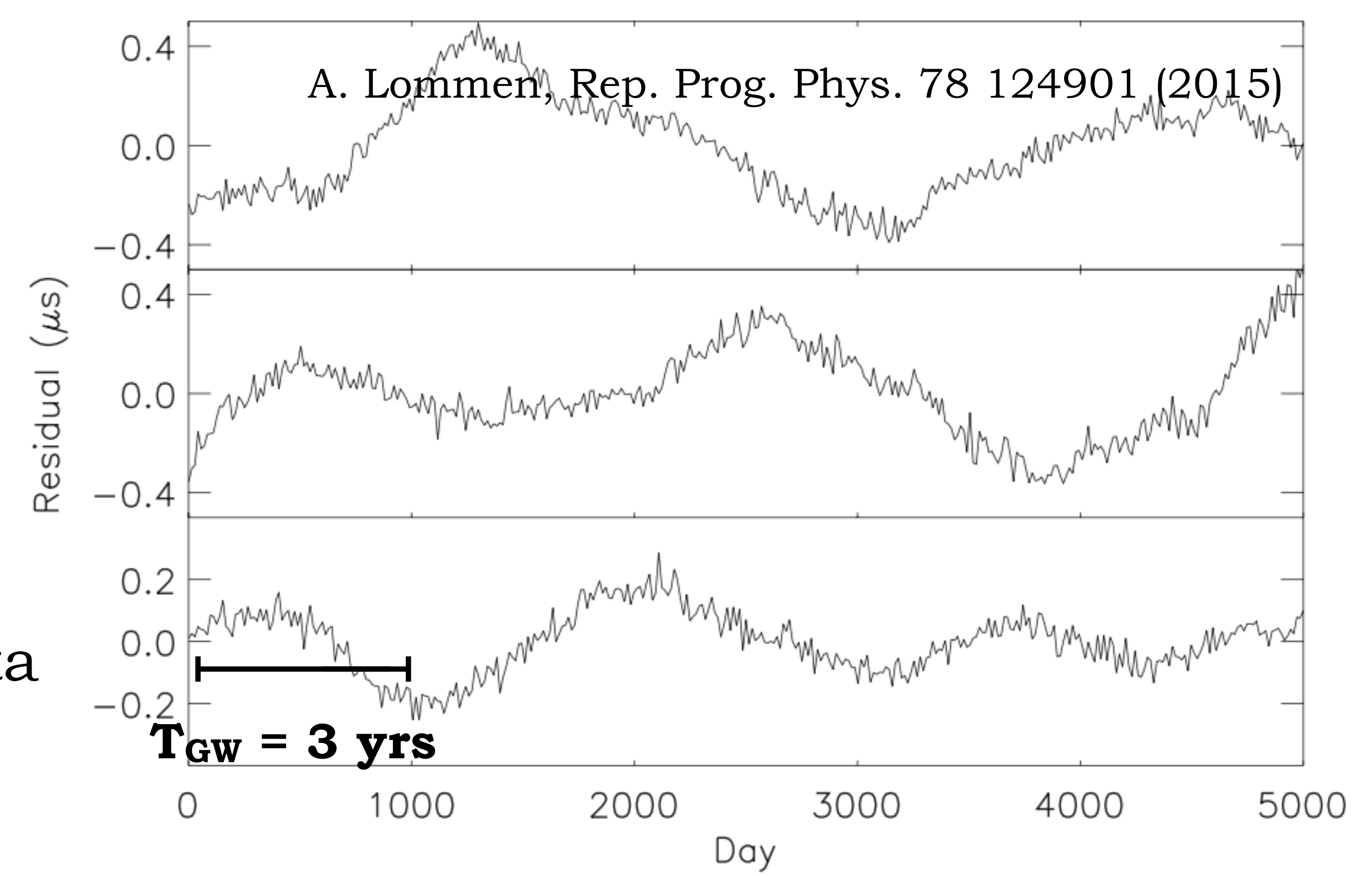

Pulsar timing arrays

HOWEVER! The signal from a single pulsar is very noisy: varying morphology of the pulses, propagation noise due to the dispersion by the interstellar medium, time referencing (time standards and solar system barycentre)...

Correlation between many pulsars to beat down the noise

$$\frac{\Delta T}{P} \simeq \frac{1}{2} \frac{\hat{u}^i \hat{u}^j}{1 - \hat{\mathbf{k}} \cdot \hat{\mathbf{u}}} \left[h_{ij}(t_e + L, \mathbf{r_o}) - h_{ij}(t_e, \mathbf{r_e}) \right]$$

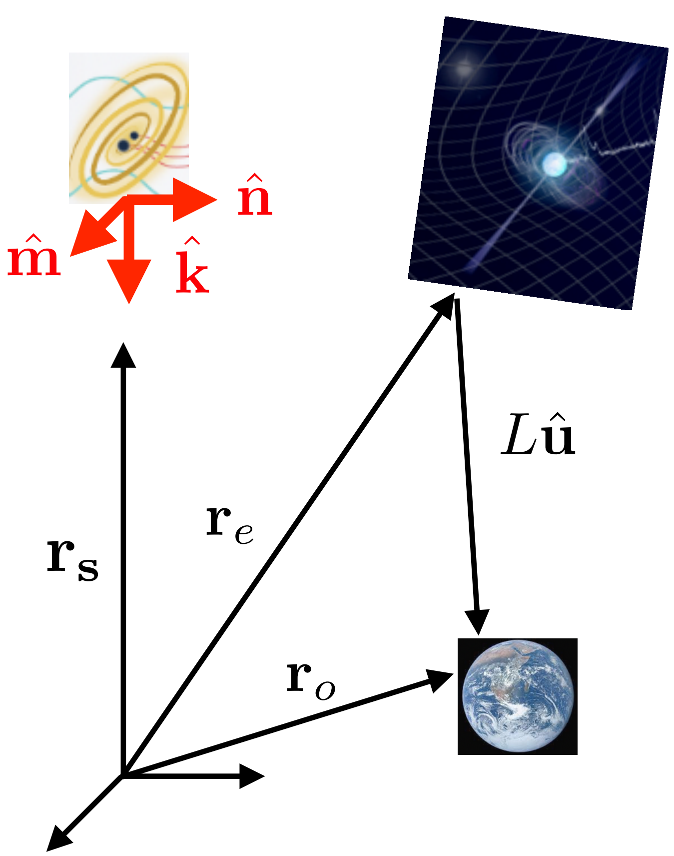

Earth term:
GW left the source at time

$$t_e + L - |\mathbf{r_o} - \mathbf{r_s}|$$

Pulsar term:
GW left the source at time

$$t_e - |\mathbf{r_e} - \mathbf{r_s}|$$

This term is different for each pulsar

In the correlation the Earth term in general dominates, but the pulsar term can create noise (unless one can determine the delay of each pulsar)

Pulsar timing arrays

Response of a pair of pulsars to a stochastic GW background

$$\langle R_a(T) R_b(T)\rangle = \int_{t_{\rm ref}}^{t_{\rm ref}+T} \mathrm{d}t' \int_{t_{\rm ref}}^{t_{\rm ref}+T} \mathrm{d}t'' \langle \frac{\Delta T}{P}(t')\Big|_a \frac{\Delta T}{P}(t'')\Big|_b \rangle$$

$$\frac{\Delta T}{P}(t')\Big|_a = \sum_r \int \frac{\mathrm{d}\mathbf{k}^3}{(2\pi)^3} h_r(\mathbf{k}) F_a^r(\hat{\mathbf{k}}) e^{-ik(t'-\hat{\mathbf{k}}\cdot\mathbf{r}_o)} \left[1 - e^{ikL_a(1-\hat{\mathbf{k}}\cdot\hat{\mathbf{u}}_a)}\right]$$

"Detector response" $F_a^r(\hat{\mathbf{k}}) = \dfrac{\hat{u}_a^i \hat{u}_a^j e_{ij}^r(\hat{\mathbf{k}})}{2(1-\hat{\mathbf{k}}\cdot\hat{\mathbf{u}})}$

put Earth at origin to simplify

Earth term

Pulsar term

Use SGWB power spectrum

$$\langle h_r(\mathbf{k},\eta)\, h_p^*(\mathbf{q},\eta)\rangle = \frac{8\pi^5}{k^3}\,\delta^{(3)}(\mathbf{k}-\mathbf{q})\,\delta_{rp}\, h_c^2(k,\eta)$$

The Earth term dominates

$$\left[1 - e^{ikL_a(1-\hat{\mathbf{k}}\cdot\hat{\mathbf{u}}_a)}\right]\left[1 - e^{-ikL_b(1-\hat{\mathbf{k}}\cdot\hat{\mathbf{u}}_b)}\right] \simeq 1$$

$a \neq b$

and SMBHB not in pulsar direction

$$kL_a = \mathcal{O}(2\pi\cdot 10^{-8}\,\mathrm{Hz}\cdot 500\,\mathrm{pc}) = \mathcal{O}(3000) \gg 1$$

Pulsar timing arrays

Response of a pair of pulsars to a stochastic GW background

$$\langle R_a(T) R_b(T)\rangle = \int_{t_{\rm ref}}^{t_{\rm ref}+T} \mathrm{d}t' \int_{t_{\rm ref}}^{t_{\rm ref}+T} \mathrm{d}t'' \langle \frac{\Delta T}{P}(t')\Big|_a \frac{\Delta T}{P}(t'')\Big|_b \rangle$$

θ_{ab} angle between pulsars

$$= \mathcal{C}(\theta_{ab}) \int_0^\infty \mathrm{d}f\, \frac{h_c^2(f)}{(2\pi)^2 f^3} \left[1 + \cos(2\pi f (T - t_{\rm ref})\right]$$

Hellings and Downs curve, characteristic of a GW signal because consequence of the quadrupolar nature of GWs

$$\mathcal{C}(\theta_{ab}) = \int \frac{\mathrm{d}\hat{\mathbf{k}}}{4\pi} \sum_r F_r^a(\hat{\mathbf{k}}) F_r^b(\hat{\mathbf{k}})$$

$$= \frac{1}{3} - \frac{1}{6} x_{ab} + x_{ab} \log(x_{ab})$$

$$x_{ab} = \frac{1}{2}(1 - \cos\theta_{ab})$$

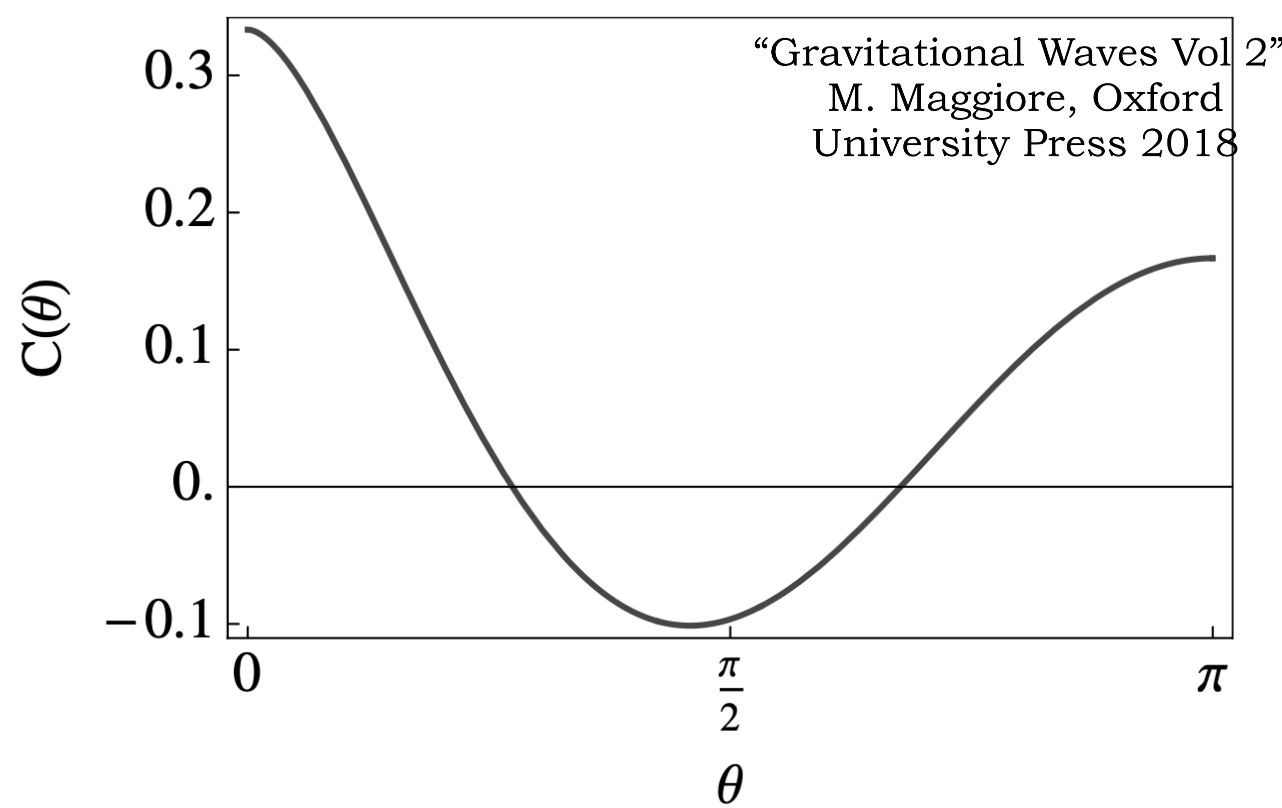

Pulsar timing arrays

Observation of the *Hellings and Downs curve* is **smoking gun evidence** of GW detection

(not only SGWB but also from a single SMBHB - Cornish & Sesana arXiv:1305.0326)

time referencing errors generate a correlated noise but:

- noise from uncertainties on the time standards on Earth is independent on the pulsar angles
- noise from uncertainties on the solar system barycentre position take the form of a (rotating) dipole (dependent on the cosinus of the angle) -> can contaminate the quadrupole

A SGWB from SMBHBs is the best candidate source in PTA frequency band

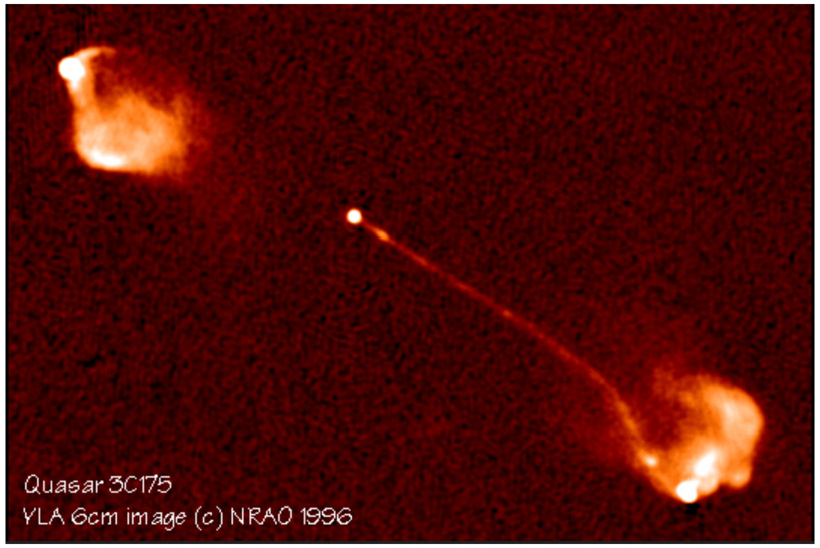

What are SMBHBs?

- They have been observed in the core of galaxies and are the central engine of active galactic nuclei
- They can originate from the collapse of massive stars (~100 $M_\odot$) or gas clouds (~ 10^4 $M_\odot$), and then grow in mass through gas accretion and/or mergers following the collision of their host galaxies (but their origin is still to be confirmed, they can also be primordial…)
- JWST sees SMBHs up to very high redshift z ~ 11
- Their presence is linked to the formation of galaxies and matter structure in the Universe

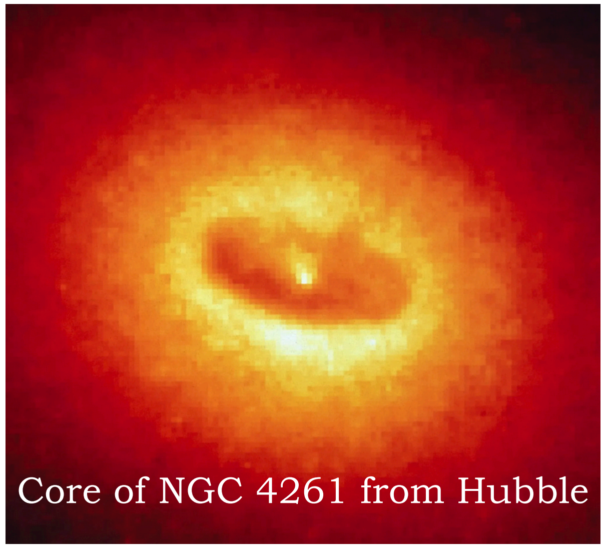
Core of NGC 4261 from Hubble

Pulsar timing arrays

HOWEVER!

- To emit GWs, SMBHs must be paired in gravitationally bound binaries in the GW emitting regime: separation of ~ 0.01-0.001 pc
- Binaires can be formed after the collision of two galaxies: the MBH previously at the centre of galaxies get to ~ kpc separation (X-ray evidence from dual AGNs)
- Dynamical friction drives the two MBH towards the centre of the new galaxy until they form a bound binary
- 3-body interaction with the surrounding stars subsequently shrinks the binary to pc separation
- How to get them to the millipc separation necessary for GW emission and merger within one Hubble time? "LAST PARSEC PROBLEM"
- maybe more stars arrive, or there is gas drag from interaction with a circumbinary disk, and/or another MBH arrives…

If PTAs observe the SGWB from SMBHBs it means that SMBHBs exist and merge in the universe!

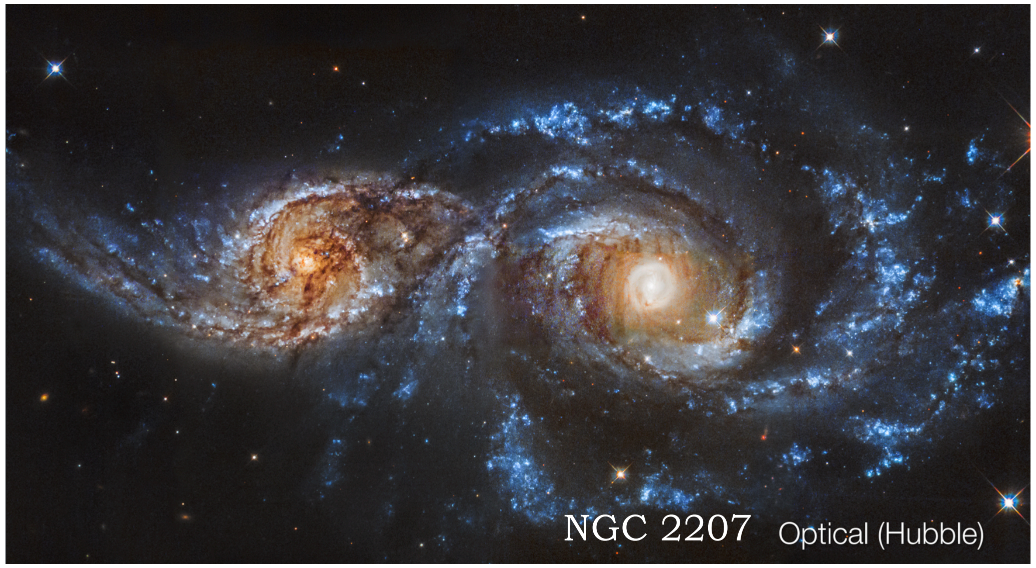
NGC 2207 Optical (Hubble)

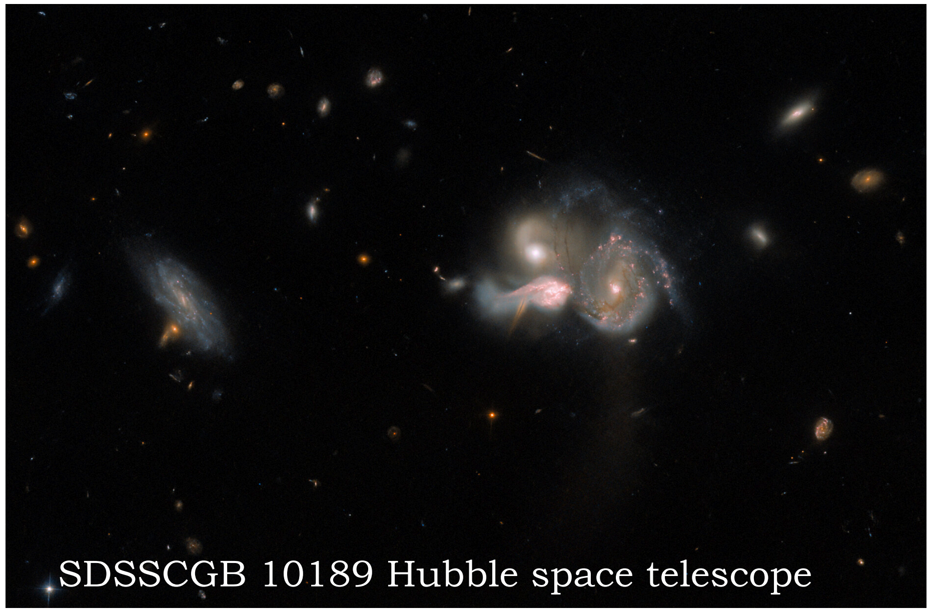
SDSSCGB 10189 Hubble space telescope

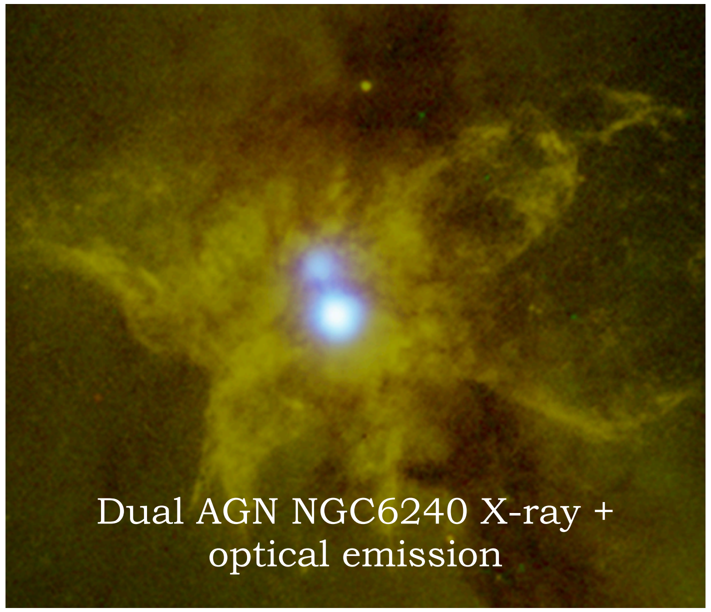
Dual AGN NGC6240 X-ray + optical emission

Pulsar timing arrays

Prediction from SMBHBs formation scenarios

How does the SGWB from SMBHBs look like?

Characteristic strain: red spectrum

$$h_c(f) = A \left(\frac{f}{f_{\rm ref}} \right)^{-\alpha} \text{ with } \alpha = \frac{2}{3}$$

$A = \mathcal{O}(10^{-15})$ at

$f_{\rm ref} = 1\,{\rm yr}^{-1}$

Circular binary

Timing residuals power spectral density: Also red spectrum

$$S_{ab}(f) = \mathcal{C}(\theta_{ab}) \Phi(f)$$

$$\Phi(f) = \frac{A^2}{(2\pi)^2} f_{\rm ref}^{-3} \left(\frac{f}{f_{\rm ref}} \right)^{-\gamma} \text{ with } \gamma = 2\alpha + 3 = \frac{13}{3}$$

Where does this spectral shape come from?

SGWB from a population of inspiralling binaries

$$h_c(f) = A\left(\frac{f}{f_{\rm ref}}\right)^{-\alpha} \text{with} \quad \alpha = \frac{2}{3}$$

in terms of the power spectrum of the GW energy density becomes

$$\Omega_{\rm GW}(f) = \frac{2\pi^2}{3H_0^2} f^2 h_c^2(f) = \Omega_{\rm GW}(f_{\rm ref})\left(\frac{f}{f_{\rm ref}}\right)^{2/3}$$

$$\frac{\rho_{\rm GW}^{\rm (tot)}}{\rho_c} = \int_0^\infty \frac{{\rm d}f}{f}\,\Omega_{\rm GW}(f) = \int {\rm d}\xi \int {\rm d}V_c \int {\rm d}\tau_c \, \frac{{\rm d}^3 N(z,\tau_c,\xi,\theta)}{{\rm d}\xi {\rm d}V_c {\rm d}\tau_c}\,\frac{\rho_{\rm GW}^{\rm (event)}}{\rho_c}$$

Parameters of the binary signal (essentially chirp mass)

Coming volume

Time to coalescence

Number density of GW sources (given within an astrophysical model for the binary population)

GW energy emitted by a single event

At the source $$\frac{\rho_{\rm GW}^{\rm (event)}}{\rho_c} = \frac{1}{16\pi G\rho_c}\,\frac{\langle \dot h_+^2 + \dot h_\times^2\rangle}{(1+z)^4}$$

SGWB from a population of inspiralling binaries

$$\dot{h}_+(t_S) = \frac{4\pi^{2/3}}{a(t_S)r}(G\,M_c)^{5/3}\left(\frac{1+\cos^2\theta}{2}\right)\underbrace{\frac{\mathrm{d}[f^{2/3}(t_S)\cos(2\Phi(t_S))]}{\mathrm{d}t_S}}$$

In the limit of circular orbit with slowly varying radius

$$\dot{f}_S \ll f_S^2$$

$$\simeq -f^{2/3}(t_S)2\,\dot{\Phi}(t_S)\sin(2\Phi(t_S))$$

$$\dot{\Phi}(t_S) \to \pi f_S$$

$$\langle \dot{h}_+^2(t_S)\rangle = \frac{32}{a_S^2 r^2}(\pi G\,M_c)^{10/3}\left(\frac{1+\cos^2\theta}{2}\right)^2 f_S^{10/3}$$

$$\frac{\rho_{\mathrm{GW}}^{(\mathrm{tot})}}{\rho_c} = \int \mathrm{d}\xi \int \mathrm{d}\tau_c \int \mathrm{d}z \frac{d_M^2}{H(z)} \frac{\mathrm{d}^3 N(z,\tau_c,\xi,\theta)}{\mathrm{d}\xi \mathrm{d}V_c \mathrm{d}\tau_c} \frac{1}{16\pi G\rho_c(1+z)^4}$$

$$\frac{32}{a_S^2 r^2}(\pi G M_c f_S)^{10/3} \int \mathrm{d}\Omega \left[\left(\frac{1+\cos^2\theta}{2}\right)^2 + \cos^2\theta\right]$$

$$d_M = a_0\, r$$

Extra factor $(1+z)^2$

$$\mathrm{d}V_c = \frac{d_M^2}{H(z)}\mathrm{d}\Omega\,\mathrm{d}z$$

$$= 16\pi/5$$

SGWB from a population of inspiralling binaries

Express the integral over time to coalescence in terms of frequency and change to frequency at the observer

$$\frac{\mathrm{d}f_S}{\mathrm{d}\tau_c} = \frac{96\pi^{8/3}}{5}(G\,M_c)^{5/3} f_S^{11/3}$$

$$f_S = f(1+z)$$

$$\frac{\rho_{\mathrm{GW}}^{(\mathrm{tot})}}{\rho_c} = \frac{\pi^{2/3}}{3\,G\rho_c}\int\frac{\mathrm{d}f}{f} f^{2/3}\int \mathrm{d}\xi\int\frac{\mathrm{d}z}{H(z)(1+z)^{4/3}}(GM_c)^{10/3}\frac{\mathrm{d}^3N(z,\tau_c,\xi,\theta)}{\mathrm{d}\xi\mathrm{d}V_c\mathrm{d}\tau_c}$$

$$\frac{\rho_{\mathrm{GW}}^{(\mathrm{tot})}}{\rho_c} = \int_0^\infty\frac{\mathrm{d}f}{f}\,\Omega_{\mathrm{GW}}(f)$$

$$\Omega_{\mathrm{GW}}(f) = \Omega_{\mathrm{GW}}(f_{\mathrm{ref}})\left(\frac{f}{f_{\mathrm{ref}}}\right)^{2/3}$$

$$\downarrow$$

SGWB amplitude determined by the population characteristics and the cosmology

SGWB from a population of inspiralling binaries

The features of the SGWB power spectrum (amplitude A, slope α…) depend on the population characteristics such as the binary merger rate, its dependence with mass and redshift, the surrounding stellar density, the initial binary eccentricity…

- The assumption of homogeneous and isotropic SGWB isn't justified at high frequency: SMBHBs are less numerous, the SGWB slope is steeper, and discreteness starts to appear with spikes due to the loudest SMBHBs
- Interactions with the binary environment makes hardening stronger and suppresses SGWB power at low frequency
- Eccentricity enhances GW emission at higher frequencies

L.Z. Kelley et al, arXiv:1702.02180

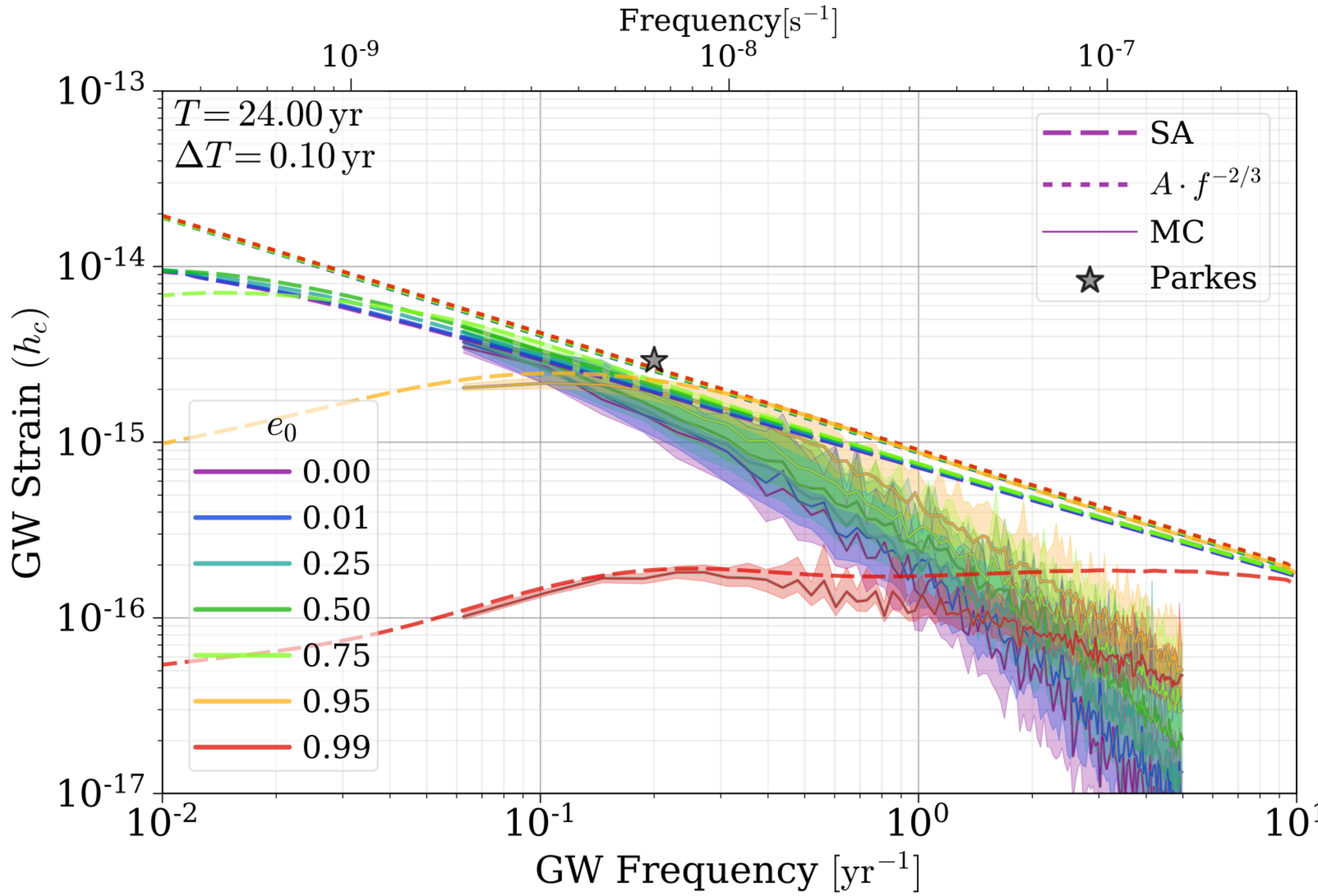

Pulsar timing arrays

In 2020, NANOGrav (followed by EPTA and PPTA) has announced the presence of a common red noise in their 12.5 years data

$$\Phi(f) = \frac{A^2}{(2\pi)^2} f_{\mathrm{ref}}^{-3} \left(\frac{f}{f_{\mathrm{ref}}}\right)^{-\gamma} \quad \text{with} \quad \gamma = 2\alpha + 3 = \frac{13}{3}$$

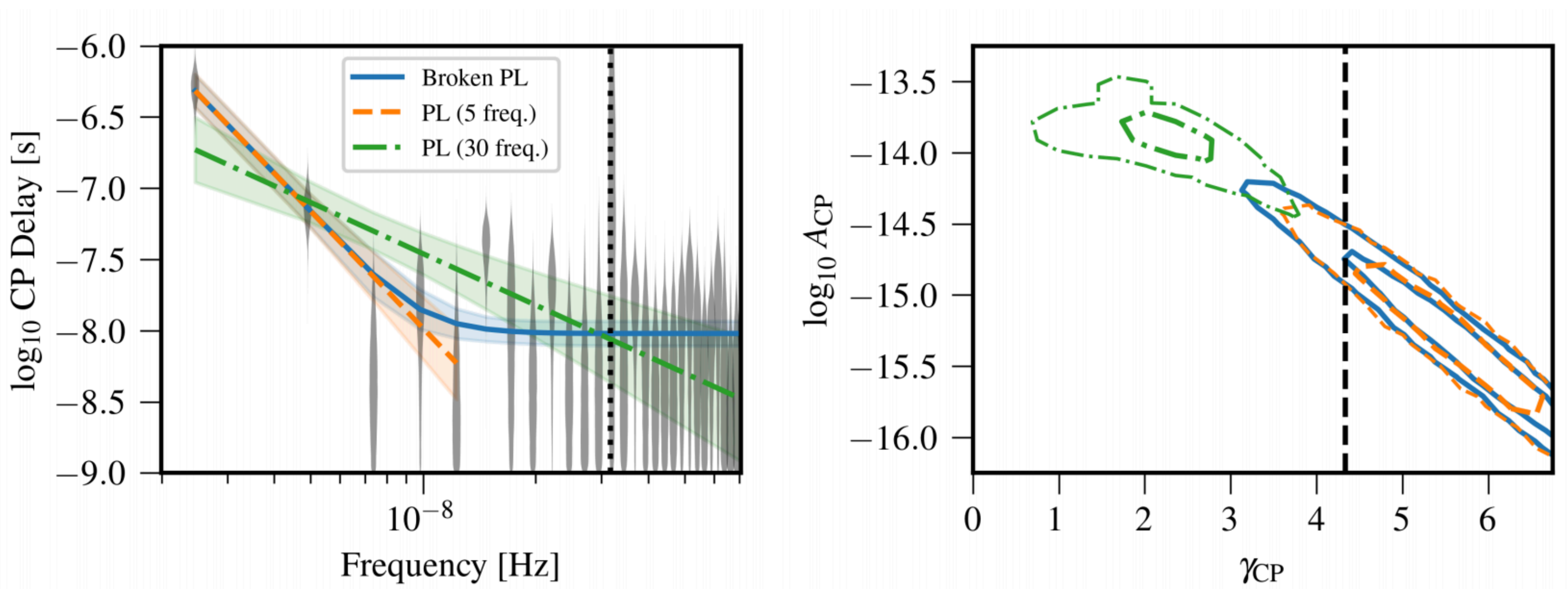

NANOGrav collaboration: arXiv:2009.04496

Pulsar timing arrays

In 2023, all PTAs have confirmed the observation of a common red noise supplemented by evidence for the Hellings-Downs correlation

EPTA results:

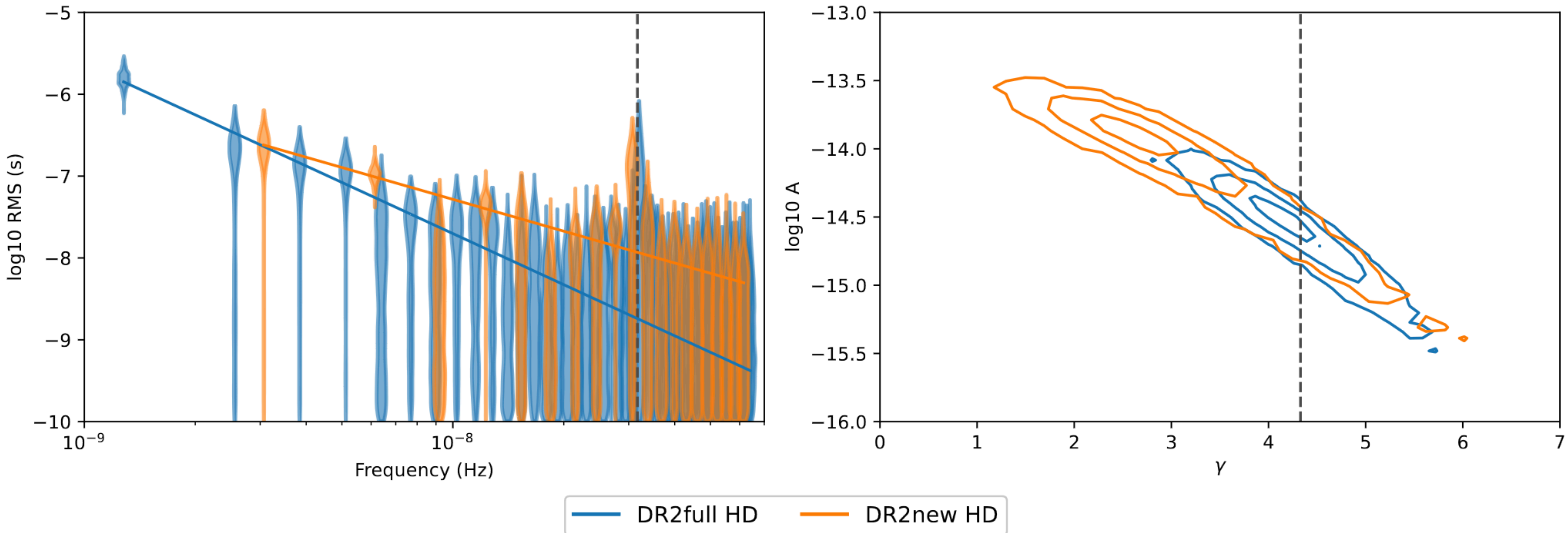

DR2new (10.3 yrs):

$$\log A = -13.94^{+0.23}_{-0.48} \quad \gamma = 2.71^{+1.18}_{-0.73} \quad \mathcal{B} = 60$$

DR2full (25 yrs):

$$\log A = -14.54^{+0.28}_{-0.41} \quad \gamma = 4.19^{+0.73}_{-0.63} \quad \mathcal{B} = 4$$

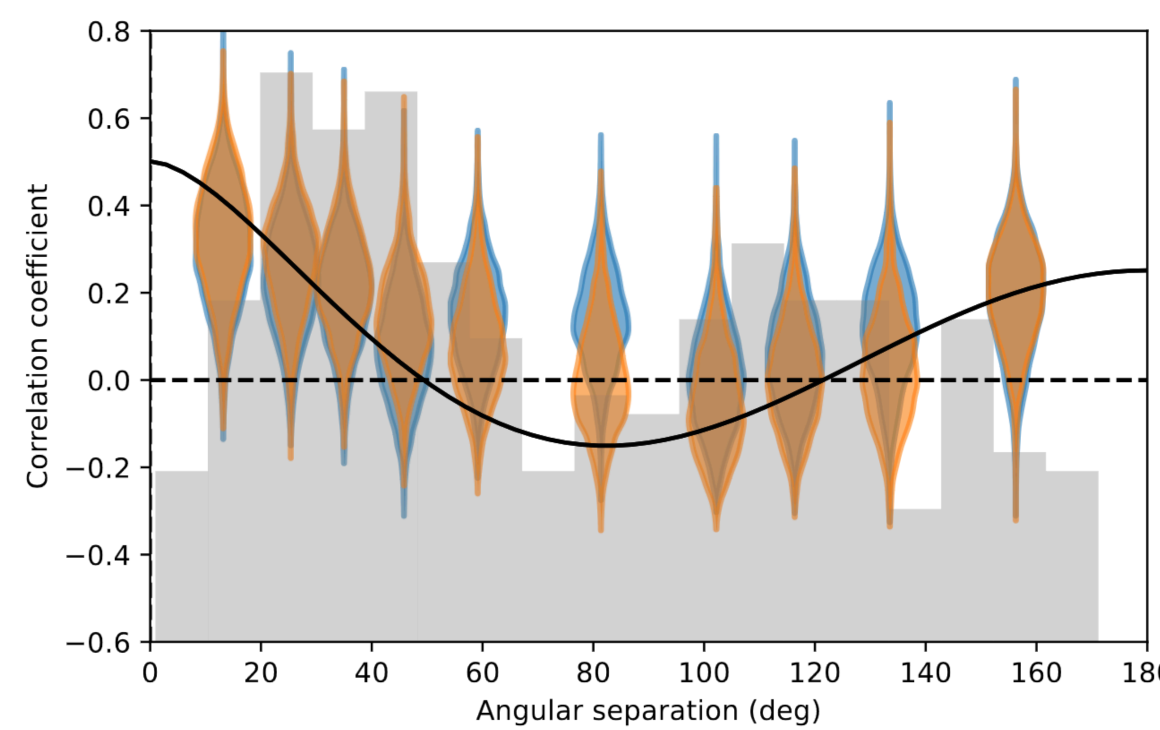

J. Antoniadis et al, arXiv:2306.16214

Pulsar timing arrays

In 2023, all PTAs have confirmed the observation of a common red noise supplemented by evidence for the Hellings-Downs correlation

NANOGrav results:

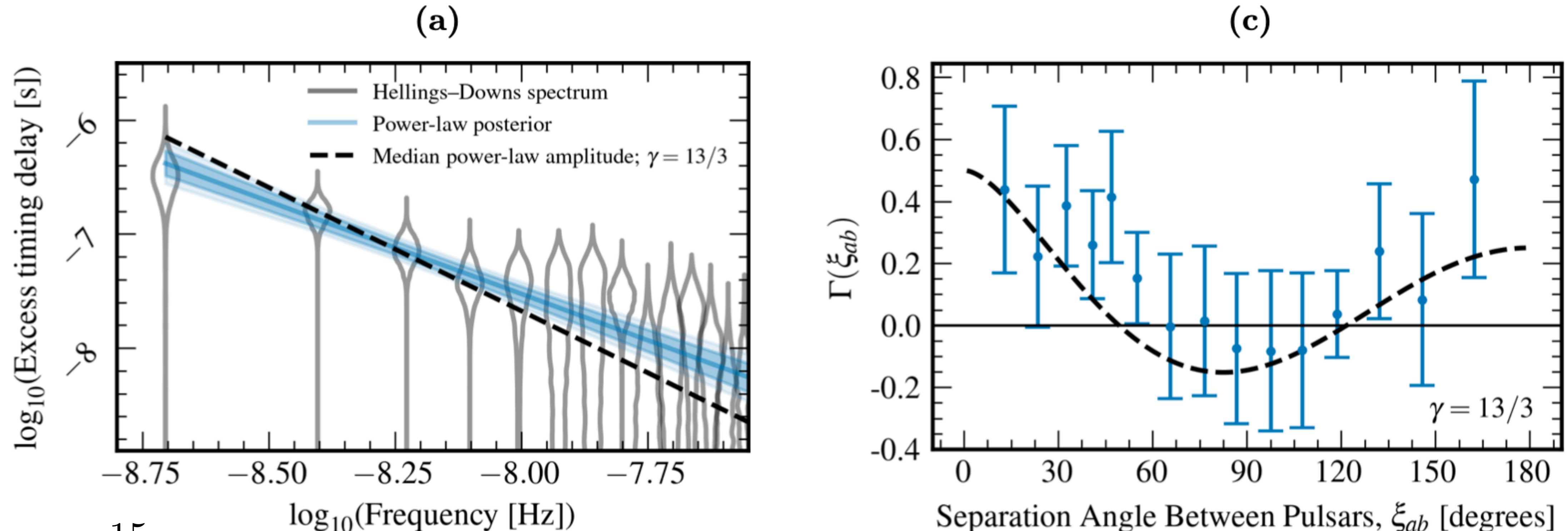

$$A = -6.4^{+4.2}_{-2.7} \times 10^{-15}$$

$$\gamma = 3.2^{+0.6}_{-0.6}$$

$$\mathcal{B} = 226$$

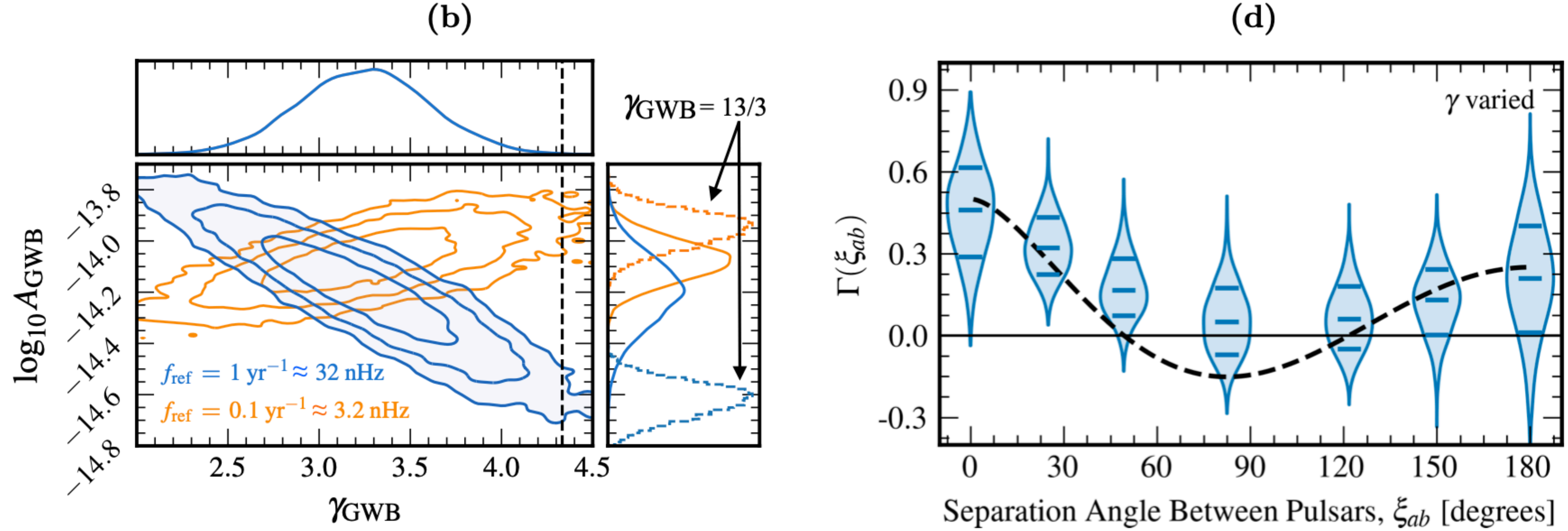

G. Agazie et al, arXiv:2306.16213

Pulsar timing arrays

- The slopes are shallower than 13/3 (but maybe the model isn't fully adapted…)
- The amplitude is consistent with the one from a SMBHBs SGWB
- All datasets are consistent within 1σ as shown by IPTA

IPTA Collaboration,
arXiv:2309.00693

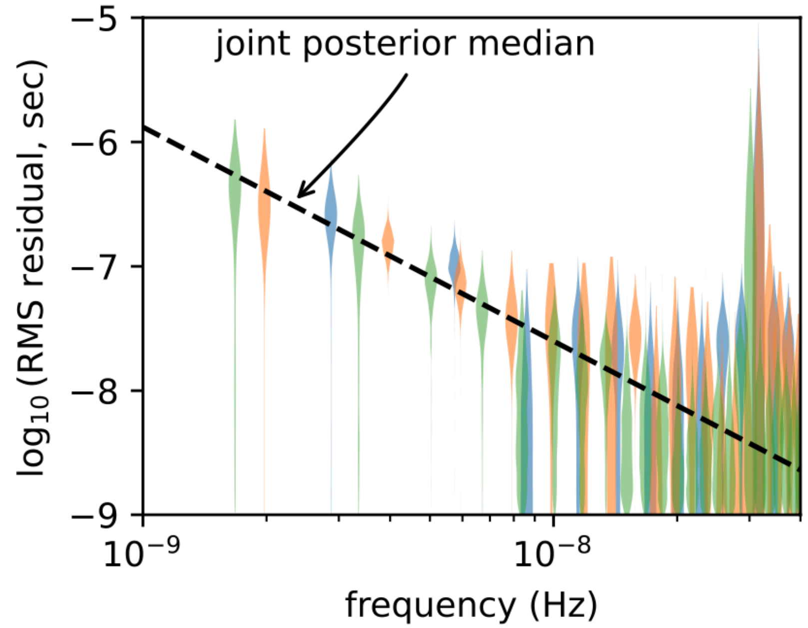

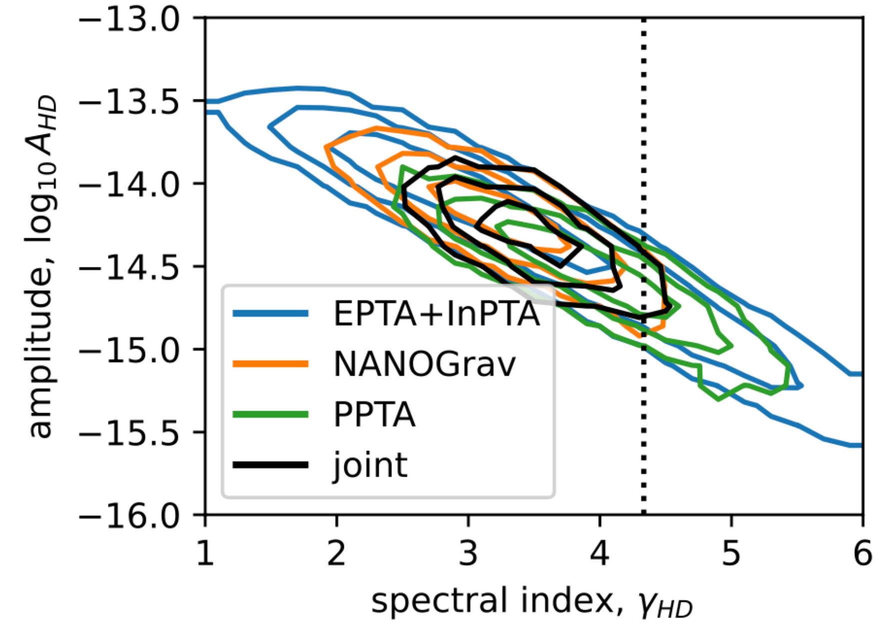

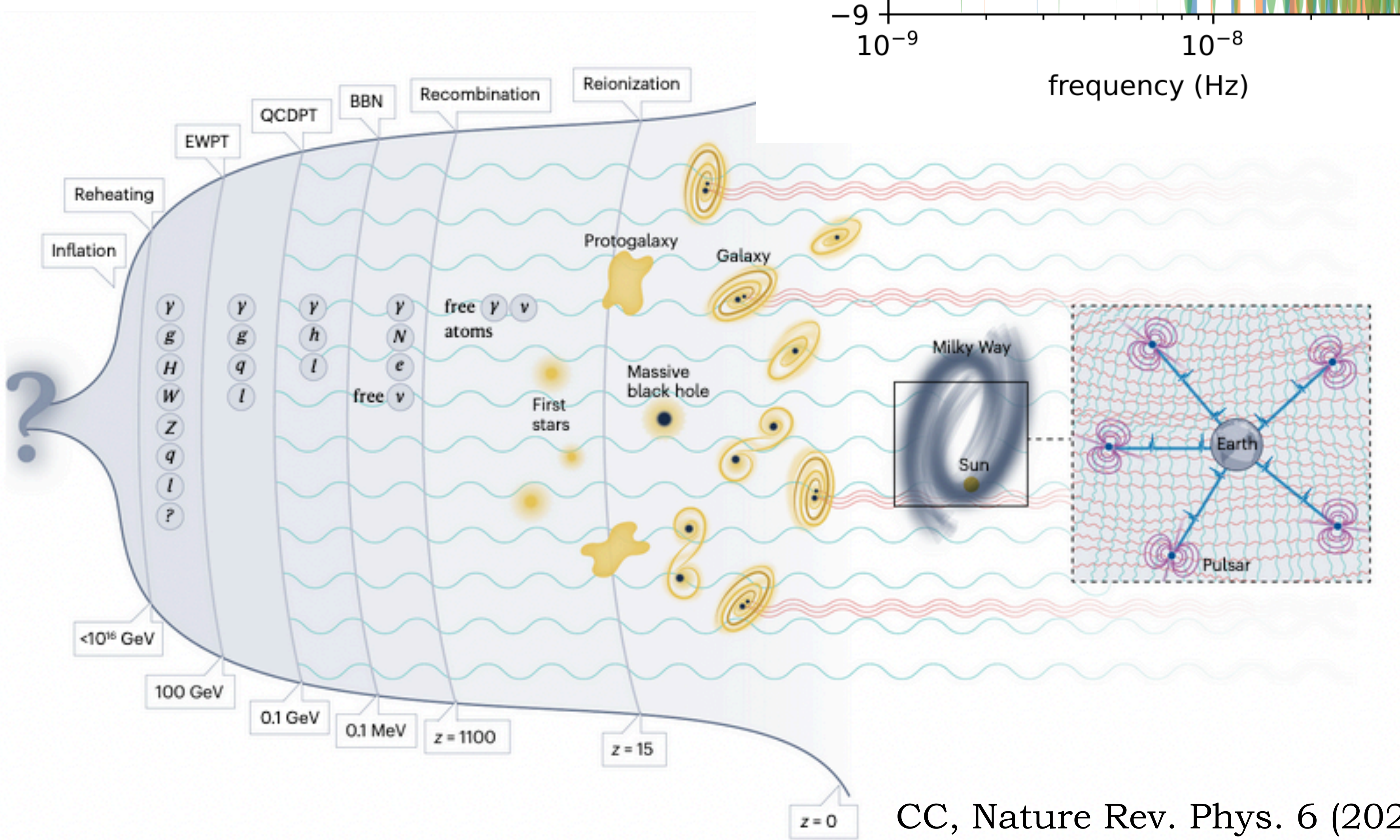

But the signal could also be of primordial origin…

CC, Nature Rev. Phys. 6 (2024), 5291-293

Examples of SGWB sources in the early universe

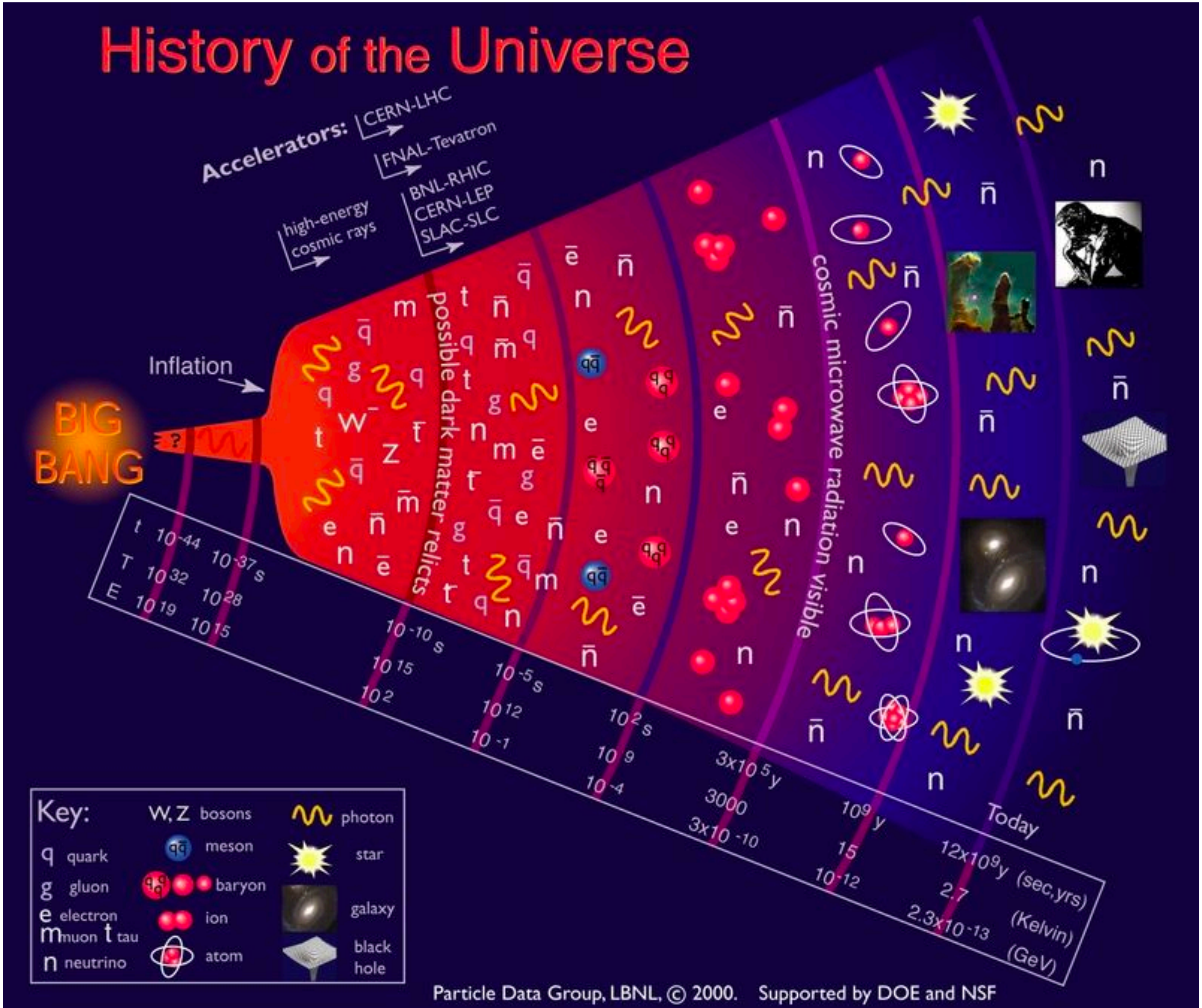

GWs can bring direct information from very early stages of the universe evolution, to which we have no direct access through em radiation —>
amazing discovery potential

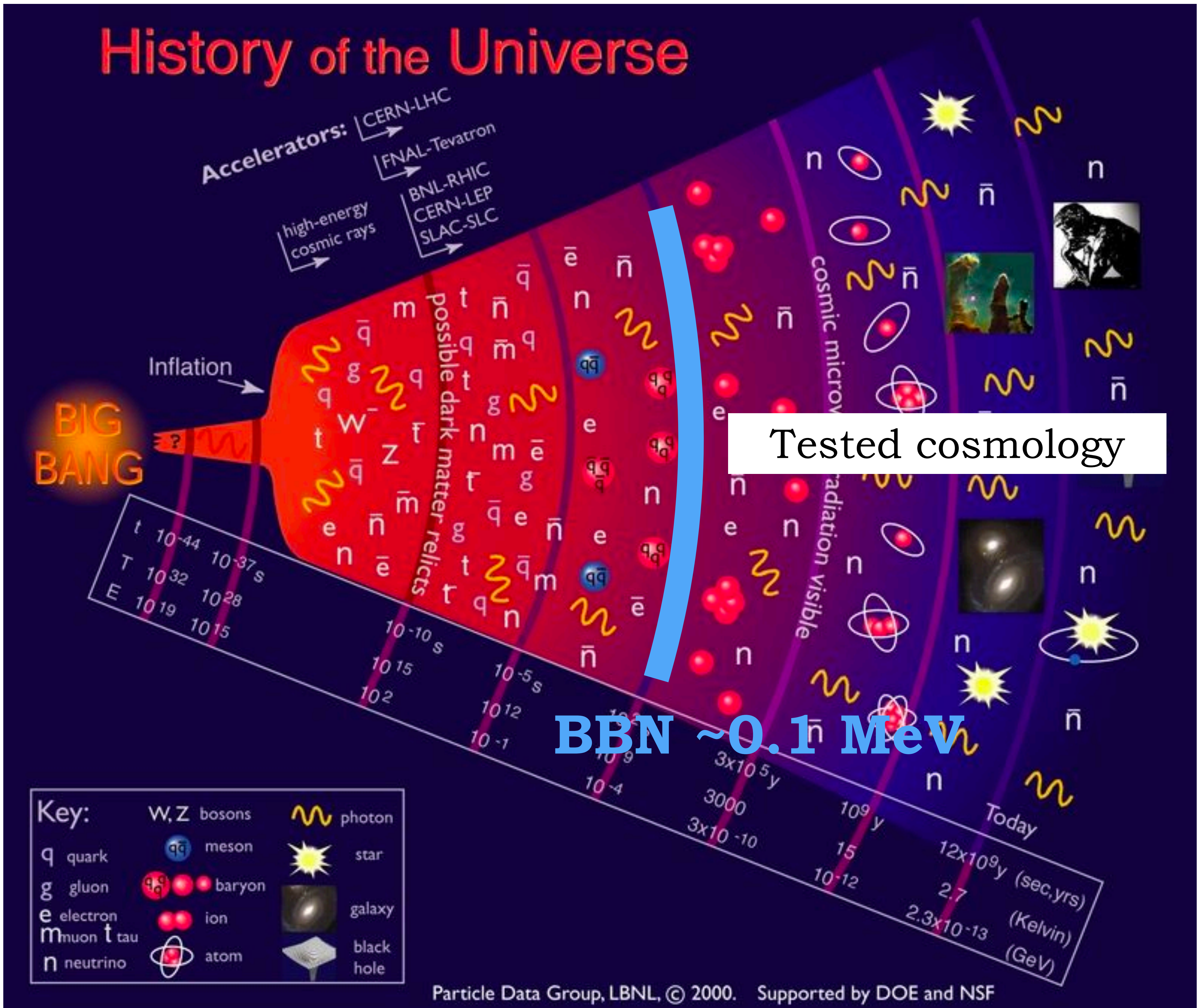

No guaranteed GW signal: predictions rely on untested phenomena, and are often difficult to estimate (non-linear dynamics, strongly coupled theories…)

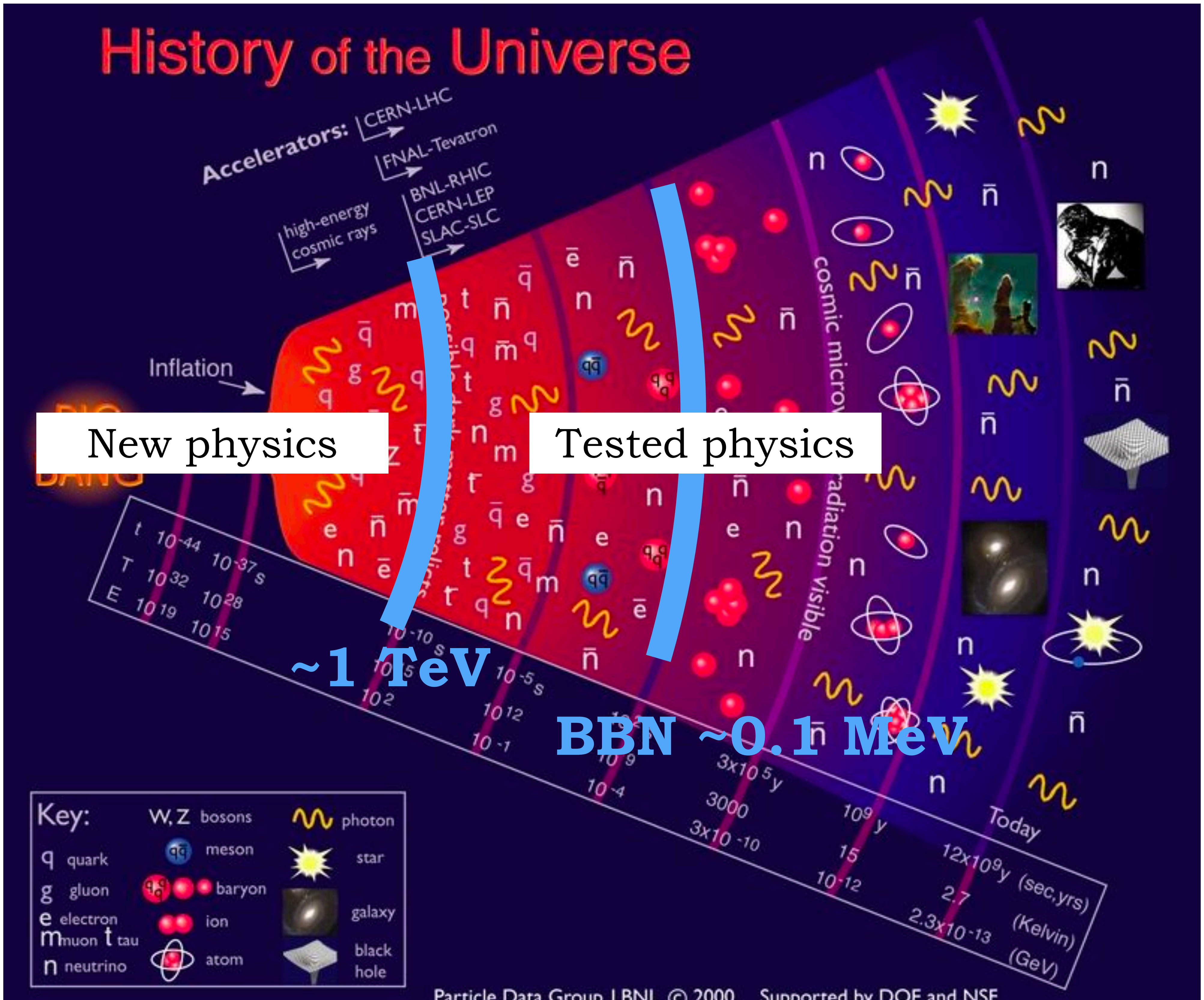

Many GW generation processes are related to PHASE TRANSITIONS

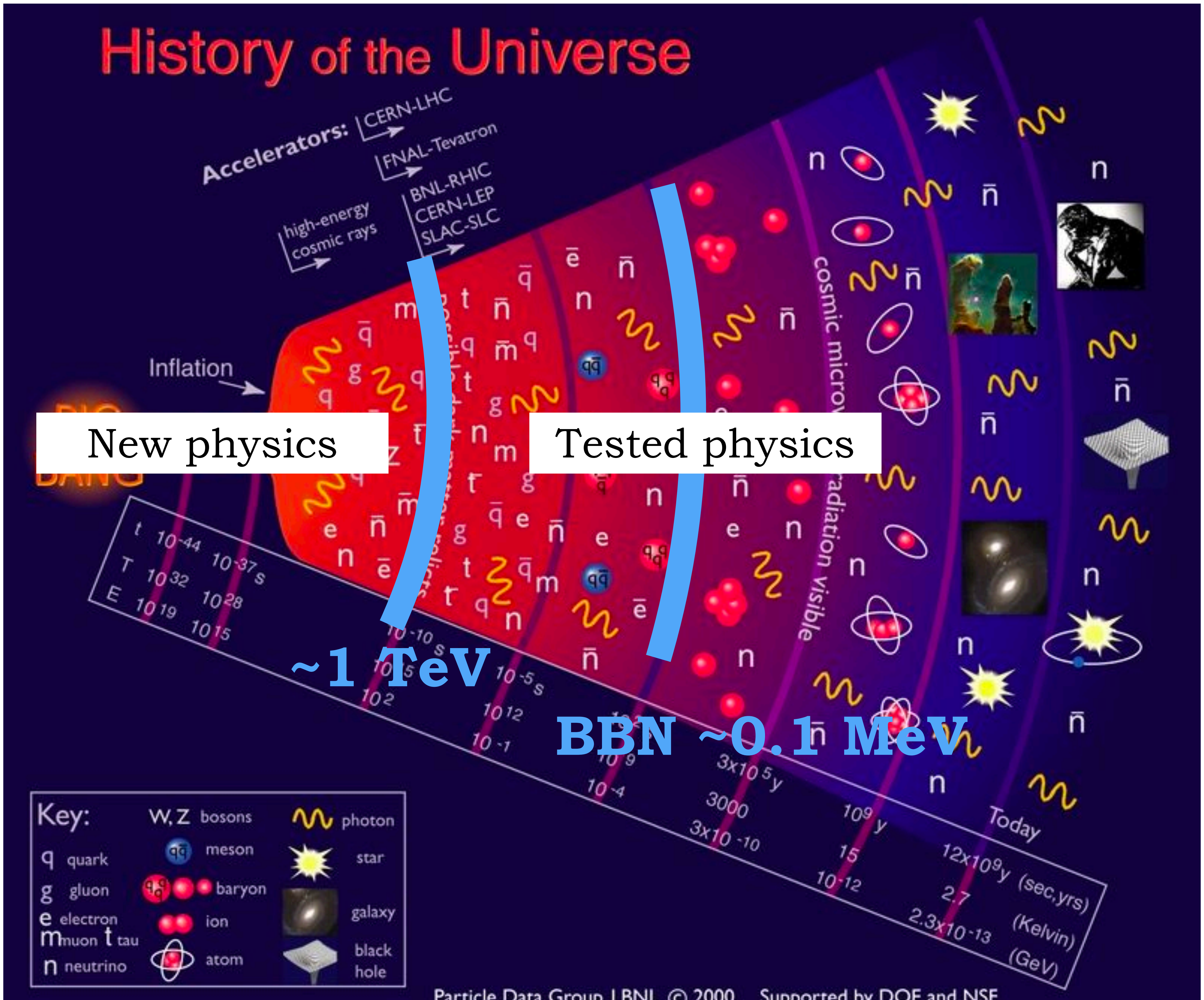

Phase transition: some field in the universe changes from one state to another, which has become more energetically favourable due to a change in external conditions (e.g. a change in temperature)

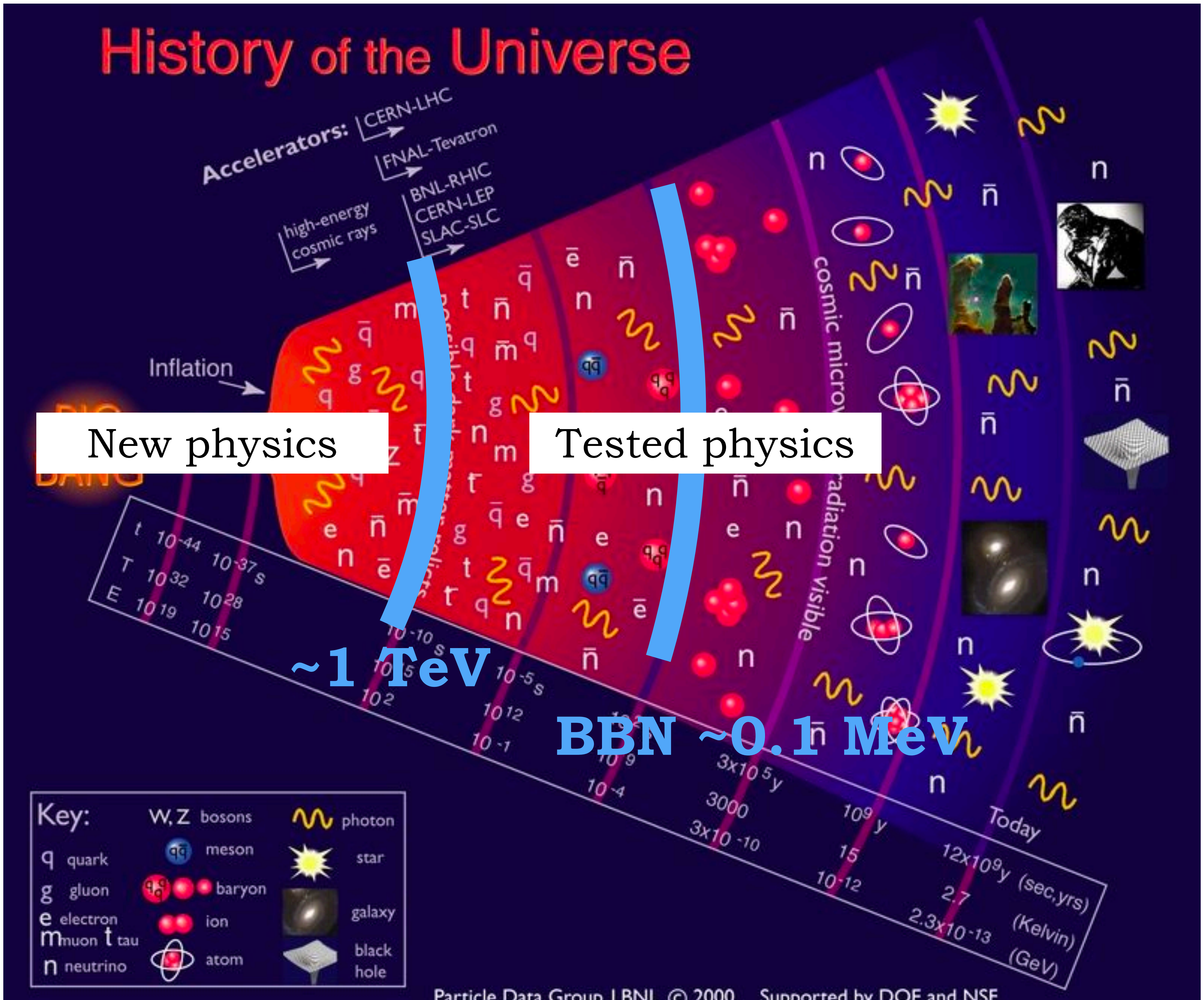

Inflation: phase transition of the Inflaton field

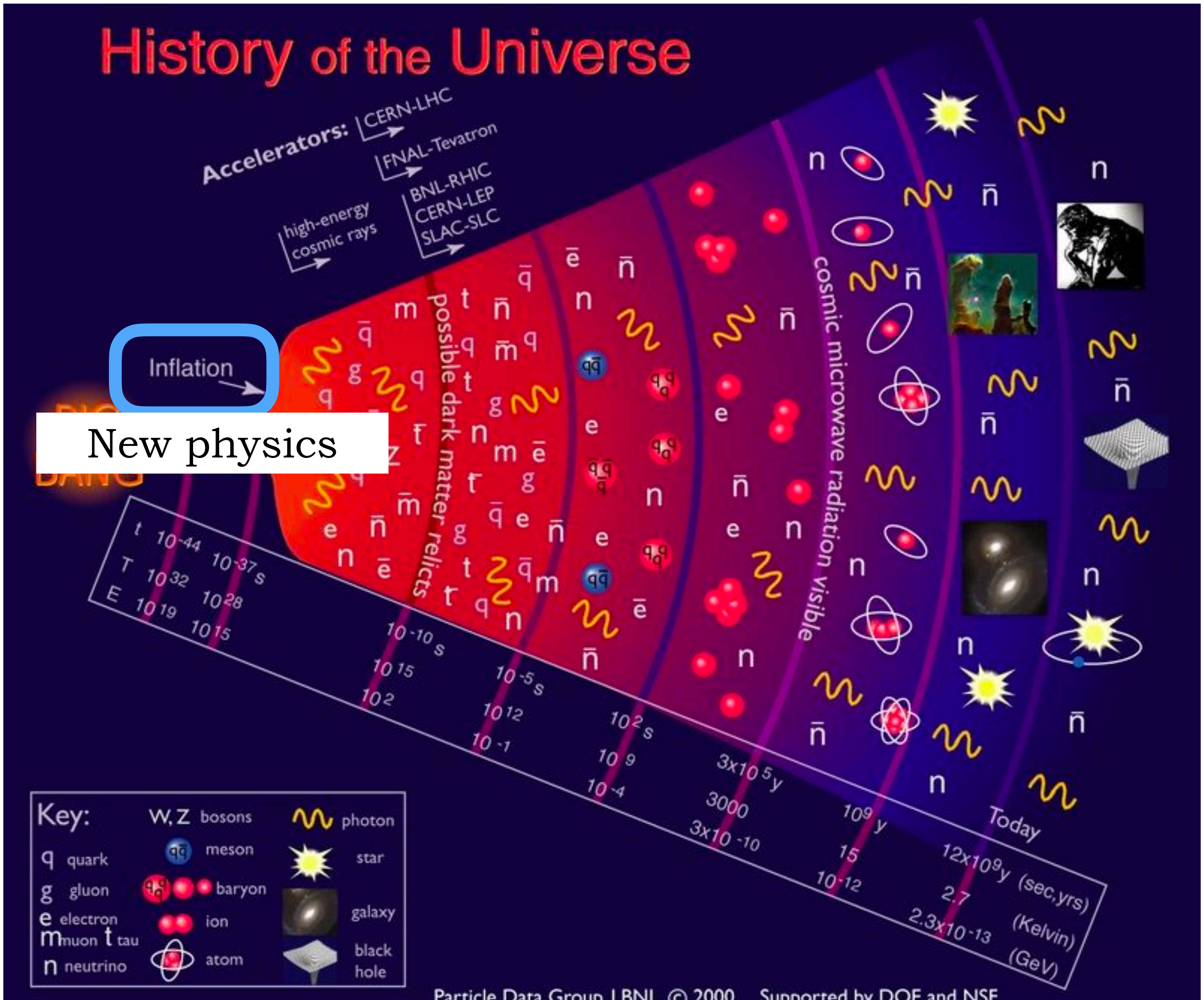

New physics

GUT phase transition or similar: related to the breaking of the symmetries of the high-energy theory describing the universe

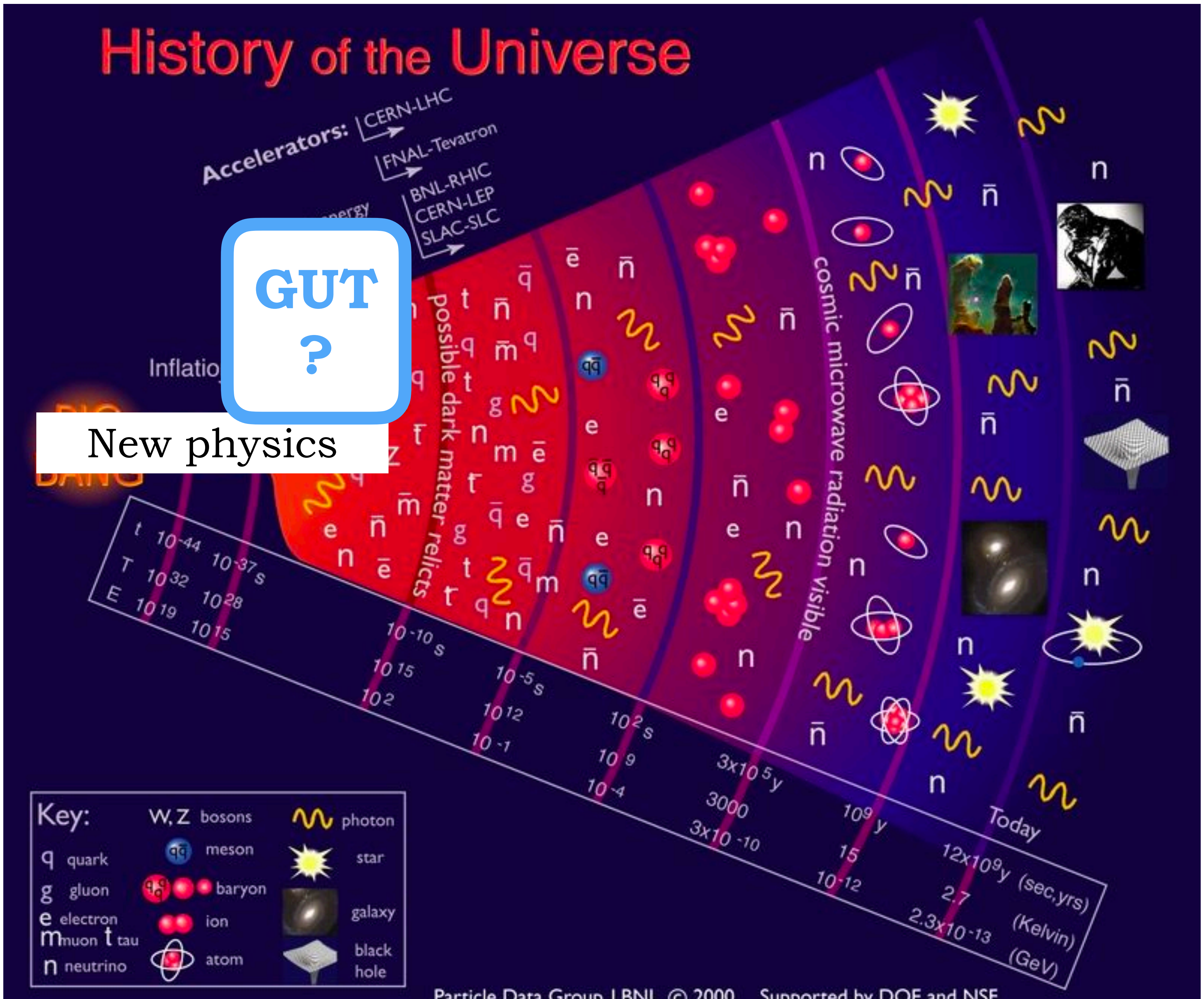

Peccei-Quinn phase transition: invoked to solve the strong CP problem

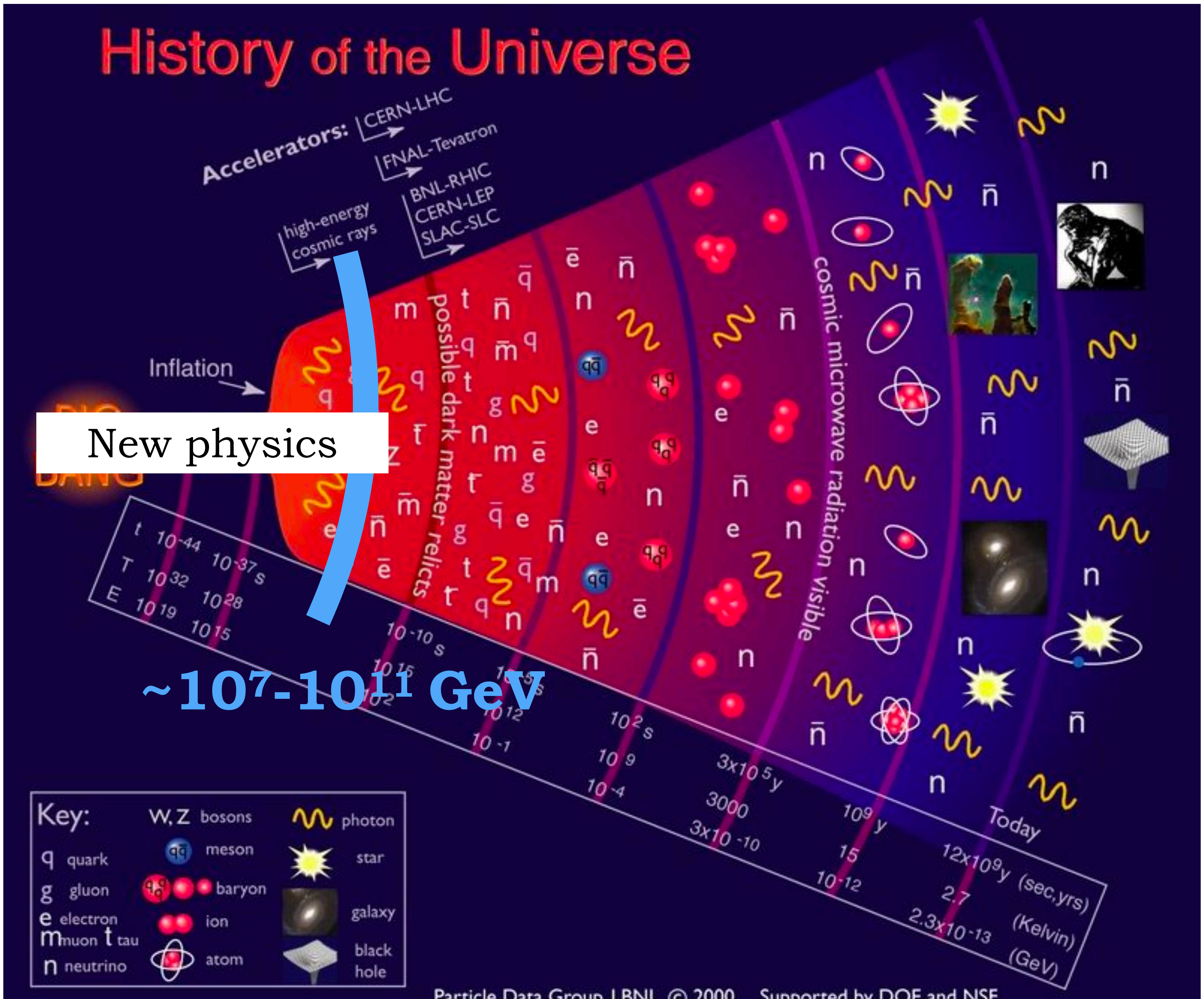

Electroweak phase transition: phase transition of the Higgs field, driven by the temperature decrease as the universe expands

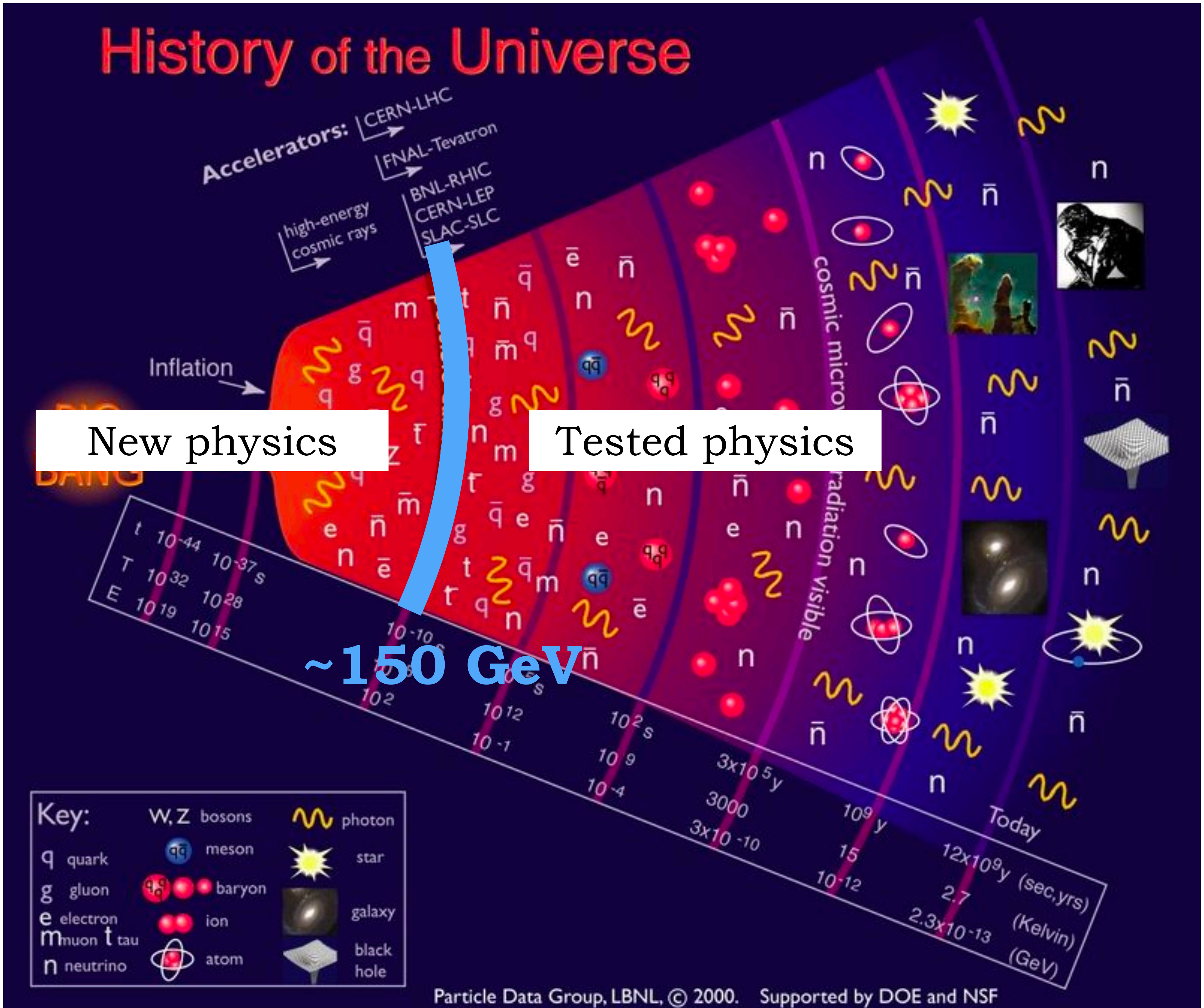

QCD phase transition: phase transition related to the strong interaction, confinement of quarks into hadrons

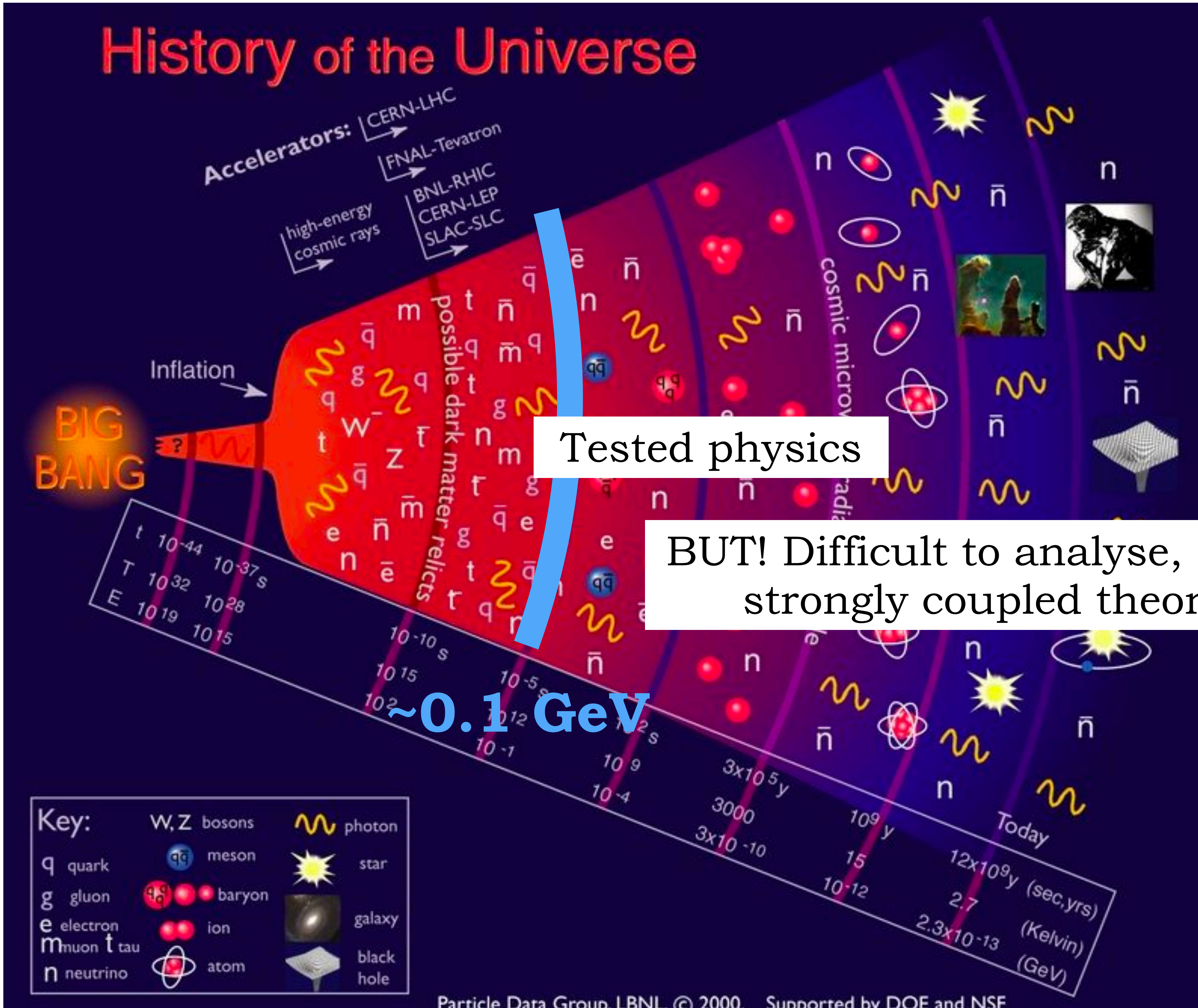

Tested physics

BUT! Difficult to analyse, since strongly coupled theory

~0.1 GeV

SGWB from a stochastic source in the radiation era

$$h_r''(\mathbf{k},\eta) + 2\,\mathcal{H}\,h_r'(\mathbf{k},\eta) + k^2\,h_r(\mathbf{k},\eta) = 16\pi G\,a^2\,\Pi_r(\mathbf{k},\eta)$$

Possible sources of tensor anisotropic stress in the early universe:

- Scalar field gradients $\Pi_{ij} \sim [\partial_i\phi\partial_j\phi]^{TT}$
- Bulk fluid motion $\Pi_{ij} \sim [\gamma^2(\rho+p)v_iv_j]^{TT}$
- Gauge fields $\Pi_{ij} \sim [-E_iE_j - B_iB_j]^{TT}$
- Second order scalar perturbations, Π_{ij} from a combination of $\partial_i\Psi, \partial_i\Phi$
- …

The components of the anisotropic stress must be treated as
random variables
because we cannot access the detailed properties of the generation processes at the moment they operated

SGWB from a stochastic source in the radiation era

Anisotropic stress power spectral density at unequal time

unequal time correlator of the anisotropic stress

$$\langle \Pi_r(\mathbf{k},\tau)\,\Pi_p^*(\mathbf{q},\zeta)\rangle = \frac{(2\pi)^3}{4}\,\delta^{(3)}(\mathbf{k}-\mathbf{q})\,\delta_{rp}\,\Pi(k,\tau,\zeta)$$

We now proceed with two approximate analytical solutions of the GW propagation equation:

- **Fast source** operating for less than one Hubble time -> peaked SGWB power spectrum
- **Continuous source** operating for several Hubble times -> extended SGWB power spectrum

---

Fast source operating in a time interval $\eta_{\rm fin}$ - $\eta_{\rm in}$ in the radiation dominated era

Typical example: first order phase transition

$$H_r^{\rm rad}(\mathbf{k},\eta>\eta_{\rm fin}) = A_r^{\rm rad}(\mathbf{k})\cos(k\eta) + B_r^{\rm rad}(\mathbf{k})\sin(k\eta)$$

$$A_r^{\rm rad}(\mathbf{k}) = \frac{16\pi G}{k}\int_{\eta_{\rm in}}^{\eta_{\rm fin}} d\tau\, a(\tau)^3\,\sin(-k\tau)\,\Pi_r(\mathbf{k},\tau),$$

$$B_r^{\rm rad}(\mathbf{k}) = \frac{16\pi G}{k}\int_{x_{\rm in}}^{x_{\rm fin}} d\tau\, a(\tau)^3\,\cos(k\tau)\,\Pi_r(\mathbf{k},\tau)$$

SGWB from a **FAST** stochastic source in the radiation era

GW amplitude power spectrum today for modes $k\eta_0 \gg 1$

$$\langle h_r(\mathbf{k},\eta_0)\, h_p^*(\mathbf{q},\eta_0)\rangle = \frac{1}{a_0^2}[\langle A_r(\mathbf{k})\, A_p^*(\mathbf{q})\rangle + \langle B_r(\mathbf{k})\, B_p^*(\mathbf{q})\rangle]$$
$$= 8\pi^5\, \delta^{(3)}(\mathbf{k}-\mathbf{q})\, \delta_{rp}\, \frac{h_c^2(k,\eta_0)}{k^3}$$

GW energy density power spectrum today for modes $k\eta_0 \gg 1$

$$\frac{d\rho_{\rm GW}}{d\log k} = \frac{k^2\, h_c^2(k,\eta_0)}{16\pi G\, a_0^2}$$

(freely propagating sub-Hubble modes)

$$\frac{d\rho_{\rm GW}}{d\log k}(k,\eta_0) = \frac{4}{\pi}\,\frac{G}{a_0^4} k^3 \int_{\eta_{\rm in}}^{\eta_{\rm fin}} d\tau\, a^3(\tau) \int_{\eta_{\rm in}}^{\eta_{\rm fin}} d\zeta\, a^3(\zeta)\, \cos[k(\eta-\zeta)]\, \Pi(k,\tau,\zeta)$$

SGWB from a **FAST** stochastic source in the radiation era

GW amplitude power spectrum today for modes $k\eta_0 \gg 1$

$$\langle h_r(\mathbf{k},\eta_0)\, h_p^*(\mathbf{q},\eta_0)\rangle = \frac{1}{a_0^2}[\langle A_r(\mathbf{k})\, A_p^*(\mathbf{q})\rangle + \langle B_r(\mathbf{k})\, B_p^*(\mathbf{q})\rangle]$$
$$= 8\pi^5\, \delta^{(3)}(\mathbf{k}-\mathbf{q})\, \delta_{rp}\, \frac{h_c^2(k,\eta_0)}{k^3}$$

GW energy density power spectrum today for modes $k\eta_0 \gg 1$

$$\frac{d\rho_{\rm GW}}{d\log k} = \frac{k^2\, h_c^2(k,\eta_0)}{16\pi G\, a_0^2}$$

(freely propagating sub-Hubble modes)

$$\frac{d\rho_{\rm GW}}{d\log k}(k,\eta_0) = \frac{4}{\pi}\,\frac{G}{a_0^4} k^3 \int_{\eta_{\rm in}}^{\eta_{\rm fin}} d\tau\, \underbrace{\cancel{a^3(\tau)}}_{a_*^3} \int_{\eta_{\rm in}}^{\eta_{\rm fin}} d\zeta\, \underbrace{\cancel{a^3(\zeta)}}_{a_*^3}\, \underbrace{\cancel{\cos[k(\eta-\zeta)]}}_{\simeq 1}\, \underbrace{\cancel{\Pi(k,\tau,\zeta)}}_{\Pi(k)}$$

SUPPOSE:

$\Delta\eta = \eta_{\rm fin} - \eta_{\rm in} \ll \mathcal{H}_*^{-1}$ $\qquad k\eta_{\rm in} \ll 1$ $\qquad \Pi(k,\tau,\eta)$ constant over $\Delta\eta$

SGWB from a **FAST** stochastic source in the radiation era

GW energy density parameter today for modes $1/\eta_0 \ll k \ll 1/\eta_{in}$

$$h^2\Omega_{\rm GW}(k,\eta_0) = \frac{3}{2\pi^2} h^2\Omega^0_{\rm rad}\left(\frac{g_0}{g_*}\right)^{\frac{1}{3}} (\Delta\eta\mathcal{H}_*)^2 \left(\frac{\rho_\Pi}{\rho_{\rm rad}}\right)^2 \underbrace{(k\ell_*)^3 \tilde{P}_{\rm GW}(k)}$$

$$\Pi(k) = \ell_*^3\, \rho_\Pi^2\, \tilde{P}_{\rm GW}(k)$$

From the time integrals

SGWB from a **FAST** stochastic source in the radiation era

GW energy density parameter today for modes $1/\eta_0 \ll k \ll 1/\eta_{in}$

$$h^2\Omega_{GW}(k,\eta_0) = \frac{3}{2\pi^2} h^2 \Omega^0_{rad} \left(\frac{g_0}{g_*}\right)^{\frac{1}{3}} (\Delta\eta\mathcal{H}_*)^2 \left(\frac{\rho_\Pi}{\rho_{rad}}\right)^2 (k\ell_*)^3 \tilde{P}_{GW}(k)$$

$\mathcal{O}(10^{-9})$ $\quad$ $\mathcal{O}(10^{-6})$ $\quad$ $\mathcal{O}(10^{-3})$

Value detected at PTA

Factor depending slightly on the generation epoch through the number of relativistic d.o.f.

Only slow, very anisotropic processes have the chance to generate detectable SGWB signals for sub-Hubble sources

Value for detection at LISA

$\mathcal{O}(10^{-11})$ $\quad$ $\mathcal{O}(10^{-6})$ $\quad$ $\mathcal{O}(10^{-5})$

SGWB from a **FAST** stochastic source in the radiation era

GW energy density parameter today for modes $1/\eta_0 \ll k \ll 1/\eta_{in}$

$$h^2\Omega_{\rm GW}(k,\eta_0) = \frac{3}{2\pi^2} h^2\Omega^0_{\rm rad} \left(\frac{g_0}{g_*}\right)^{\frac{1}{3}} (\Delta\eta\mathcal{H}_*)^2 \left(\frac{\rho_\Pi}{\rho_{\rm rad}}\right)^2 (k\ell_*)^3 \tilde{P}_{\rm GW}(k)$$

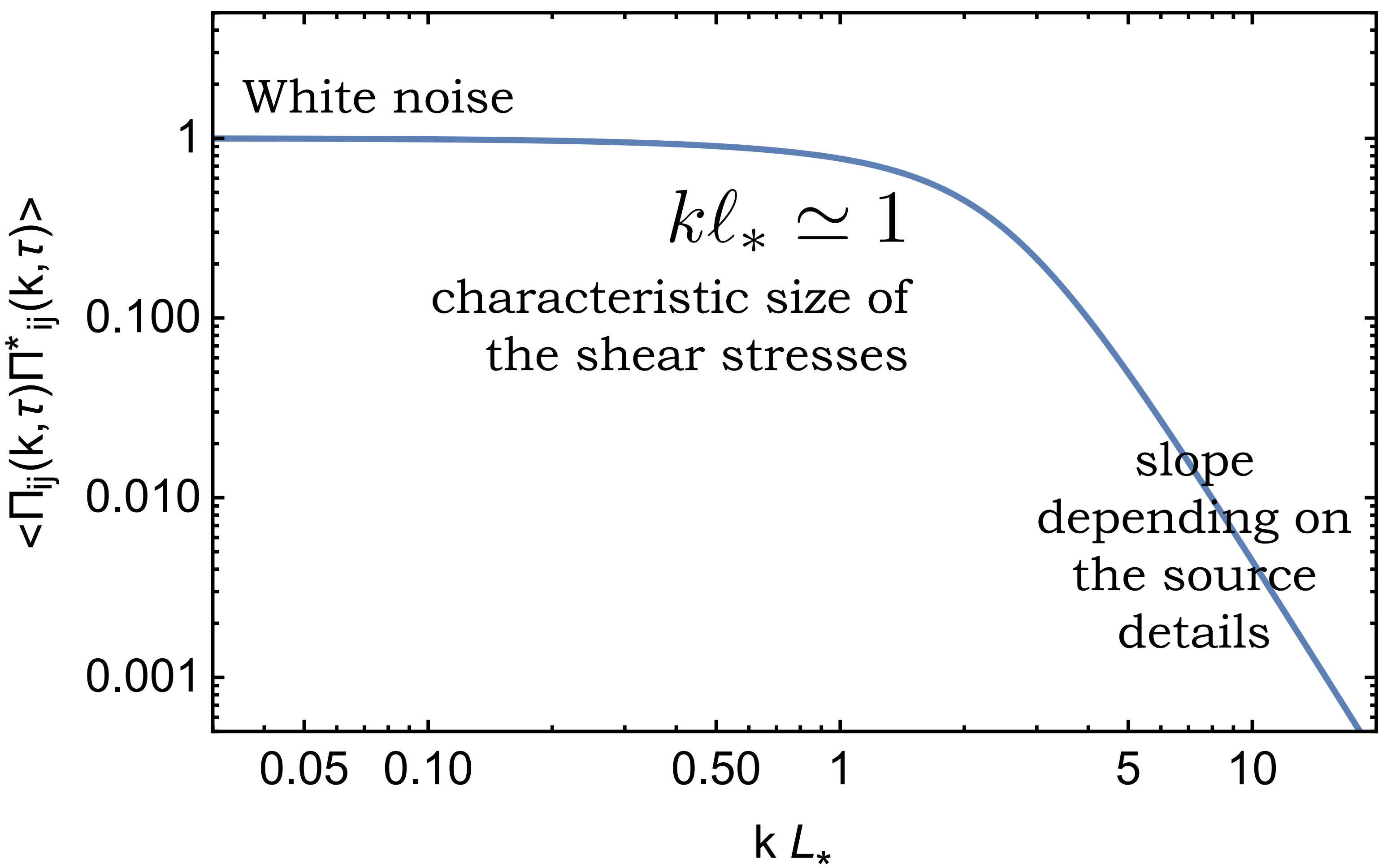

Fast source: independent on k for large enough scales (uncorrelated)

$$\boxed{\ell_* \leq H_*^{-1}}$$

SGWB from a **FAST** stochastic source in the radiation era

GW energy density parameter today for modes $1/\eta_0 \ll k \ll 1/\eta_{in}$

$$h^2\Omega_{\rm GW}(k,\eta_0) = \frac{3}{2\pi^2}h^2\Omega^0_{\rm rad}\left(\frac{g_0}{g_*}\right)^{\frac{1}{3}}(\Delta\eta\mathcal{H}_*)^2\left(\frac{\rho_\Pi}{\rho_{\rm rad}}\right)^2(k\ell_*)^3\tilde{P}_{\rm GW}(k)$$

$$1/\eta_0 \ll \underbrace{k \ll \mathcal{H}_*}_{\substack{\text{Range of validity}\\ \text{of the solution}}} \ll \underbrace{\,}_{\substack{\text{Causality of the}\\ \text{sourcing process}}} 1/(a_*\ell_*)$$

$$\boxed{\Omega_{\rm GW}(k) \propto (k\ell_*)^3}$$

SGWB from a **FAST** stochastic source in the radiation era

- Characteristic time of the source evolution $\delta t_c = \dfrac{\ell_*}{v_{\rm rms}}$

- Characteristic time of the GW production from the Green's function: $\delta t_{\rm gw} \sim \dfrac{1}{k}$

- GW production goes faster than source evolution for all relevant wave-numbers including the spectrum peak $k > \dfrac{v_{\rm rms}}{\ell_*}$

- One assumes that the source is constant in time for a finite time interval (which can be larger than the Hubble time) $\delta t_{\rm fin} \sim \mathcal{N} \delta t_c$

- One can then easily integrate to find the GW spectrum

$$\boxed{h^2 \Omega_{\rm GW}(k, \eta_0) \propto h^2 \Omega^0_{\rm rad} \left(\frac{g_0}{g_*}\right)^{\frac{1}{3}} \left(\frac{\rho_\Pi}{\rho_{\rm rad}}\right)^2 (k\ell_*)^3 \tilde{P}_{\rm GW}(k) \begin{cases} \ln^2[1 + \mathcal{H}_* \delta t_{\rm fin}] & \text{if } k\,\delta t_{\rm fin} < 1 \\ \ln^2[1 + (k/\mathcal{H}_*)^{-1}] & \text{if } k\,\delta t_{\rm fin} \geq 1 \end{cases}}$$

A. Roper Pol et al, arXiv:2201.05630

SGWB from a **FAST** stochastic source in the radiation era

$$k_{\rm peak} \simeq 4\pi/\ell_*$$

$$\Omega_{\rm gw,\, peak} \propto \left(\frac{\rho_\Pi}{\rho_{\rm rad}}\right)^2 (\mathcal{H}_*\ell_*)^2$$

Transition from k^3 to k^1

at $k \simeq 1/\delta t_{\rm fin}$

Can be smoother if

$\delta t_{\rm fin} > 1/\mathcal{H}_*$

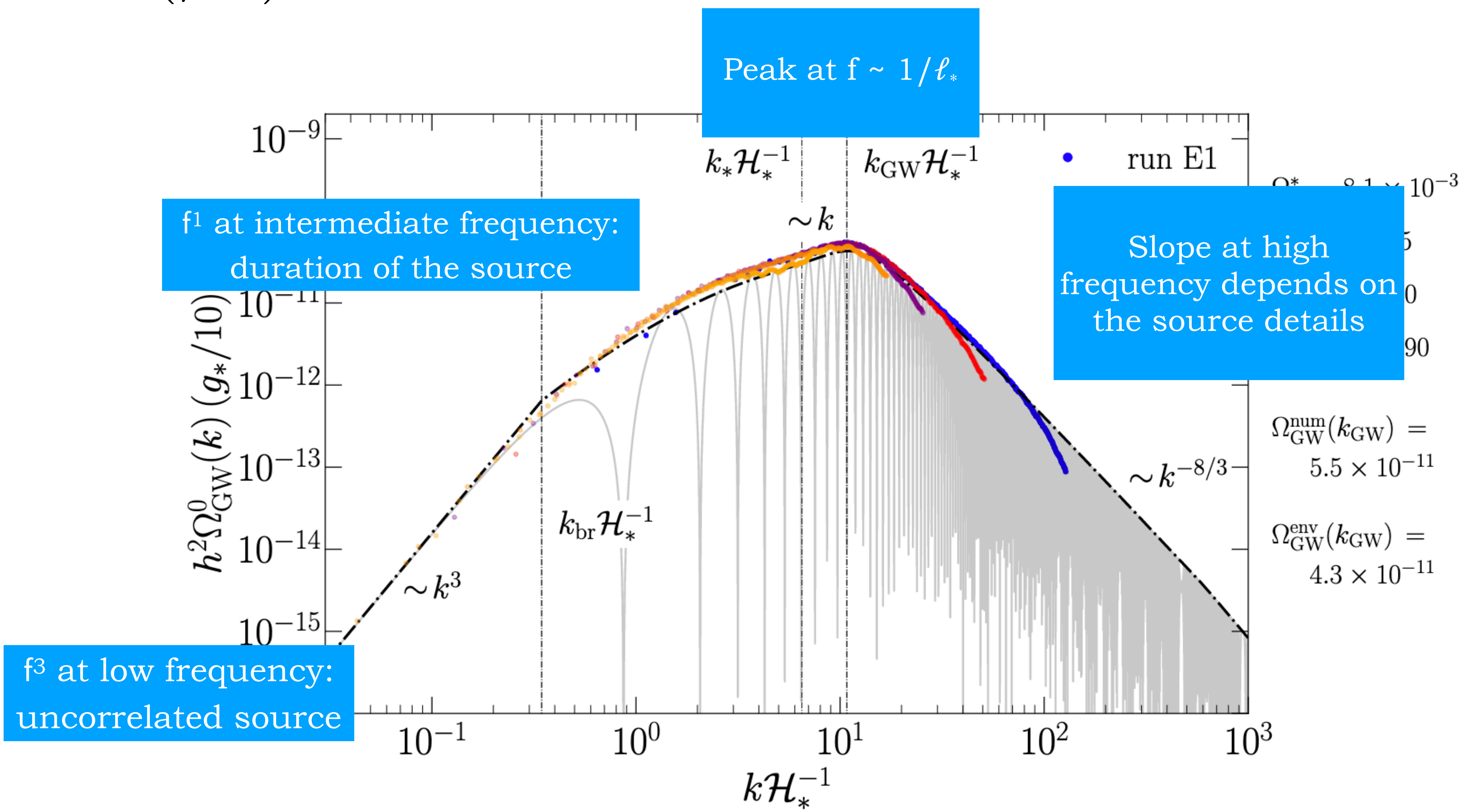

A. Roper Pol et al, arXiv:2201.05630

SGWB from a **CONTINUOUS** stochastic source in the radiation era

Typical example: topological defects

Suppose the source is operating continuously in the radiation dominated era

- No matching at the end time of the source
- No *free* sub-Hubble modes

$$H_r(\mathbf{k},\eta) = a\, h_r(\mathbf{k},\eta)$$

$$H_r^{\rm rad}(\mathbf{k},\eta) = \frac{16\pi G}{k}\int_{\eta_{\rm in}}^{\eta} d\tau\, a(\tau)^3\, \sin[k(\eta-\tau)]\,\Pi_r(\mathbf{k},\tau)$$

$$h_r{}'(\mathbf{k},\eta) = \frac{16\pi G}{a(\eta)}\int_{\eta_{\rm in}}^{\eta} d\tau\, a(\tau)^3\, \cos[k(\eta-\tau)]\,\Pi_r(\mathbf{k},\tau)$$

$$\langle h_r'(\mathbf{k},\eta)\, h_p'^{\,*}(\mathbf{q},\eta)\rangle = \frac{8\pi^5}{k^3}\,\delta^{(3)}(\mathbf{k}-\mathbf{q})\,\delta_{rp}\, h_c'^{\,2}(k,\eta) \qquad \frac{d\rho_{\rm GW}}{d\log k} = \frac{h_c'^{\,2}(k,\eta)}{16\pi G\, a^2(\eta)}$$

$$\frac{d\rho_{\rm GW}}{d\log k}(k,\eta) = \frac{4}{\pi}\frac{G}{a^4}\,k^3\int_{\eta_{\rm in}}^{\eta} d\tau\, a(\tau)^3\int_{\eta_{\rm in}}^{\eta} d\zeta\, a(\zeta)^3\,\mathcal{G}(k,\eta,\tau,\zeta)\,\Pi(k,\tau,\zeta)$$

SGWB from a **CONTINUOUS** stochastic source in the radiation era

Typical example: topological defects

Suppose the source is operating continuously in the radiation dominated era

- Scaling (property of the topological defects network)
- Decays very fast in off-diagonal $k\tau \neq k\zeta$
- Decays as a power law on the diagonal $k\tau = k\zeta$

D. Figueroa et al, arXiv:1212.5458

$$\Pi(k,\tau,\zeta) = \frac{v^4}{\sqrt{\tau\zeta}}\,\frac{\mathcal{U}(k\tau,k\zeta)}{a(\tau)a(\zeta)}$$

$$\frac{d\rho_{\rm GW}}{d\log k}(k,\eta) = \frac{4}{\pi}\frac{G}{a^4}\,k^3\int_{\eta_{\rm in}}^{\eta} d\tau\, a(\tau)^3\int_{\eta_{\rm in}}^{\eta} d\zeta\, a(\zeta)^3\,\mathcal{G}(k,\eta,\tau,\zeta)\,\Pi(k,\tau,\zeta)$$

SGWB from a **CONTINUOUS** stochastic source in the radiation era

Typical example: topological defects

Suppose the source is operating continuously in the radiation dominated era

$$h^2\Omega_{\rm GW}(f) = \frac{32}{3}h^2\Omega_{\rm rad}\left(\frac{v}{M_{\rm Pl}}\right)^4 F_{\rm RD}^{[\mathcal{U}]}(\infty)$$

TODAY FLAT SPECTRUM
AT SUB-HORIZON MODES
IN THE RADIATION ERA

D. Figueroa et al, arXiv:1212.5458

Progressively
independent on the
upper bound

$$\frac{d\rho_{\rm GW}}{d\log k}(k,\eta) = \frac{32}{3}\Omega_{\rm rad}\frac{\rho_c}{a^4}\left(\frac{v}{M_{\rm Pl}}\right)^4\int_{x_{\rm in}}^{x}dx_1\int_{x_{\rm in}}^{x}dx_2\,\sqrt{x_1x_2}\,\mathcal{G}(x,x_1,x_2)\,\mathcal{U}(x_1,x_2)$$

D. Figueroa et al, arXiv:1212.5458

SGWB from a **CONTINUOUS** stochastic source in the radiation era

Typical example: topological defects

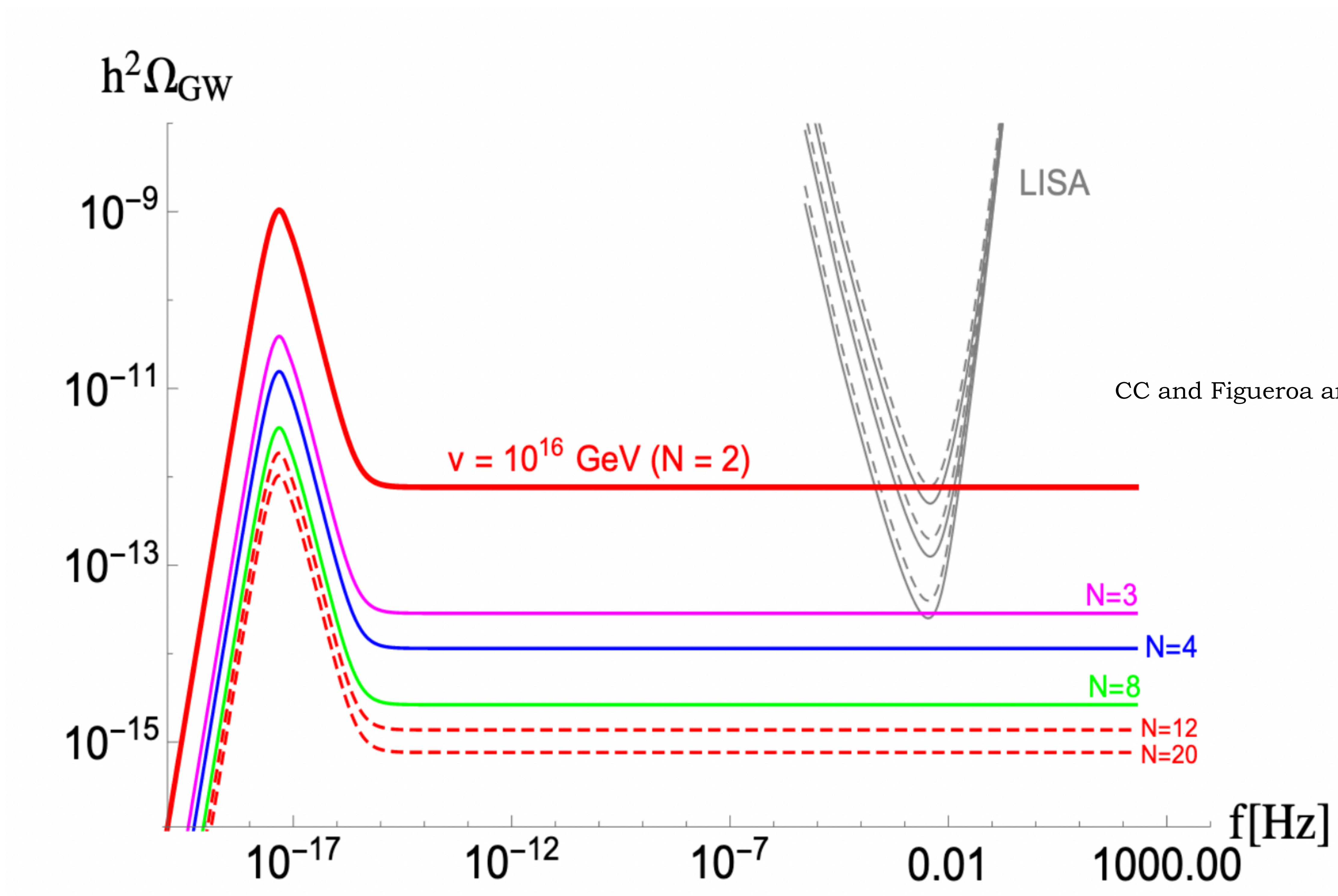

CC and Figueroa arXiv:1801.04268

Examples of signals

Inflation: phase transition of the Inflaton field

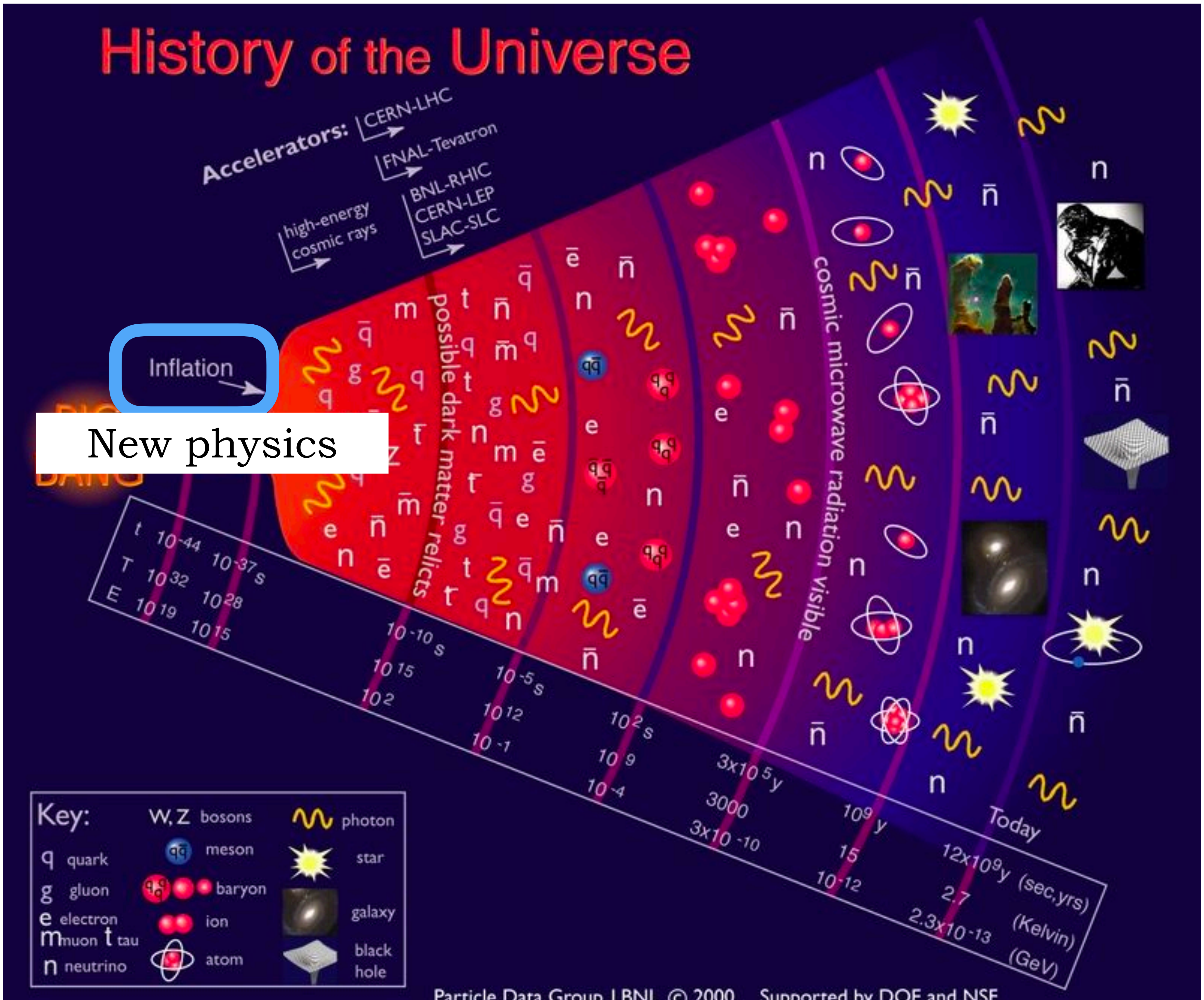

GW signal from (slow roll) inflation

Gw detectors offer the amazing opportunity to probe the inflationary power spectrum (and the model of inflation) down to the tiniest scales

BUT! The signal in the standard slow roll scenario is too low because of CMB observational bound

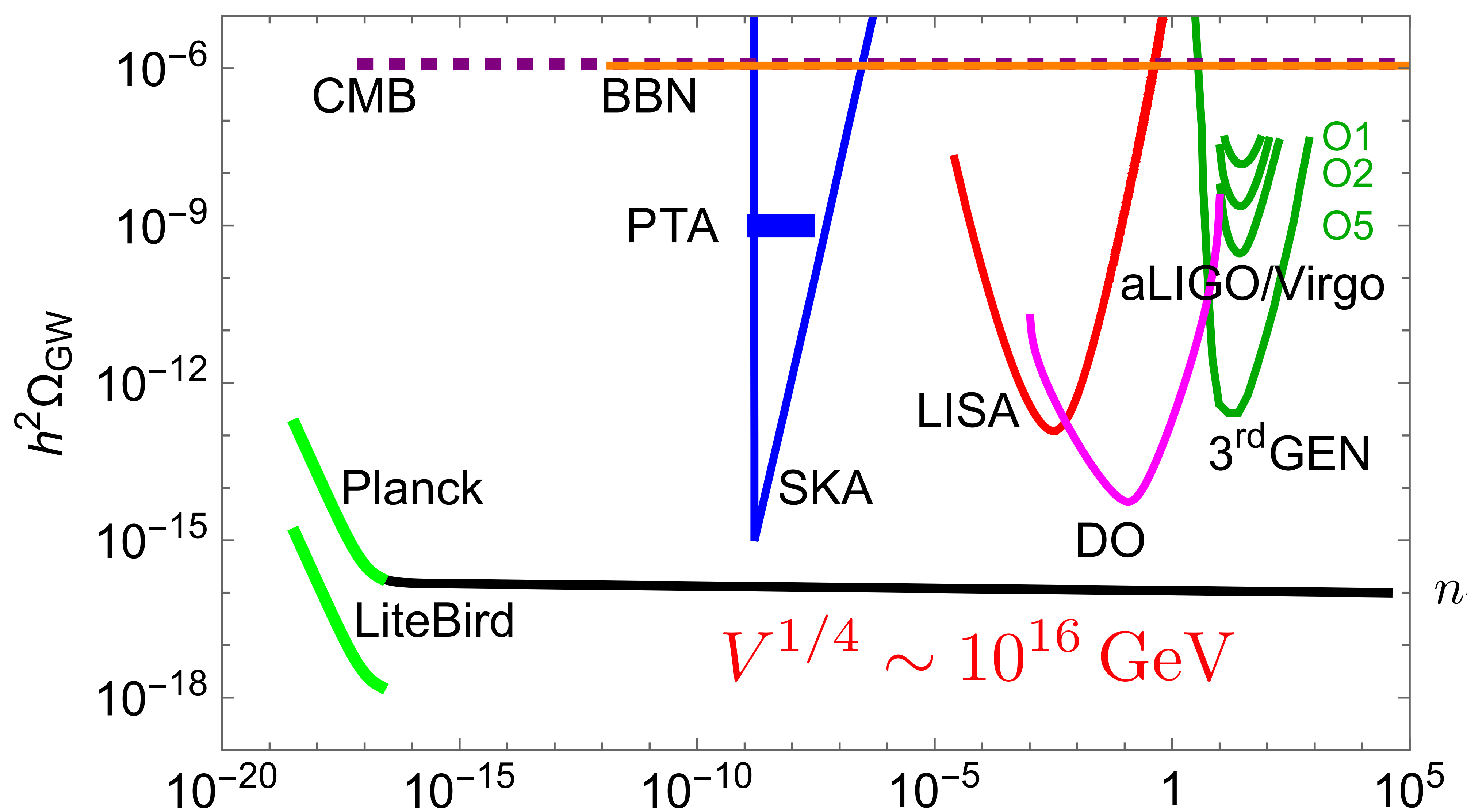

$n_T(\phi) \sim -2\epsilon(\phi)$

$$f \simeq 15\,\mathrm{mHz}\left(\frac{k}{10^{13}\,\mathrm{Mpc}^{-1}}\right)$$

GW signal from (slow roll) inflation

- tensor spectrum $$\mathcal{P}_h = \frac{2}{\pi}\frac{H^2}{m_{Pl}^2}\left(\frac{k}{aH}\right)^{-2\epsilon} \qquad \epsilon \equiv \frac{M_P^2}{2}\left(\frac{V'}{V}\right)^2 \ll 1$$
- transfer function as modes re-enter the Hubble scale

$$\Omega_{\rm GW}(f) = \frac{3}{128}\,\Omega_{\rm rad}\, r\, \mathcal{P}_{\mathcal{R}}^{*}\left(\frac{f}{f_*}\right)^{n_T}\left[\frac{1}{2}\left(\frac{f_{\rm eq}}{f}\right)^2 + \frac{16}{9}\right]$$

- tensor to scalar ratio $r = \mathcal{P}_h/\mathcal{P}_{\mathcal{R}}$ $\qquad r_* < 0.038$ Planck+BICEP+ACT+BAO limit
- scalar amplitude at CMB pivot scale $\mathcal{P}_{\mathcal{R}}^* \simeq 2\cdot 10^{-9} \qquad k_* = \frac{0.05}{\rm Mpc}$
- GW signal extended in frequency: $H_0 \leq f \leq H_{\rm inf}$

continuous sourcing of GW as modes re-enter the Hubble horizon

GW signal from (non-standard) inflation

There is the possibility to enhance the signal going beyond the standard inflationary scenario: adding extra fields, modifying the inflaton potential, modifying the gravitational interaction, adding a phase with stiff equation of state…

$$H_r''(\mathbf{k},\eta) + \left(k^2 - \frac{a''}{a}\right) H_r(\mathbf{k},\eta) = \boxed{16\pi G\, a^3\, \Pi_r(\mathbf{k},\eta)}$$

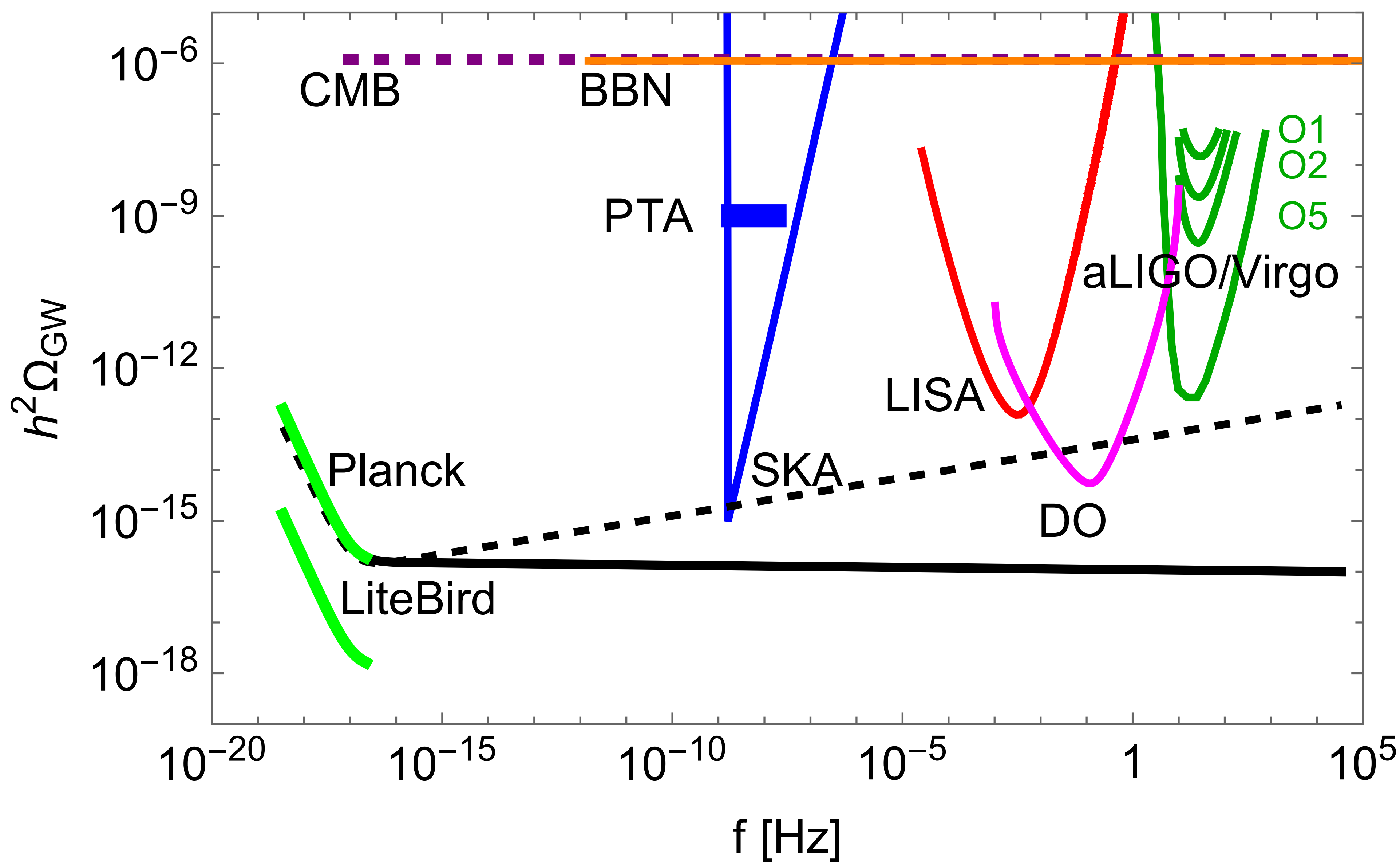

Example: inflaton-gauge field coupling

Add a term in the Lagrangian coupling pseudo-scalar inflaton to gauge fields

$$V(\phi) + \frac{\phi}{4\Lambda} F_{\mu\nu}\tilde{F}^{\mu\nu}$$

Production of gauge fields and consequently of GWs through the source

$$\Pi_{ij} \sim [-E_i E_j - B_i B_j]^{TT}$$

EXAMPLE IN THE LISA BAND:

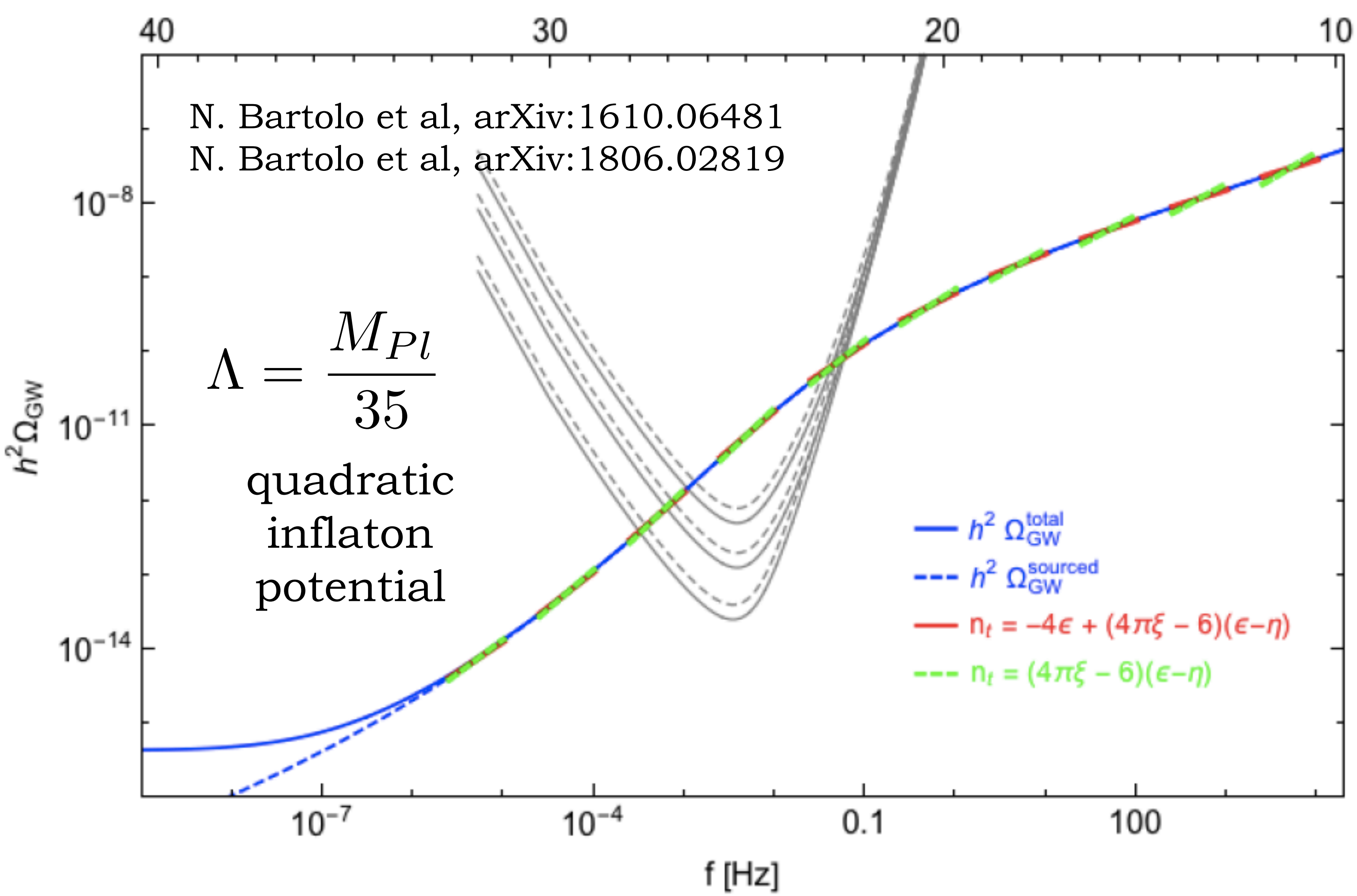

OTHER SIGNATURES/ CONSTRAINTS: non-gaussianity, chirality, primordial black holes

Predictions of the signal must be refined accounting for non-linearity of the system

Example: GW signal from second order scalar perturbations and associated primordial black holes

- At linear order in cosmological perturbation theory, scalar and tensor perturbations are decoupled and evolve separately, but *at second order they mix*
- Gradients in the scalar component *can source the tensor component at second order*: since the scalar fluctuations are order of 10^{-5}, the tensors are small $\partial_i \Psi, \partial_i \Phi$
- However, *if the scalar component is enhanced*, the induced tensor component can be important (e.g. from a phase of ultra slow-roll close to reheating)
- The enhanced scalar density fluctuations can collapse upon horizon reentry and produce *primordial black holes* whose properties are linked to those of the tensor spectrum

$$\Omega_{\rm GW}(f) = \Omega_{\rm rad} \int_0^\infty \mathrm{d}v \int_{|1-v|}^{1+v} \mathrm{d}u \, \mathcal{K}(u,v) \mathcal{P}_{\mathcal{R}}(uk) \mathcal{P}_{\mathcal{R}}(vk)$$

Second order in curvature perturbation

$\phi_0 = 3M_{\rm P}$ and $V_0 = 2.3 \cdot 10^{-10} M_{\rm P}^4$

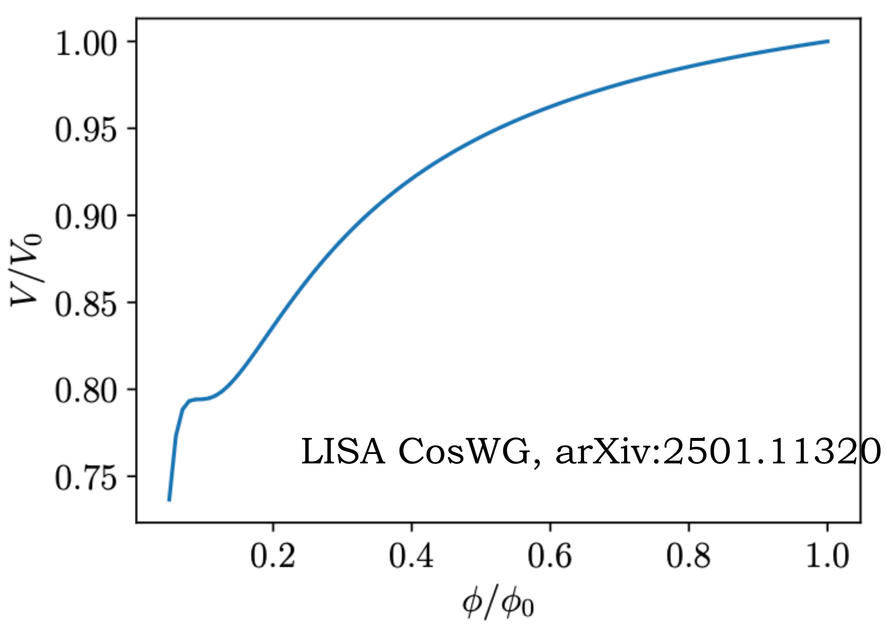

The signal depends on the shape of the curvature power spectrum, several phenomenological models are proposed

Example: GW signal from second order scalar perturbations and associated primordial black holes

Source, Π_{ij} from a combination of

$$\partial_i \Psi, \partial_i \Phi$$

EXAMPLE OF SIGNAL IN THE LISA BAND:

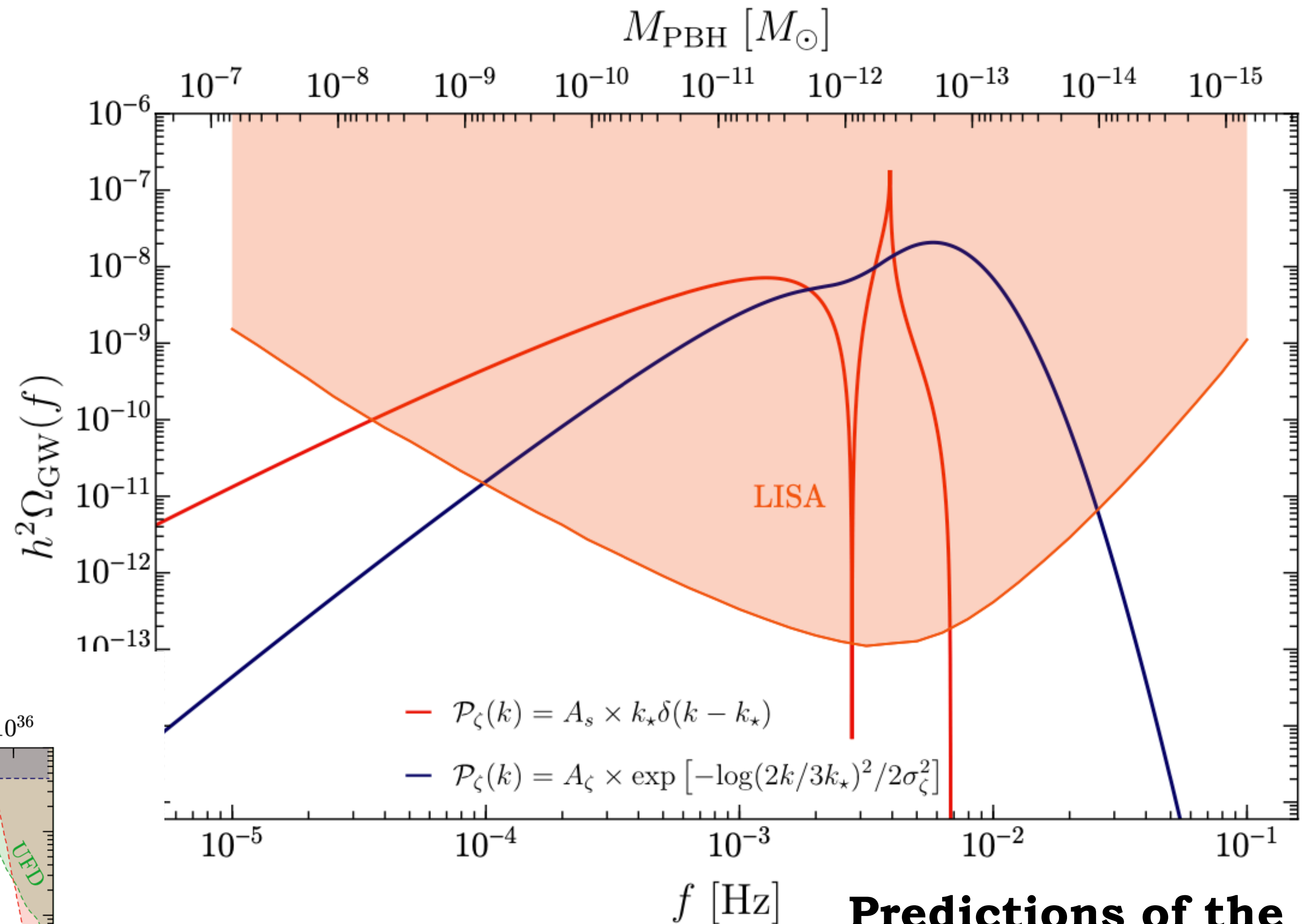

Predictions of the signal must be refined accounting for non-gaussianity

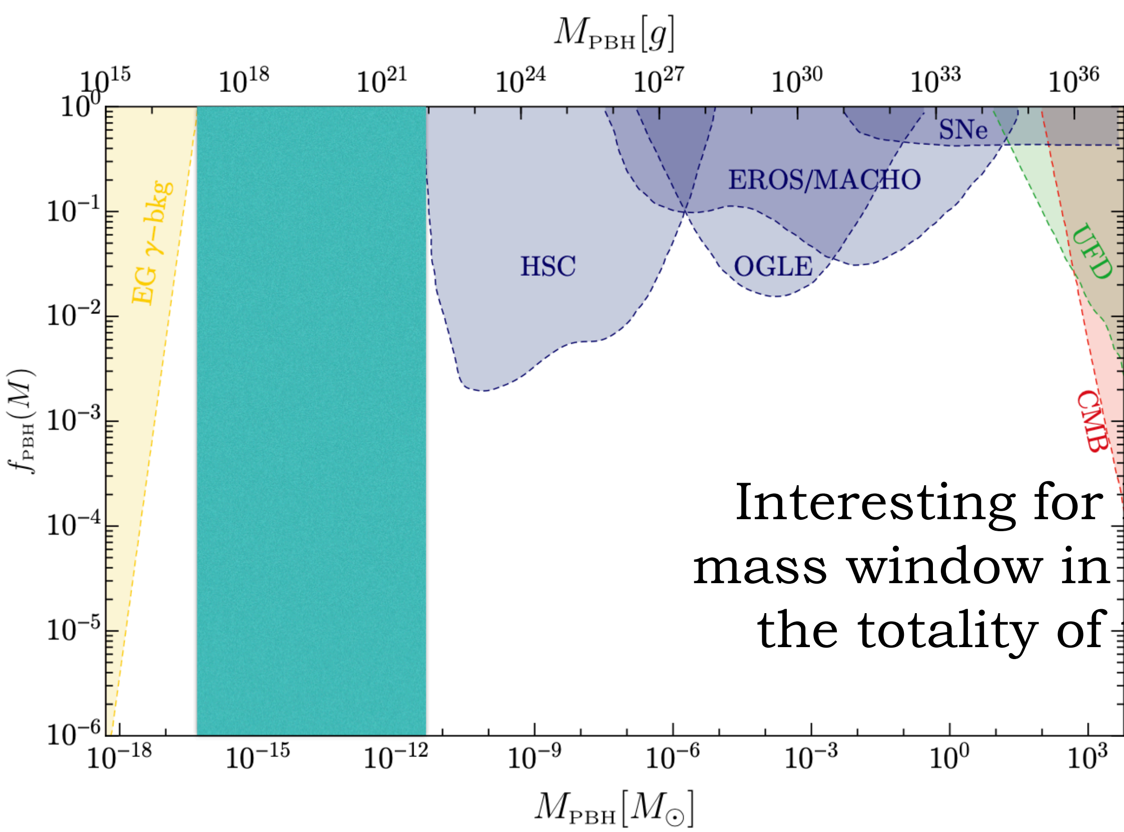

Interesting for LISA: PBH in the mass window in which they can be the totality of the Dark Matter

$$\frac{M_H}{M_\odot} \simeq 7 \times 10^{-11} \frac{k}{10^{12}\,\mathrm{Mpc}^{-1}}$$

A. Riotto, https://indico.math.cnrs.fr/event/5766/contributions/5153/attachments/2801/3587/Paris2021.pdf

Example: resonant particle production at preheating

$$V(\phi) + \frac{1}{2} g^2 \phi^2 \chi^2$$

Kofman et al. arXiv:hep-ph/9704452

GW sourced from inhomogeneous field

$$\Pi_{ij} \sim [\partial_i \chi \partial_j \chi]^{TT}$$

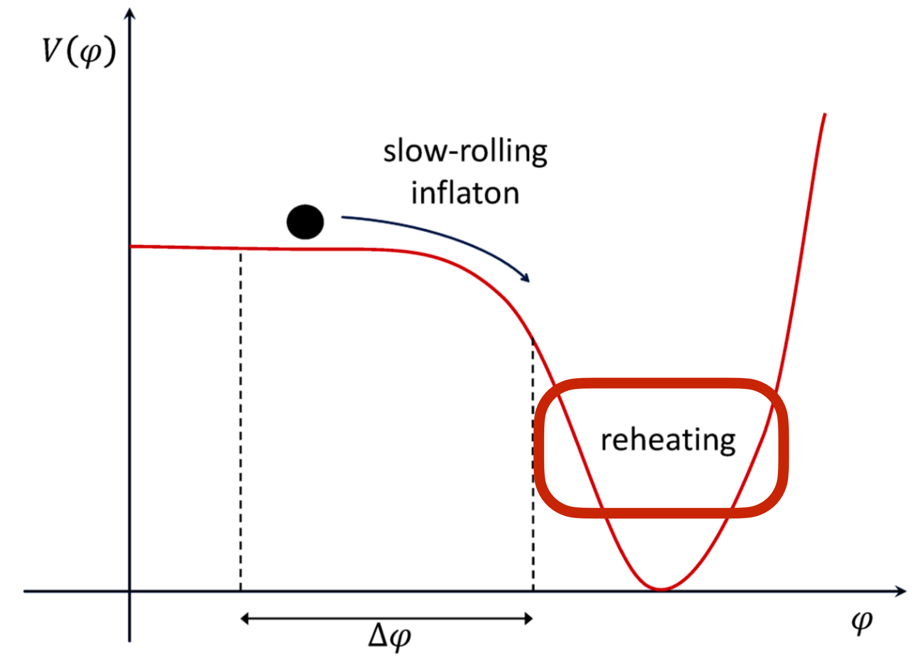

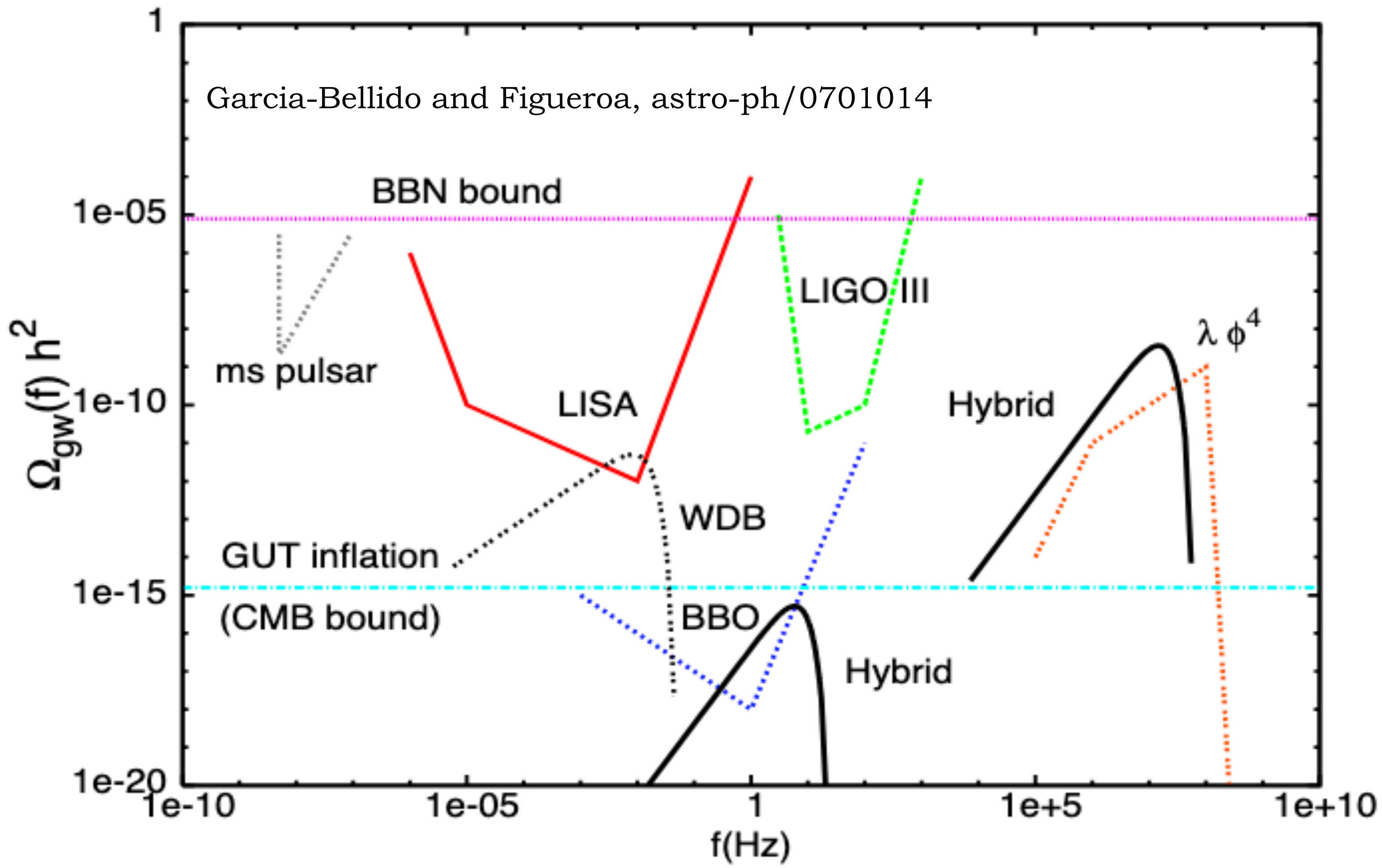

high frequency detectors up to 10^{18} GeV, sensitivity still above BBN and CMB bounds

Aggarwal et al, arXiv:2501.11723

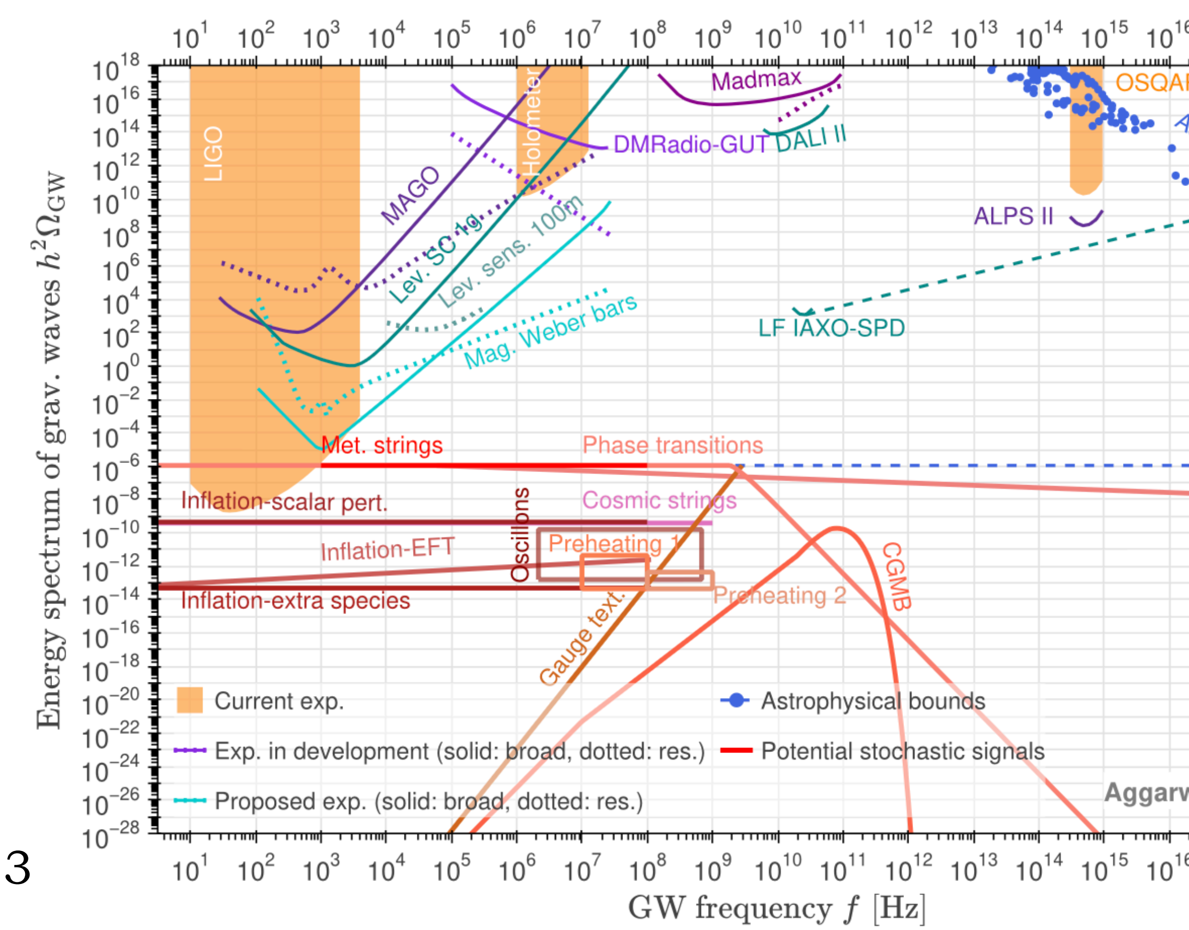

An example of possible detection at PTA?

Very small value of
r at CMB scale

$$\Omega_{\rm GW}(f) = \frac{3}{128}\,\Omega_{\rm rad}\, r\, \mathcal{P}^*_{\mathcal{R}} \left(\frac{f}{f_*}\right)^{n_T} \left[\frac{1}{2}\left(\frac{f_{\rm eq}}{f}\right)^2 + \frac{16}{9}\right]$$

$$\times \left(\frac{f}{f_{\rm RD}}\right)^{\frac{2(3w-1)}{3w+1}}$$

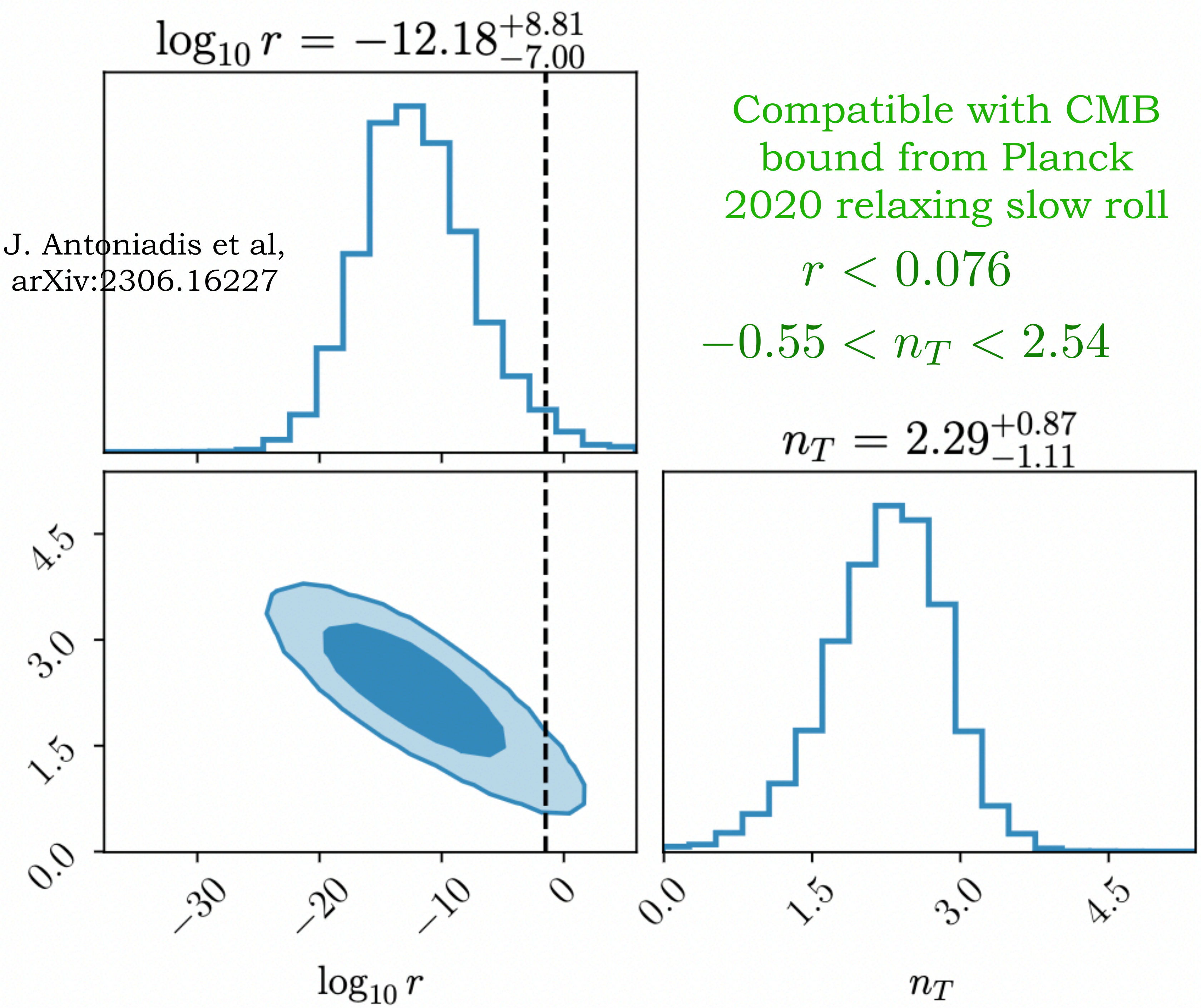

J. Antoniadis et al,
arXiv:2306.16227

Compatible with CMB
bound from Planck
2020 relaxing slow roll

$$r < 0.076$$

$$-0.55 < n_T < 2.54$$

Would this be
compatible with slow
roll and a stiff equation
of state? Marginally

$$\gamma = 5 - n_T + \frac{2(1-3w)}{3w+1}$$

Bound between 0 and -2

$$\gamma_{\rm best\ fit} \simeq 2.7 \;\longrightarrow\; n_T \gtrsim 0.3$$

Strong degeneracy between the
two parameters $\quad n_T = -0.16 \log_{10} r + 0.46$

phase transitions predicted by the standard model of particle physics: electroweak and QCD

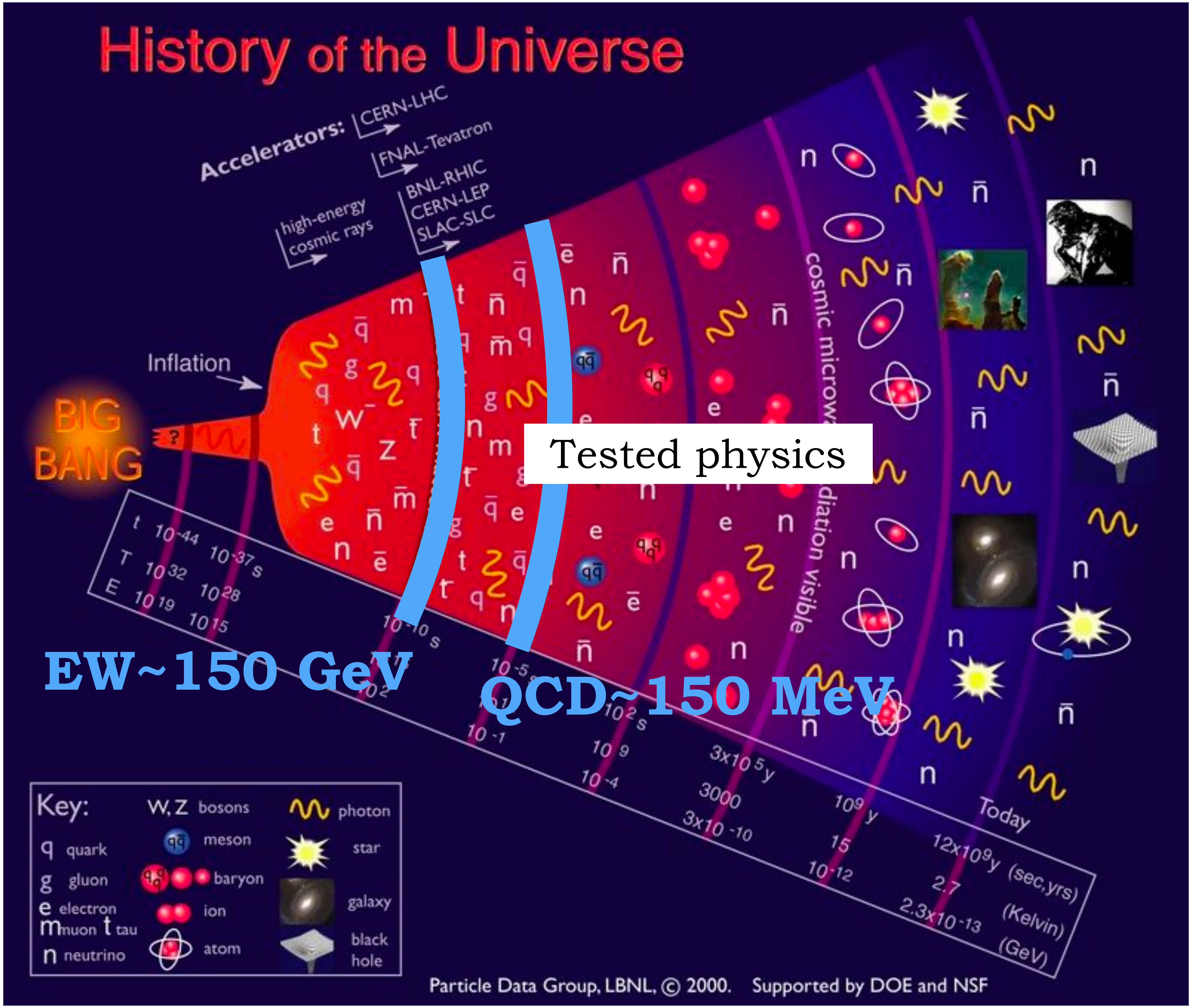

First order phase transitions

- We know that at least two PTs occurred in the universe, the EW one and the QCD one: according to the standard model, they are both **crossovers**
- However, *sizeable (detectable) GW generation requires a first order PT*, proceeding through the *nucleation of true vacuum bubbles*

Second order phase transition

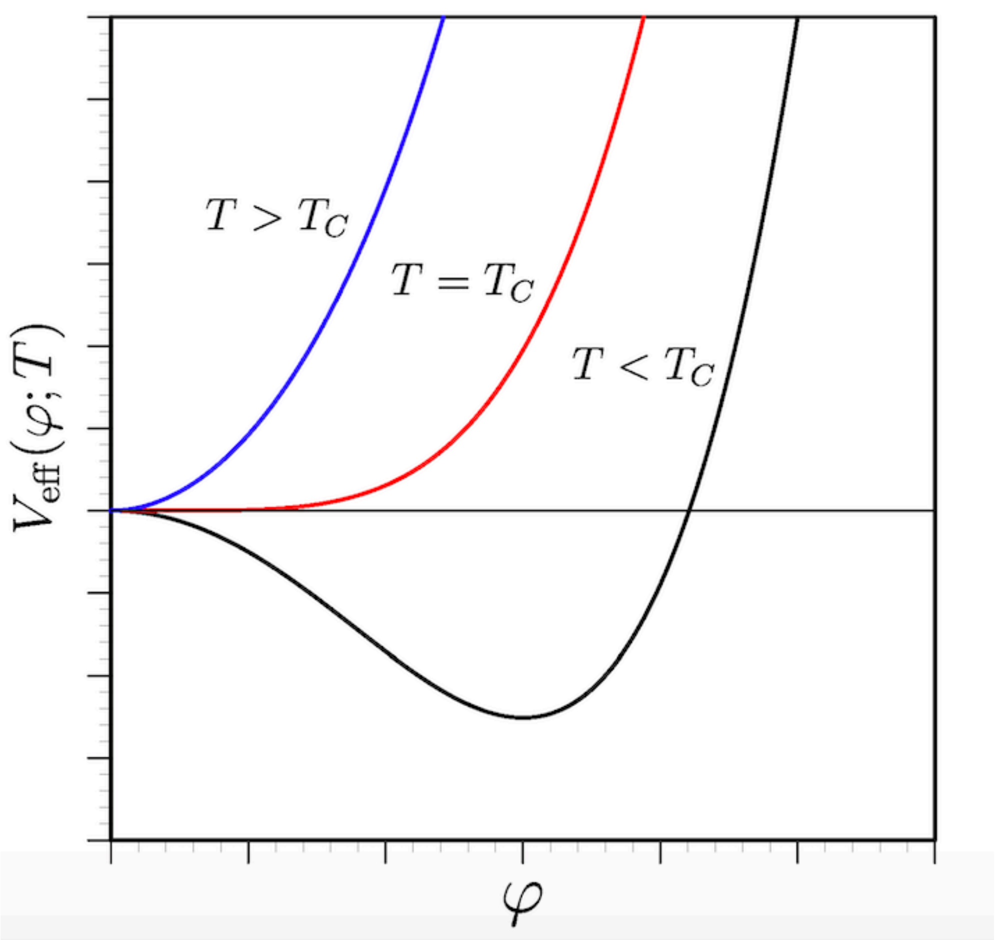

First order phase transition

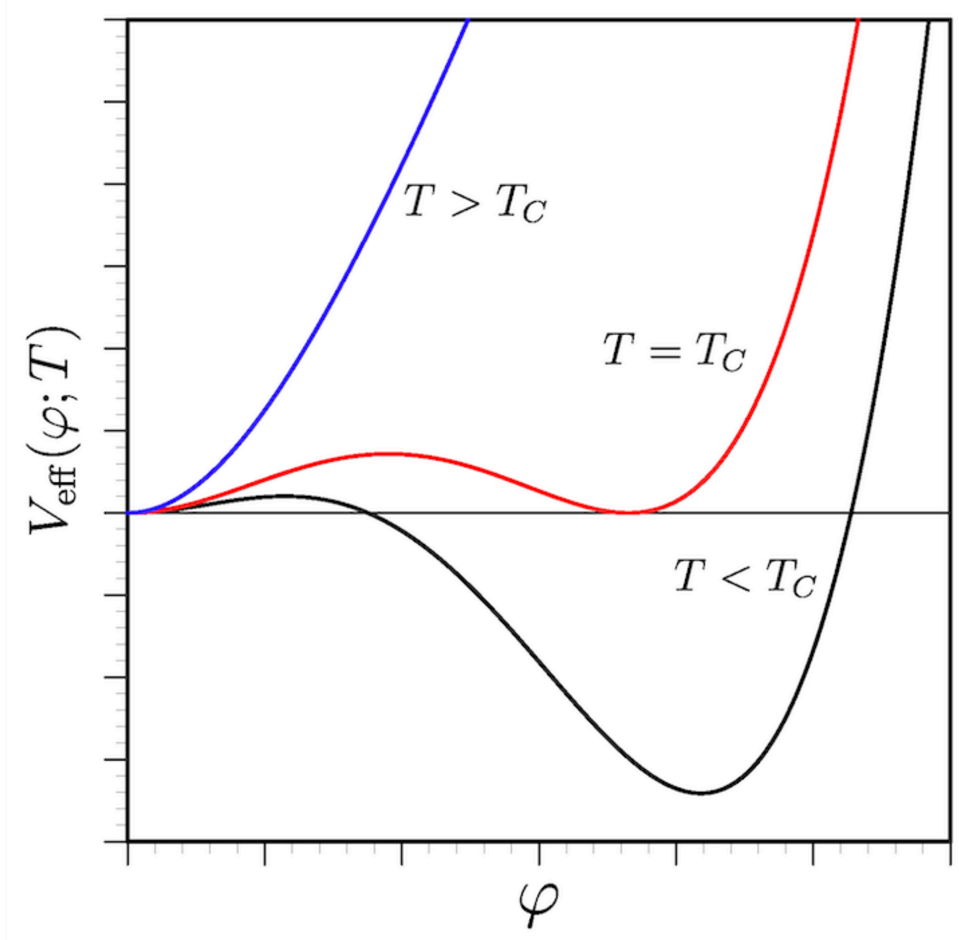

Image credit: E. Senaha, Symmetry 2020

First order phase transitions

- We know that at least two PTs occurred in the universe, the EW one and the QCD one: according to the standard model, they are both **crossovers**
- However, *sizeable (detectable) GW generation requires a first order PT*, proceeding through the *nucleation of true vacuum bubbles*

EWPT

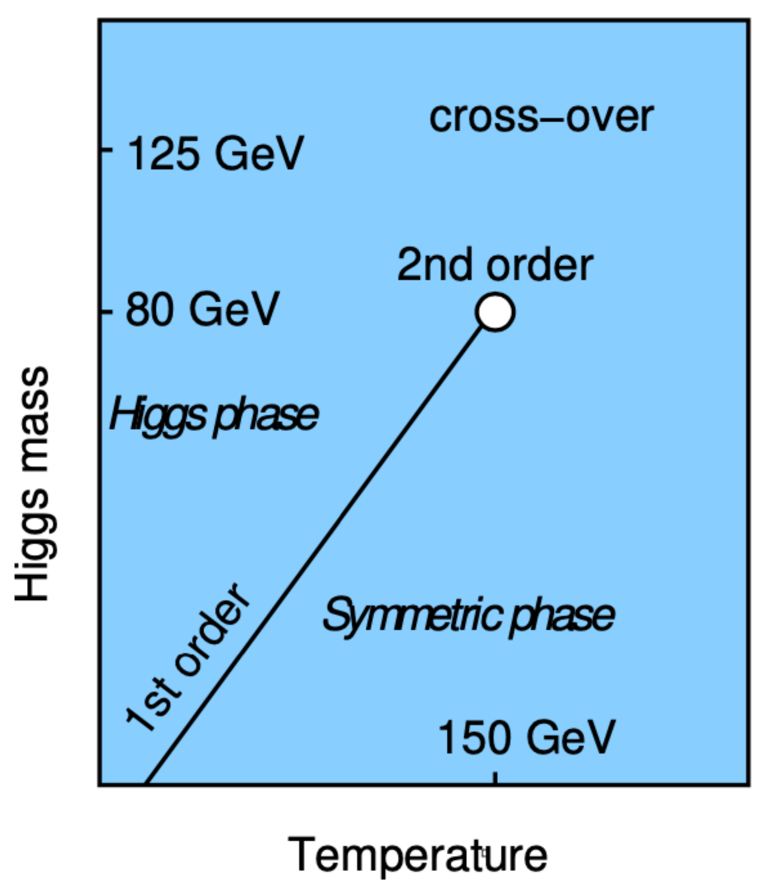

M. Hindmarsh et al, arXiv:2008.09136

QCDPT

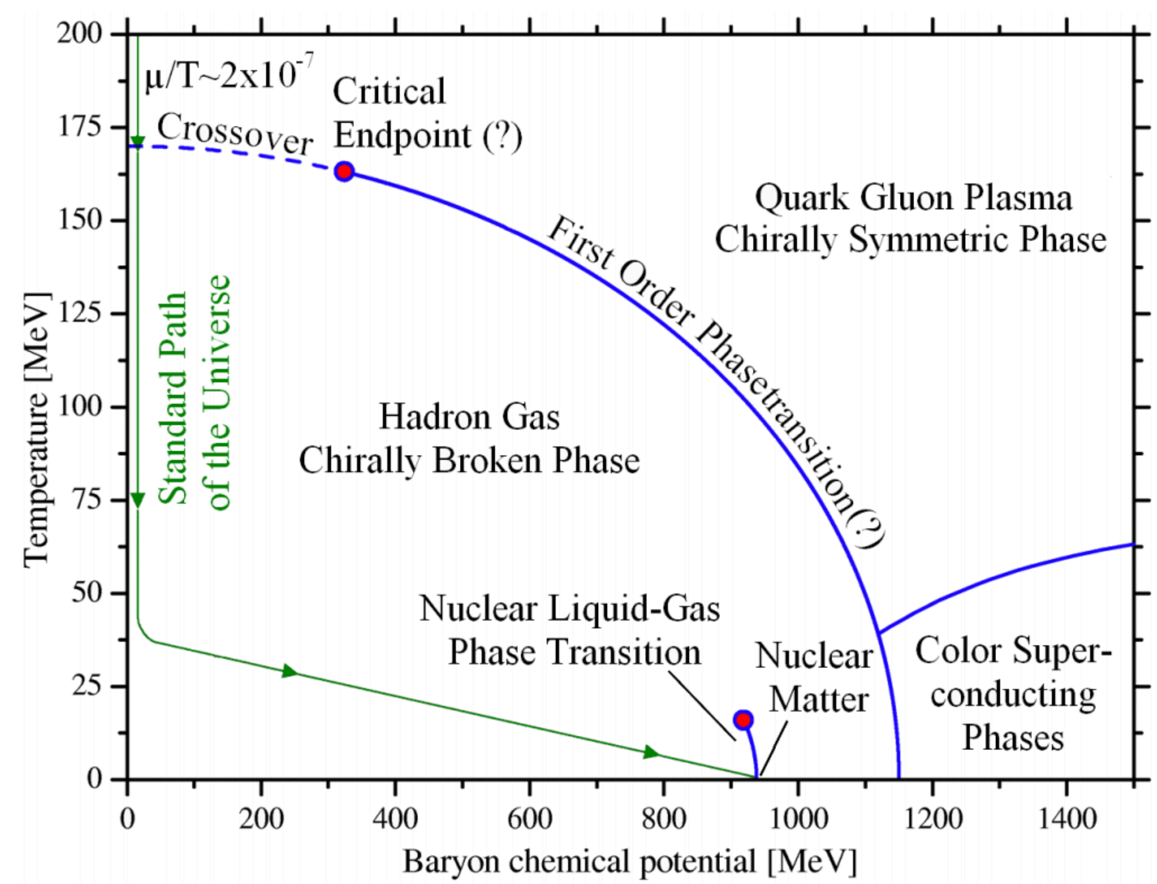

T. Boekel and J. Schaffner-Bielich, arXiv:1105.0832

First order phase transitions

- We know that at least two PTs occurred in the universe, the EW one and the QCD one: according to the standard model, they are both **crossovers**
- However, *sizeable (detectable) GW generation requires a first order PT*, proceeding through the *nucleation of true vacuum bubbles*

EWPT

might become first order in BSM EW sector extensions: SM + light scalars (SM+singlet, SUSY, 2HDM, composite Higgs…)

QCDPT

Depends on the conditions in the early universe: **might become first order if the lepton asymmetry in the universe is large**

D. Schwarz and Stuke, arXiv:0906.3434
M. Middeldorf-Wygas et al, arXiv:2009.00036

OTHER EXAMPLES OF POSSIBLE FOPTs:

- **Effective approaches:** heavy new physic represented by higher dimensional operators
- **Conformal models:** e.g. conformal symmetry breaking with dilaton
- **New symmetries:** extend the SM with e.g. $U(1)_{B-L}$
- **Hidden sectors:** provide also dark matter candidates, PT can be as strong as one wants
- **Peccei Quinn** can be first order depending on the realisation

Opportunity to probe high energy physics scenarios beyond the standard model

First order phase transitions

Sources of tensor anisotropic stress (and thereby GWs) at a first order phase transition:

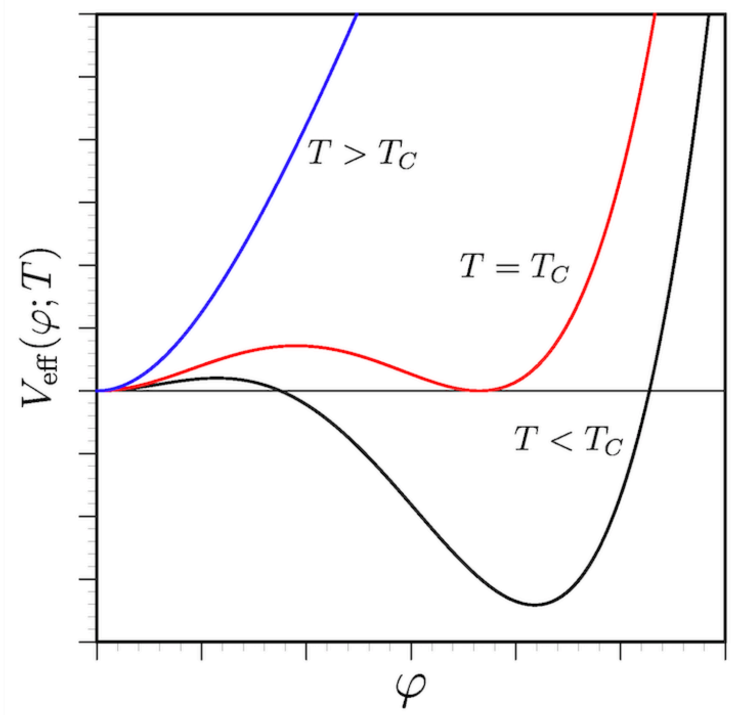

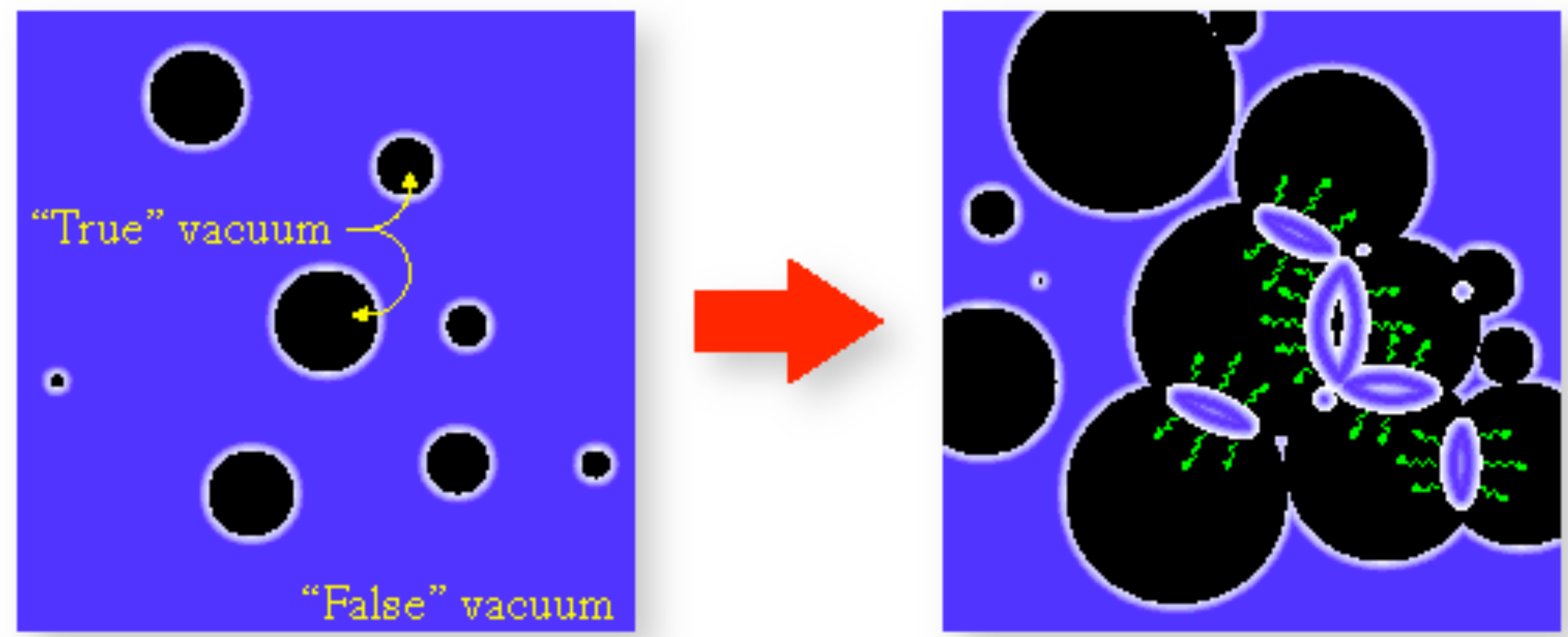

Several processes, rich phenomenology!

- Bubble collision (scalar field gradients) $\quad \Pi_{ij}^{TT} \sim [\partial_i\phi\partial_j\phi]^{TT}$
- Bulk fluid motion $\quad \Pi_{ij}^{TT} \sim [\gamma^2(\rho+p)v_iv_j]^{TT}$ sound waves and/ or turbulence
- Electromagnetic fields $\quad \Pi_{ij}^{TT} \sim [-E_iE_j - B_iB_j]^{TT}$

First order phase transitions

The signal depends on the following parameters

- The temperature of the FOPT T_*
- The amount of energy available in the source K, connected to the PT strength
- The size of the anisotropic stresses, connected to the bubble size $R_* = v_w/\beta$
- The bubble wall velocity v_w

$T_*,\ \alpha,\ \dfrac{\beta}{H_*}$ → Determined by the effective potential

v_w, K → Determined by the bubble expansion dynamics and interaction, and by the fluid dynamics (sound speed fixed)

If the PT is strong and non-linearities in the bulk fluid develop: fraction of kinetic energy in turbulent motions $\varepsilon = \dfrac{K_{\rm turb}}{K}$

Most of these parameters are known (at least in principle) given a PT model + numerical simulations of the fluid dynamics

numerical simulations are necessary to infer the GW signal because of non-linear dynamics and/or complicated fluid shells profiles and/or intrinsic randomness of the process

First order phase transitions

The signal depends on the following parameters

- The temperature of the FOPT T_*
- The amount of energy available in the source K, connected to the PT strength
- The size of the anisotropic stresses, connected to the bubble size $R_* = v_w/\beta$
- The bubble wall velocity v_w

$T_*,\ \alpha,\ \dfrac{\beta}{H_*}$ → Determined by the effective potential

v_w, K → Determined by the bubble expansion dynamics and interaction, and by the fluid dynamics (sound speed fixed)

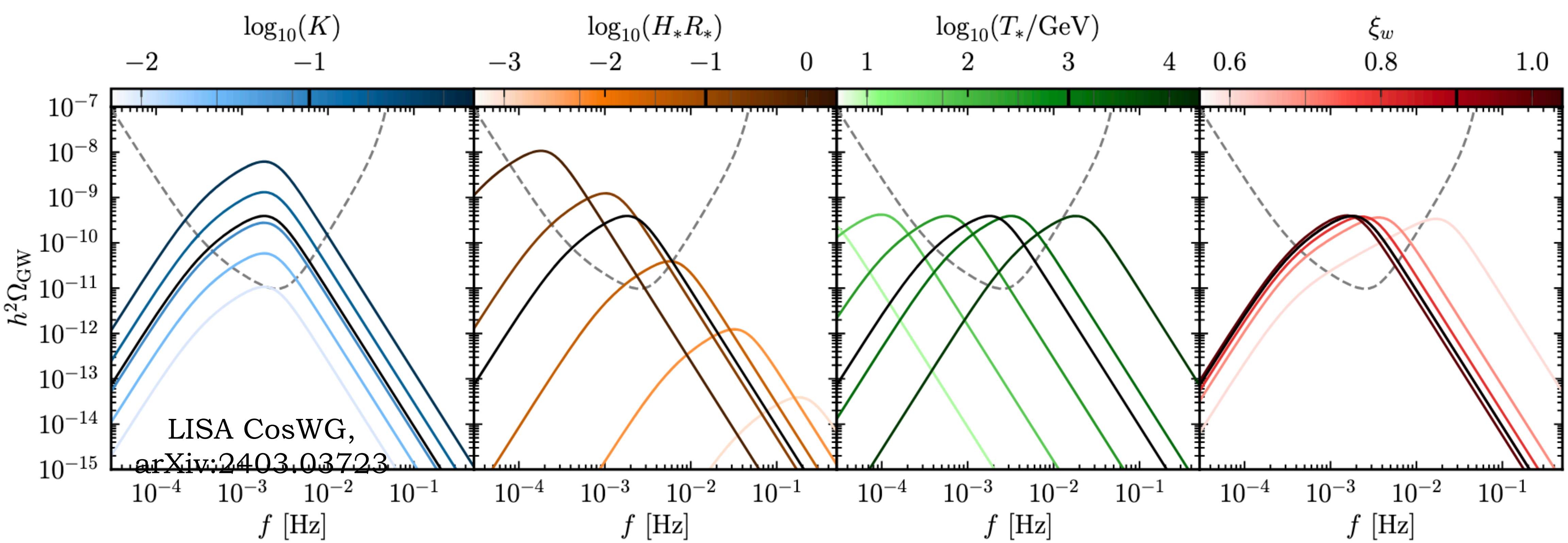

(b) sound waves (black: $K = 0.1$, $H_*R_* = 0.1$, $\xi_w = 0.9$, $T_* = 1\,\mathrm{TeV}$)

First order phase transitions

LIGO Virgo Kagra

$$1\,\mathrm{Hz} < f < 1000\,\mathrm{Hz} \quad \longrightarrow \quad 10^6\,\mathrm{GeV} \lesssim T_* \lesssim 10^{10}\,\mathrm{GeV}$$

CC et al, ArXiv:2406.02359

LVK constraints from non-detection

Badger et al, arXiv:2209.14707

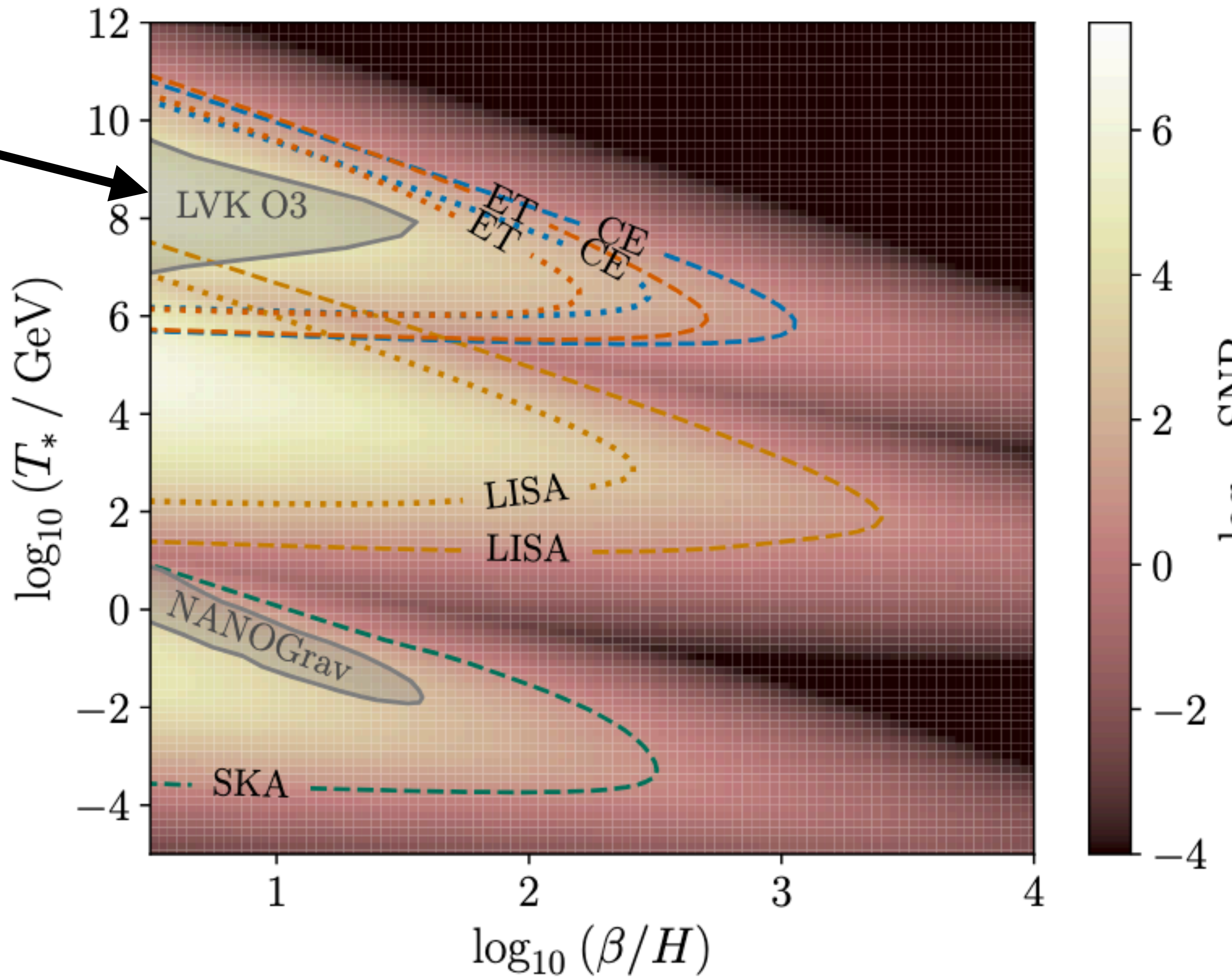

Parameter to which the signal amplitude is *inversely* proportional

Peccei-Quinn phase transition

$$T_{\mathrm{PQ}} \sim F_a$$

$$10^{7-8}\,\mathrm{GeV} \lesssim F_a \lesssim 10^{10-11}\,\mathrm{GeV}$$

First order phase transitions

Pulsar Timing Arrays

$$10^{-9}\,\mathrm{Hz} < f < 10^{-7}\,\mathrm{Hz} \quad \longrightarrow \quad 1\,\mathrm{MeV} \lesssim T_* \lesssim 1\,\mathrm{GeV}$$

CC et al, ArXiv:2406.02359

PTAs offer the possibility
to probe the
QCD energy scale

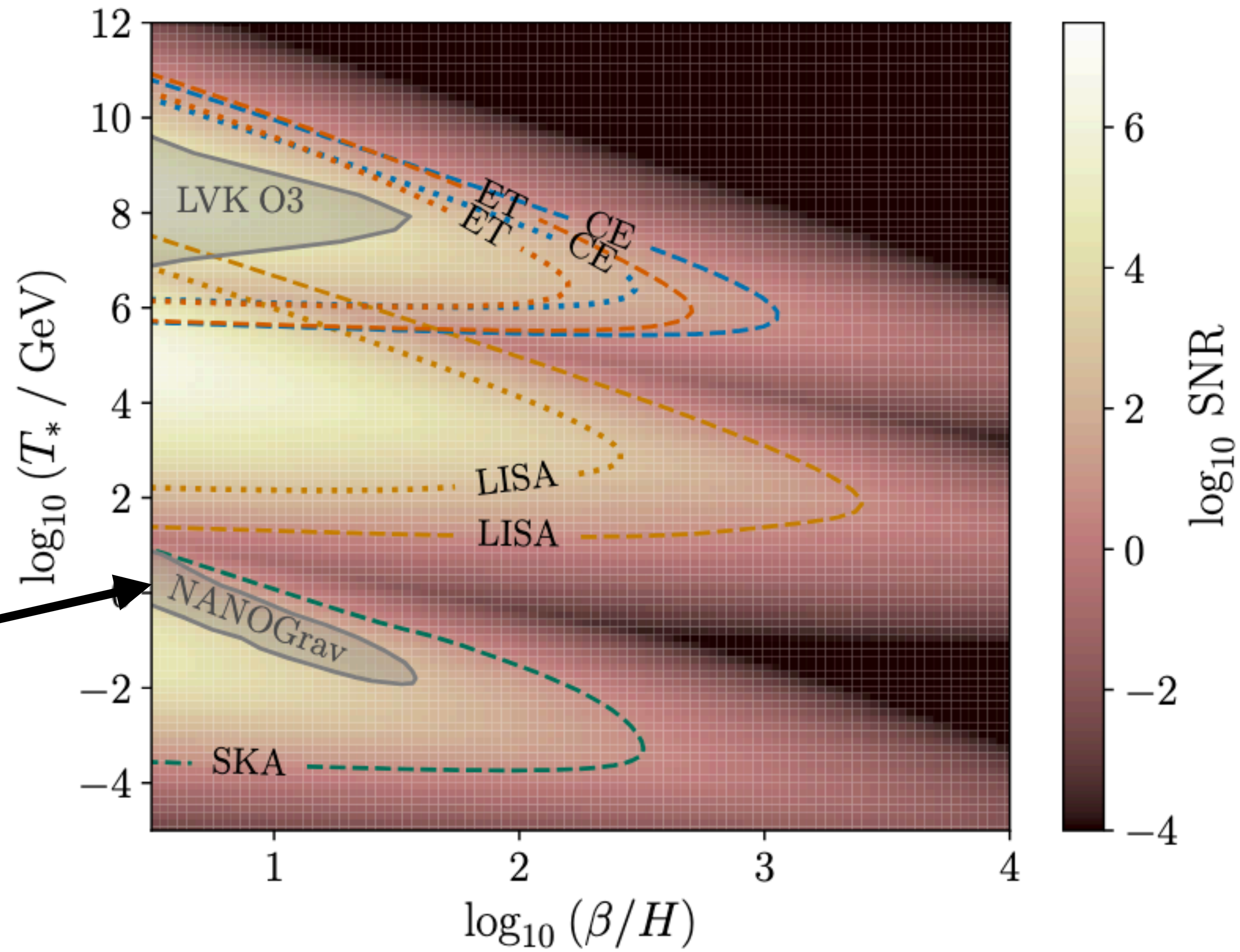

Parameter space
region that could
explain the
measurement

Afzal et al arXiv:2306.16219

Parameter to which the signal amplitude is *inversely* proportional

First order phase transitions

Laser interferometer space antenna

$$10^{-5}\,\mathrm{Hz} < f < 0.1\,\mathrm{Hz} \quad \longrightarrow \quad 10\,\mathrm{GeV} \lesssim T_* \lesssim 10^5\,\mathrm{GeV}$$

CC et al, ArXiv:2406.02359

LISA offers the possibility to probe the **EW energy scale and beyond**

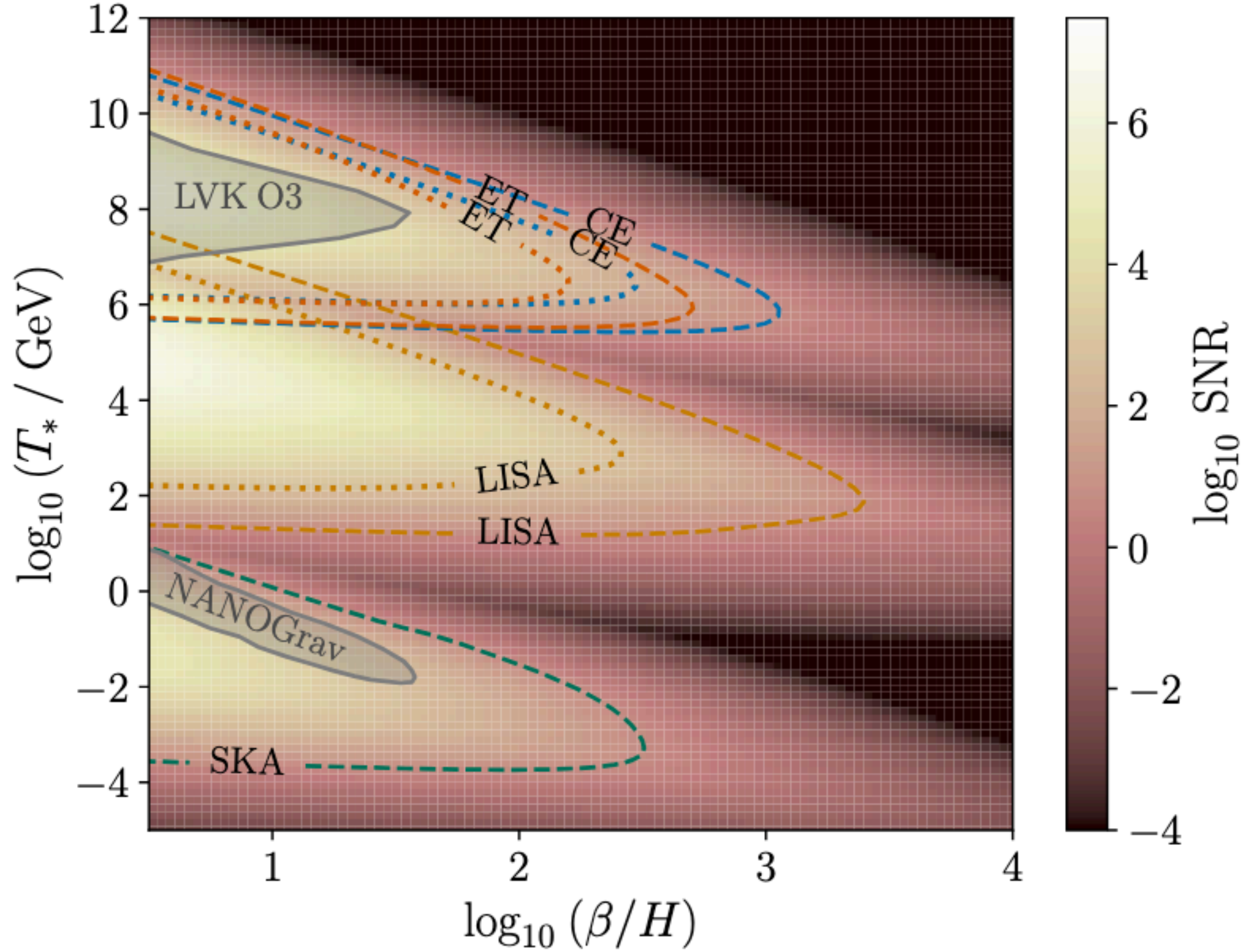

Parameter to which the signal amplitude is *inversely* proportional

Examples of detectable signal from the EWPT

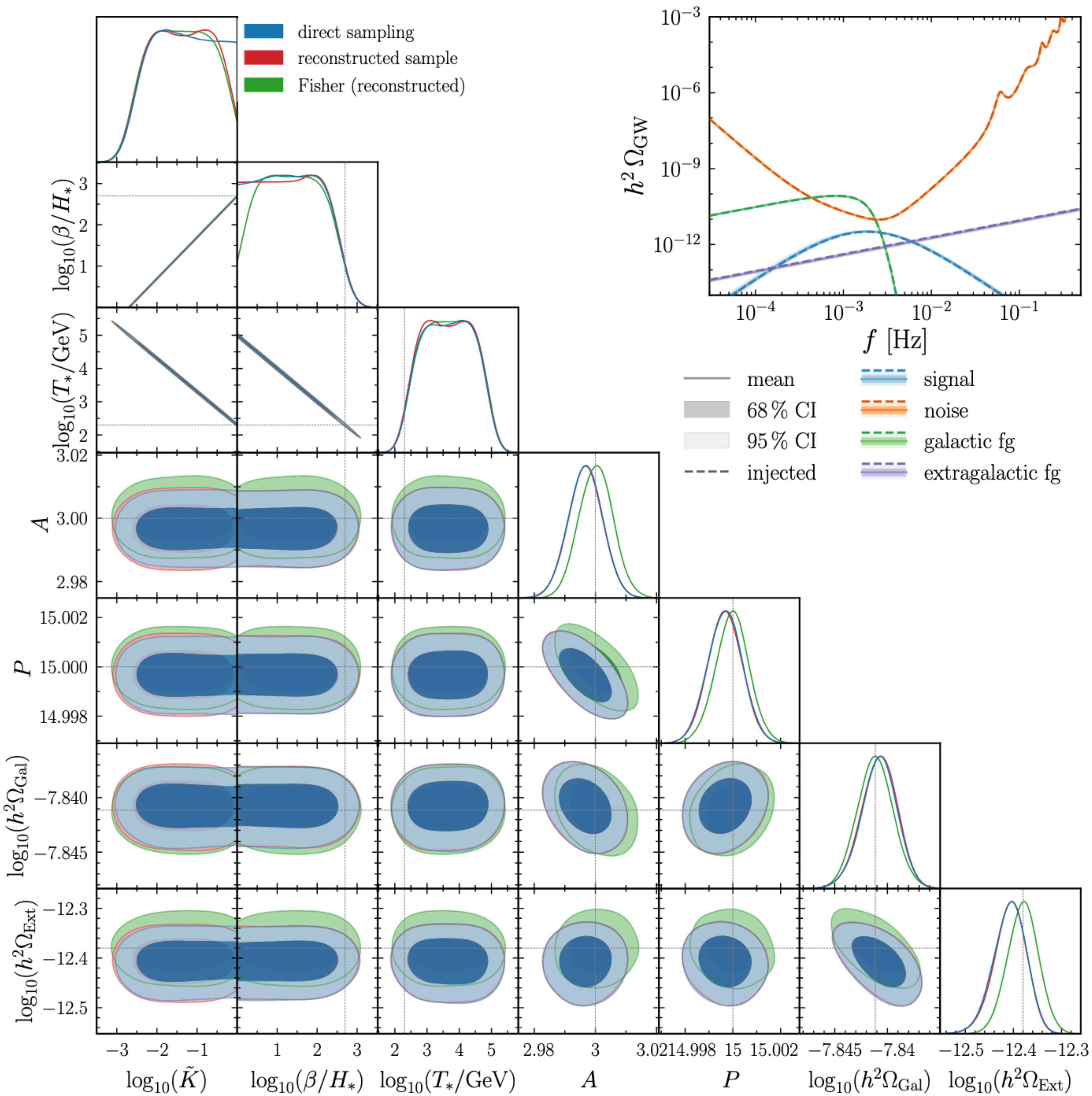

Template-based reconstruction of the *thermodynamic parameters* of the first order PT for **bubble collisions**

accounting for **foregrounds** and **assuming a two-parameters noise model**

LISA CosWG, arXiv:2403.03723

Examples of detectable signal from the EWPT

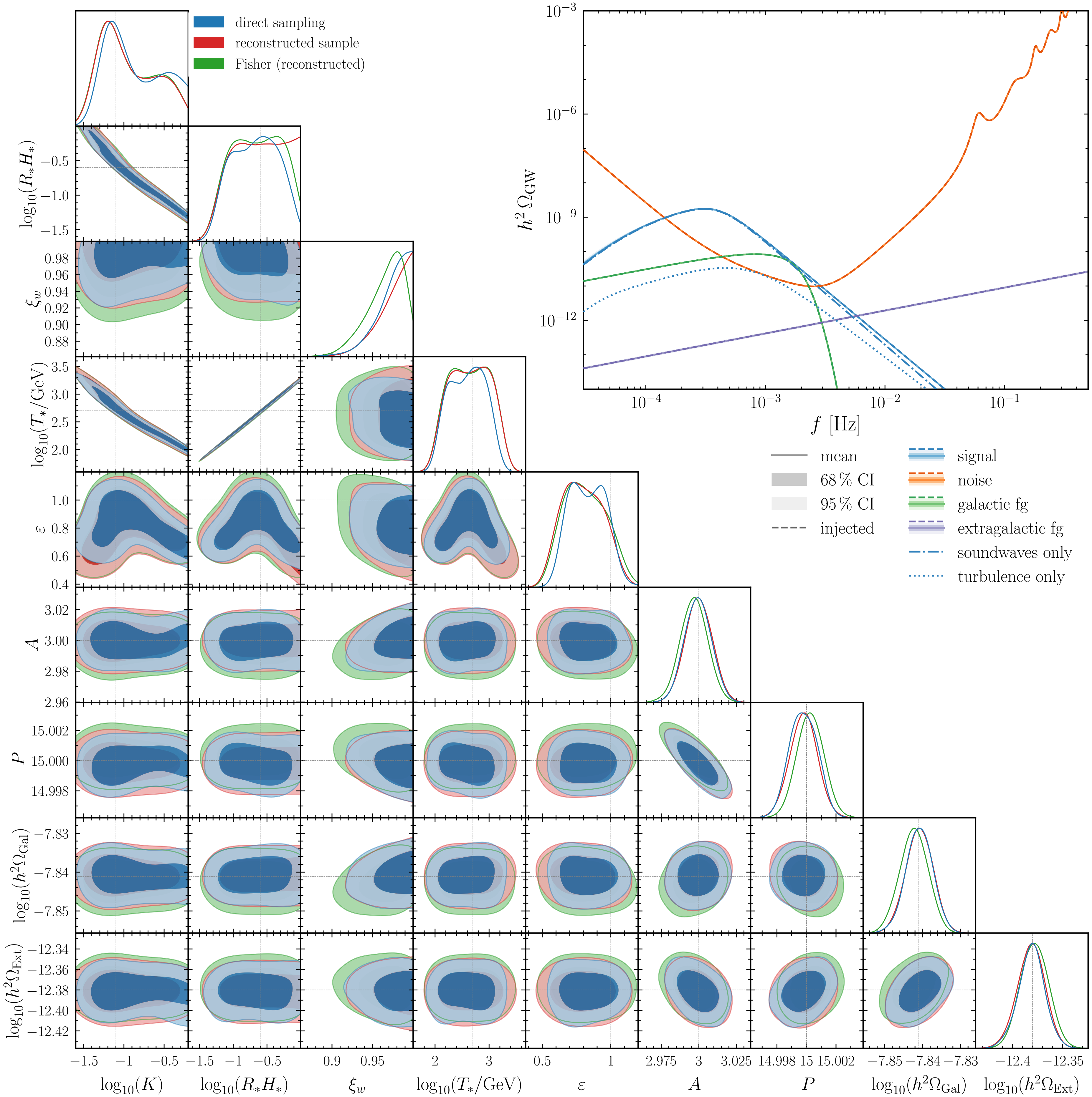

Template-based reconstruction of the *thermodynamic parameters* of the first order PT for **sound waves + turbulence**

accounting for **foregrounds** and **assuming a two-parameters noise model**

LISA CosWG, arXiv:2403.03723

An example of possible detection at PTA?

The PTA signal is compatible with GWs generated by MHD turbulence at the QCD scale

- T_* must be close to the QCD scale, the amount of energy available in anisotropic stress K must be high (at least 10% of the total energy density of the universe, and size of the anisotropic stresses $R_* = v_w/\beta$ must be close to the horizon

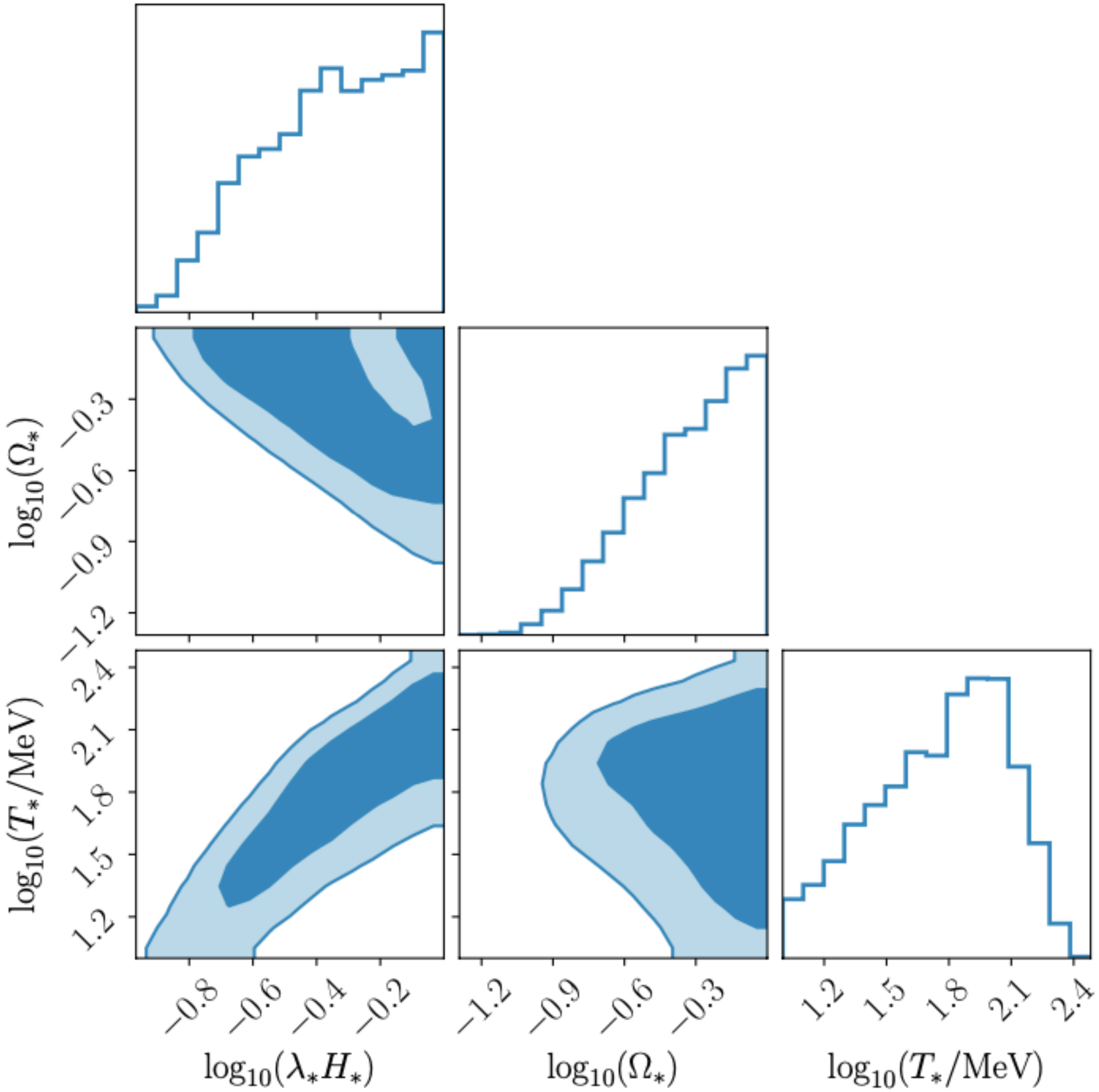

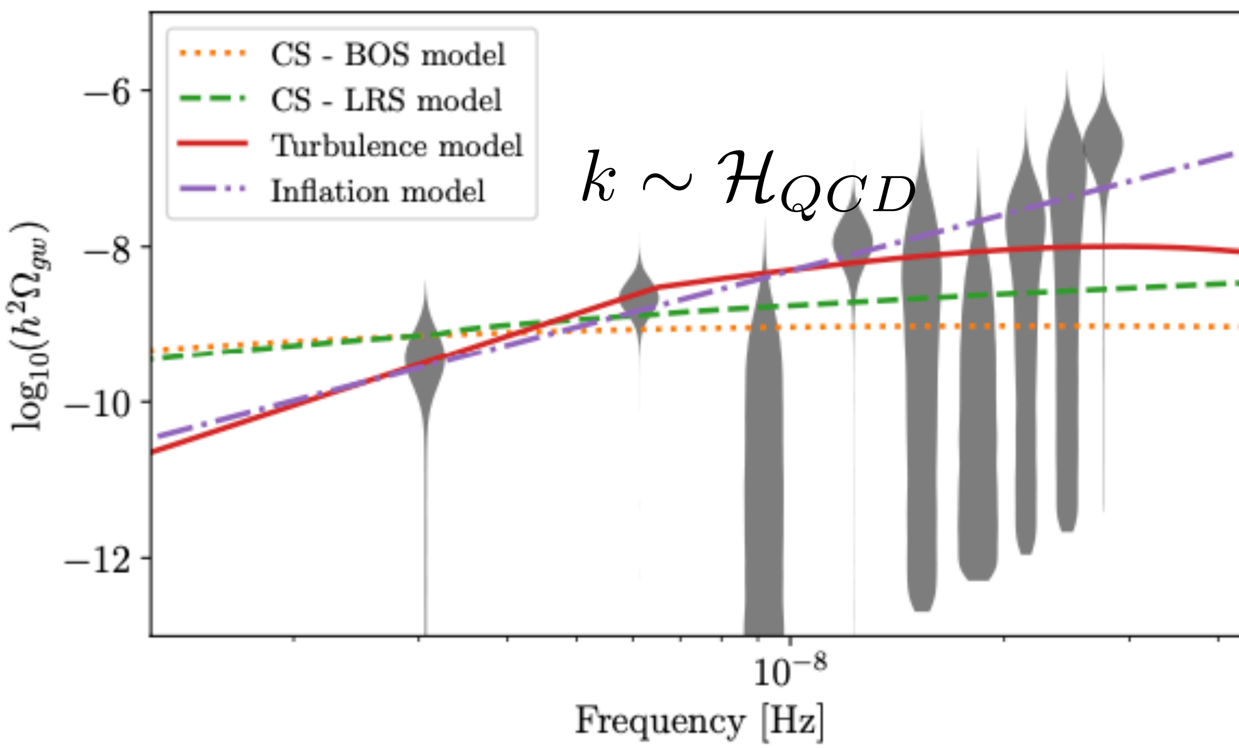

The the signal is fit with the low frequency tail, and the spectrum has a break at a scale comparable to the horizon at the QCD PT

To summarise:

- SGWB might reveal a powerful tool to probe the early universe and high energy physics
- The spectral shape must be predicted with good accuracy in order to disentangle the different sources (and also for foregrounds)
- General considerations about the characteristics of the spectral shape are possible in some cases, to pin down at least the class of SGWB sources
- Inflation: new physics but observationally compelling, extended GW signal in frequency, only accessible by CMB unless one goes beyond the standard slow roll scenario (there are well motivated scenarios!)
- Topological defects: amazing potential to probe high energy theory, but need to account for GW signal model dependent
- Electroweak PT: at the limit of tested physics, GW signal can be accessed/ constrained by LISA only for models beyond the standard model of particle physics
- QCD PT: tested physics but difficult to predict, GW signal can be accessed/ constrained by PTA only for models beyond the standard model of particle physics
- **SGWBs from the primordial universe might seem speculative but their potential to probe fundamental physics is great and amazing discoveries can be around the corner, especially after the PTA results!**